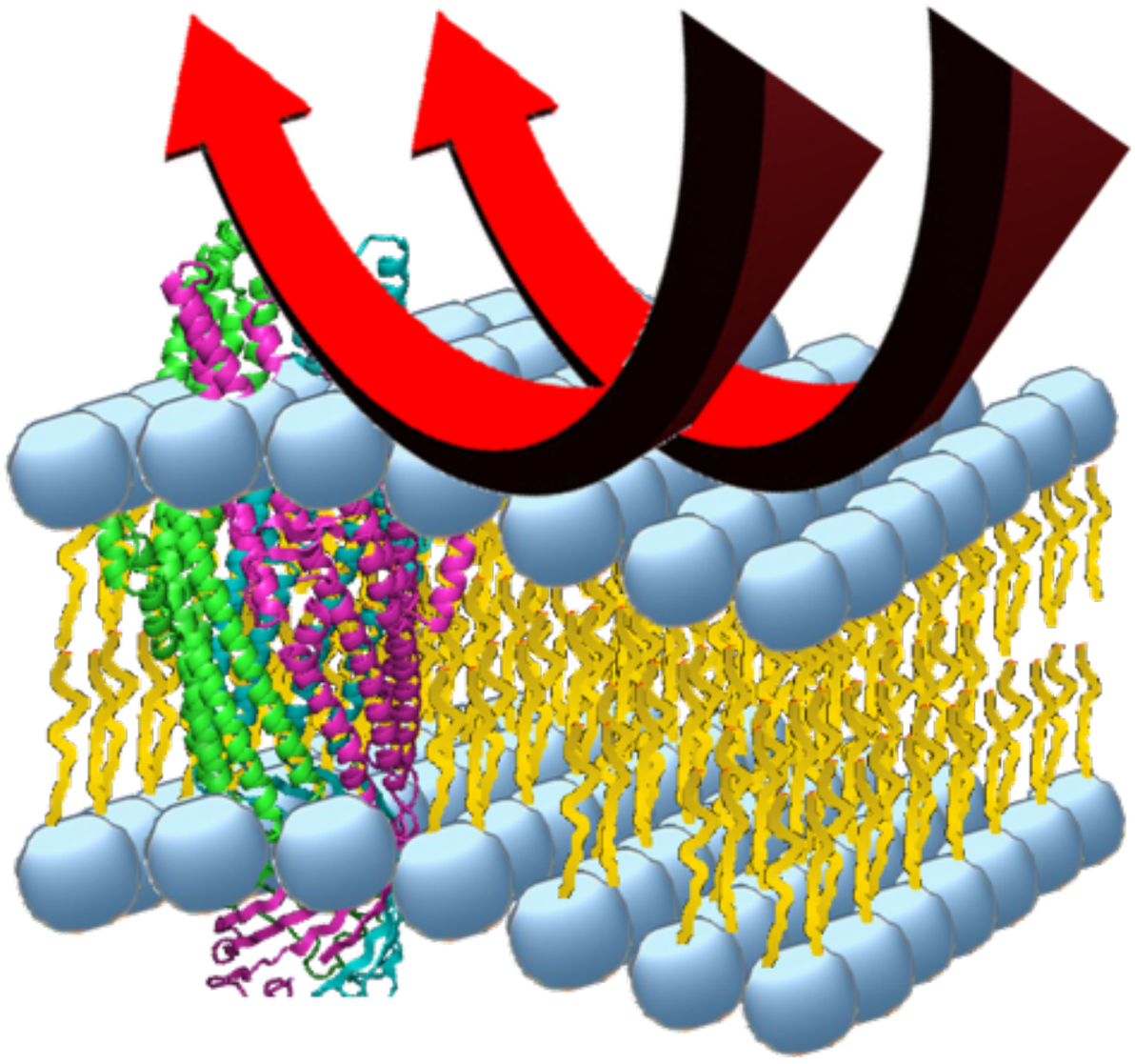

INTRODUCTION TO NEUTRON REFLECTOMETRY

Giovanna Fragneto
Institut Laue-Langevin

The importance of interfaces

They are everywhere: our body, food we eat, drinks, plants, animals, soil, atmosphere, manufacturing, chemical factories….

In many cases interfaces have a significant effect in the behaviour of a system

Examples:

Inner lining of lung: surfactants prevent lung from collapsing at the end of expiration

Nanotechnology: solid surfaces are the places where the processes of interest take place

Detergency

Biofouling

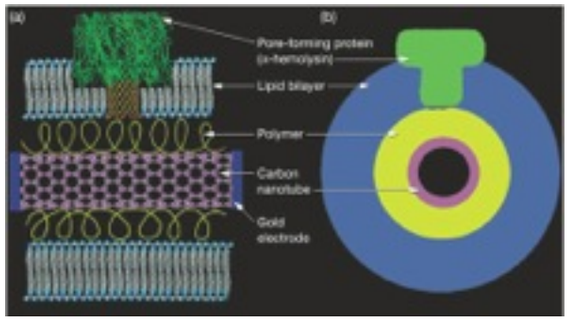

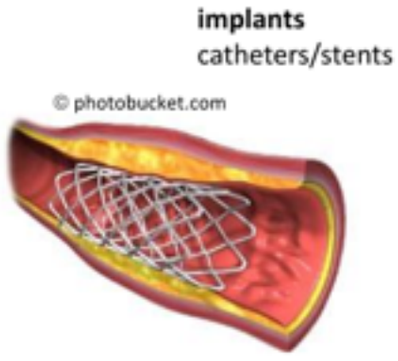

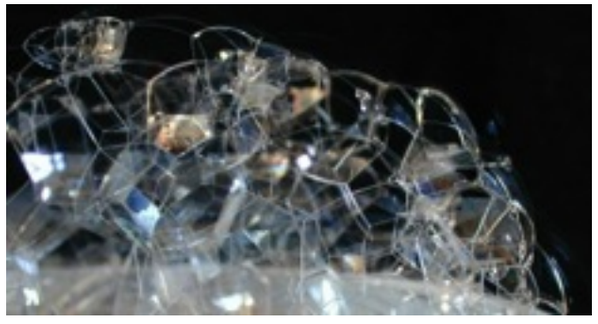

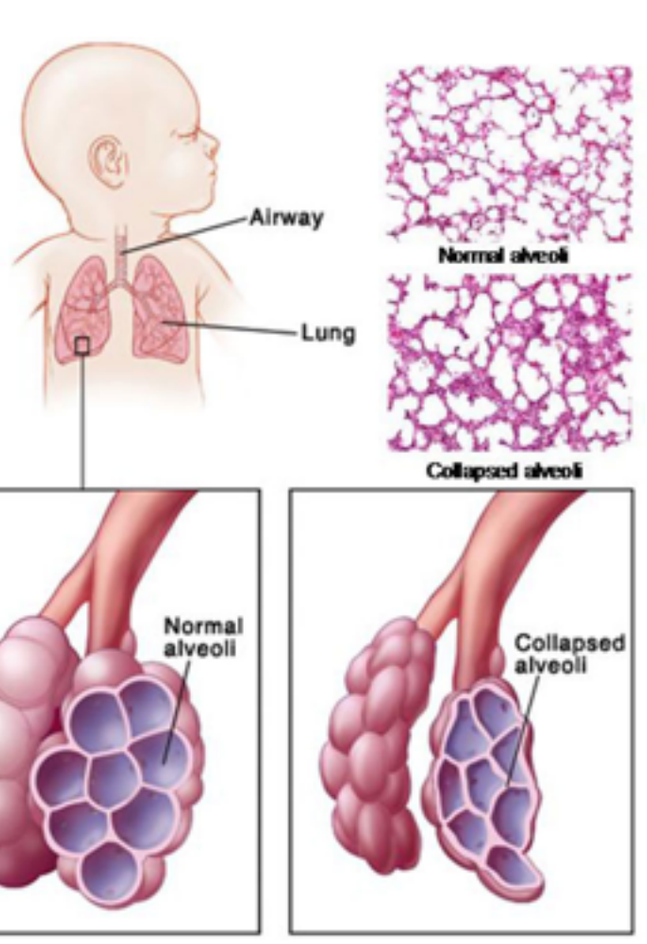

Why Neutron Reflectometry?

Probe relevant lengths (**Å to μm**)

Sensitive to light elements (H, C, O, N)

Buried systems and complex sample environment

Possibility of **isotopic labelling**

Non-destructive

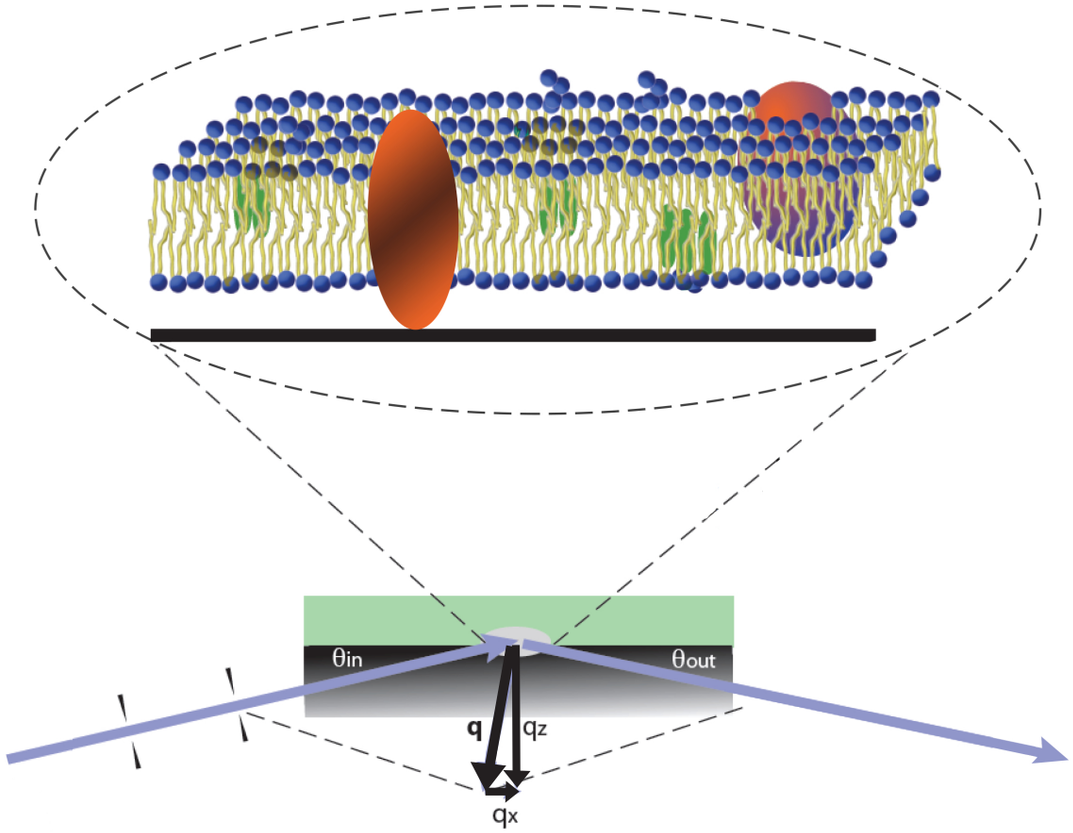

Schematic view of elastic neutron scattering spectra

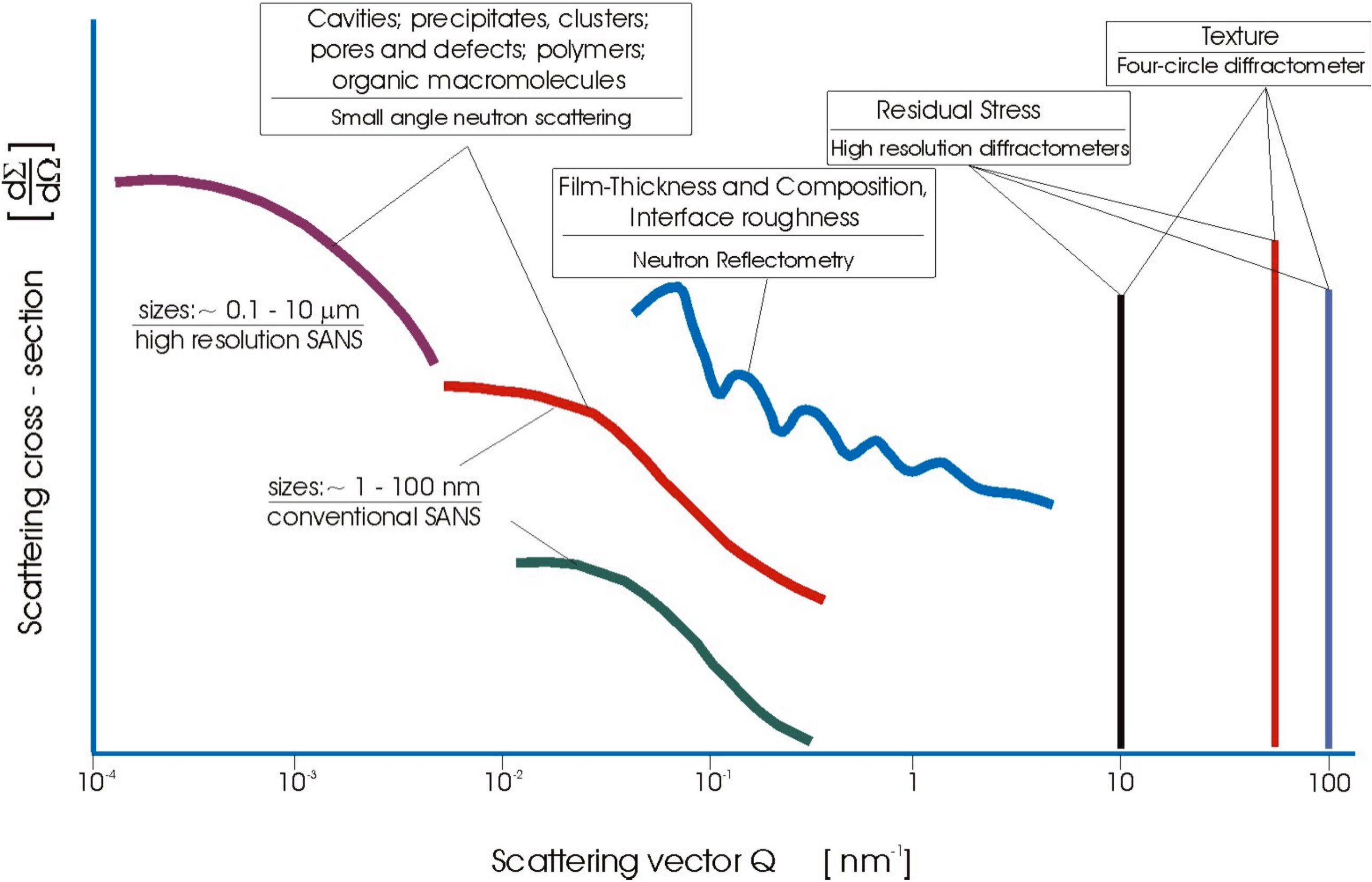

Crystallography Microstructure Structure

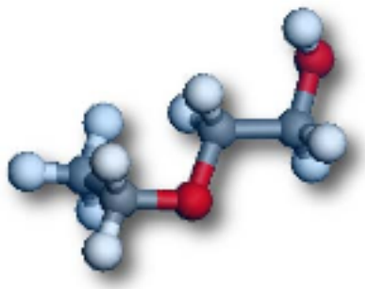

Atomic Structures

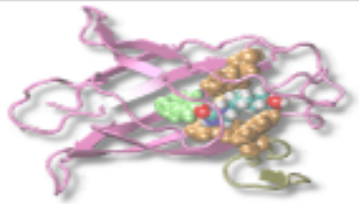

Proteins

Viruses

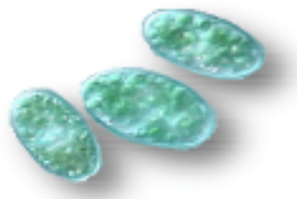

Bacteria

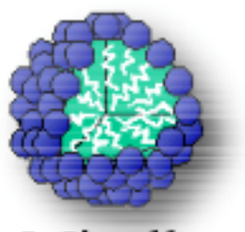

Micelles

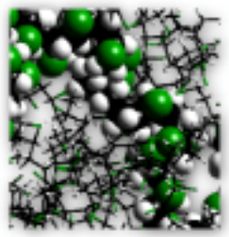

Polymers

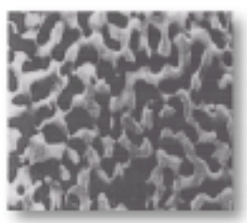

Porous Media

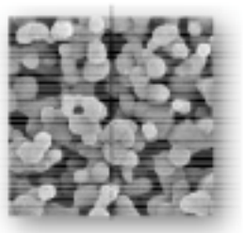

Precipitates

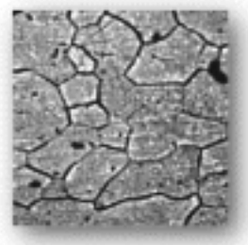

Grain Structures

TEM

USANS

DIFFRACTION SANS/SAXS

X-ray, n, e REFLECTOMETRY Optical microscopy

1-5000 Å Light scattering

10^{-11} m 10^{-9} 10^{-7} 10^{-5} 10^{-3}

Reflectivity measurements:

Specular $\theta_i=\theta_f$

- *Thickness of layers at interfaces*
- *Roughness/interdiffusion*
- *Composition in the direction normal to the interface*

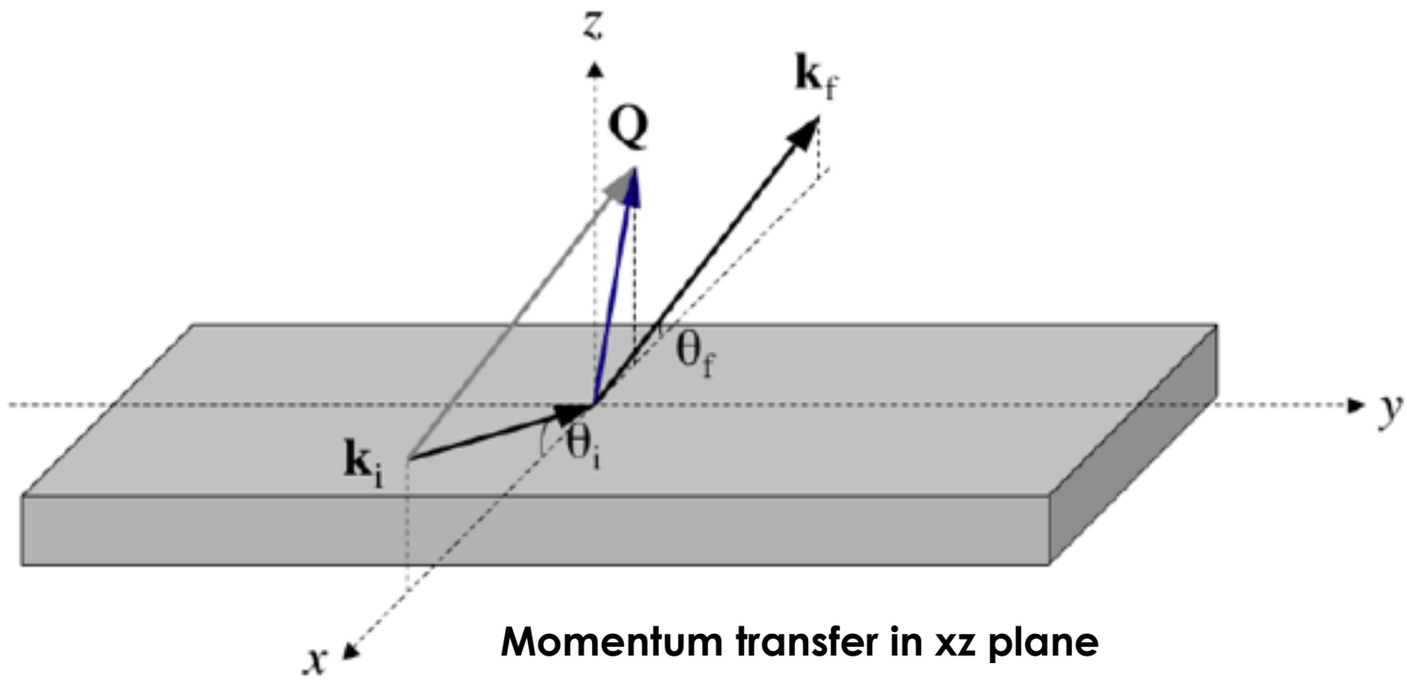

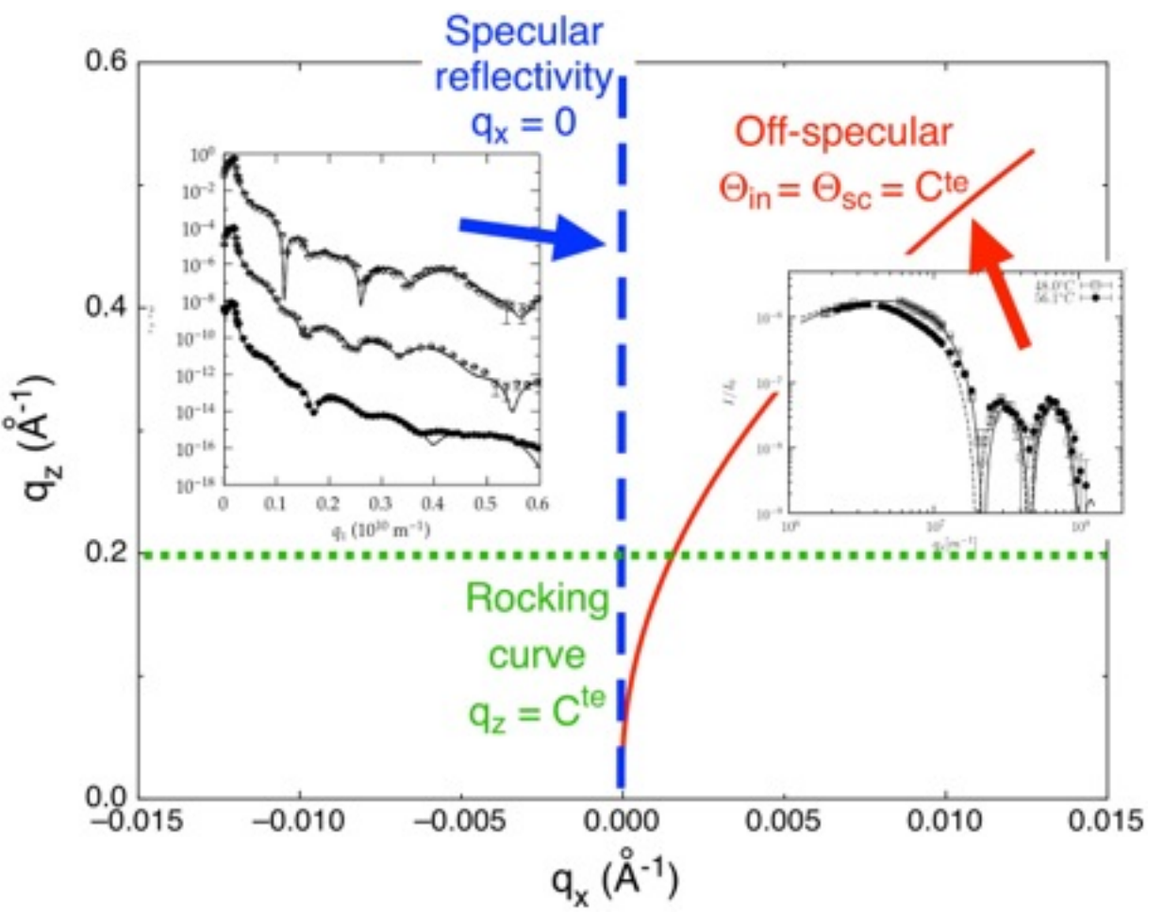

In-plane features (height fluctuations, domains, holes ...) can be probed by ***off-specular*** *measurements: for thin films synchrotron radiation is more suitable*

$$R(\vartheta,\lambda) = \frac{I_{out}(\vartheta,\lambda)}{I_{in}(\lambda)}$$

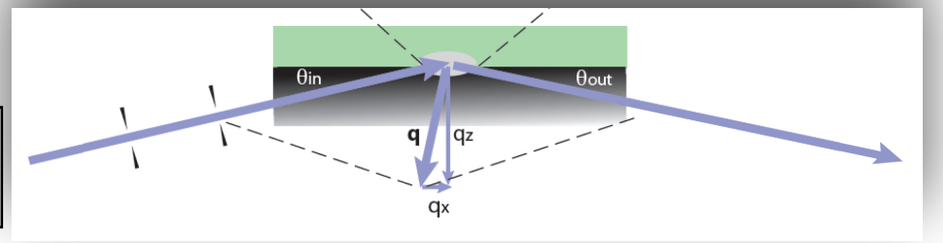

Scattering length density profile extracted from data analysis

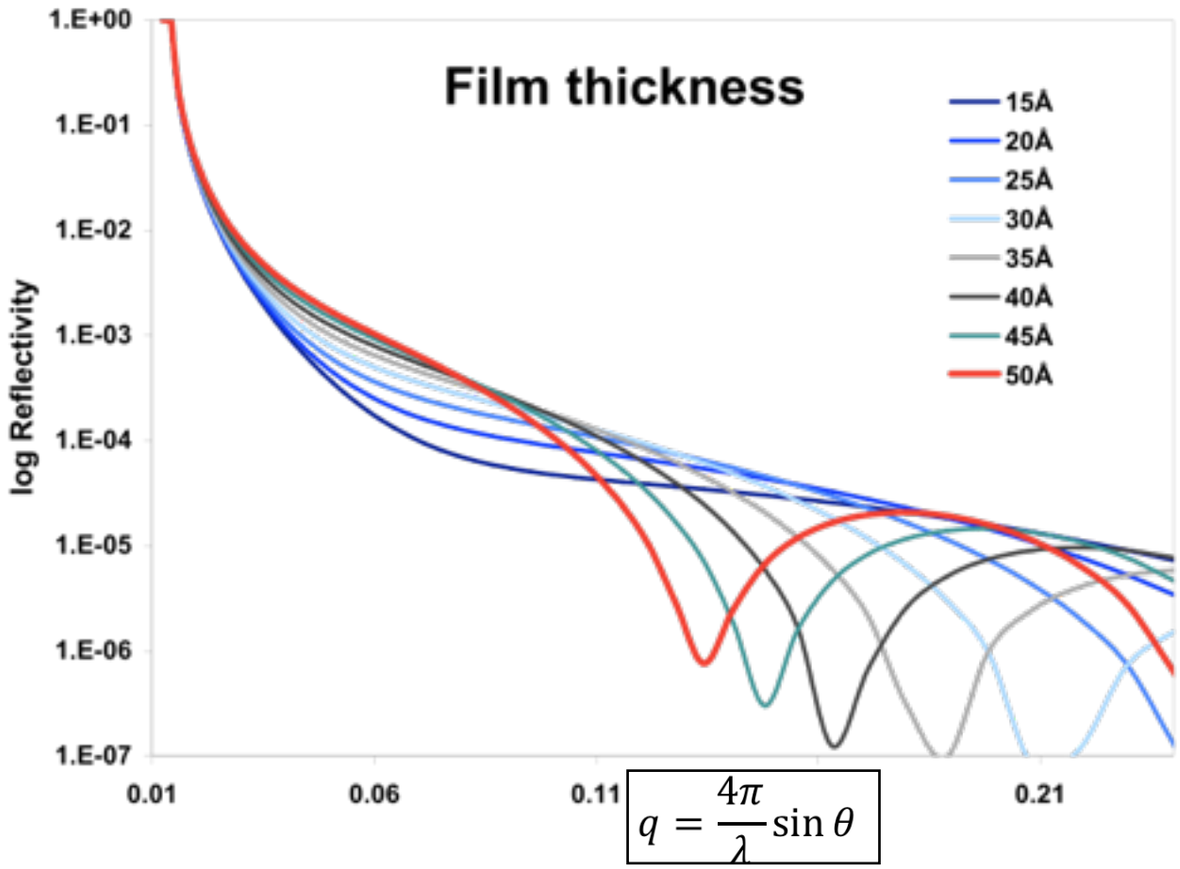

$$q = \frac{4\pi}{\lambda}\sin\theta$$

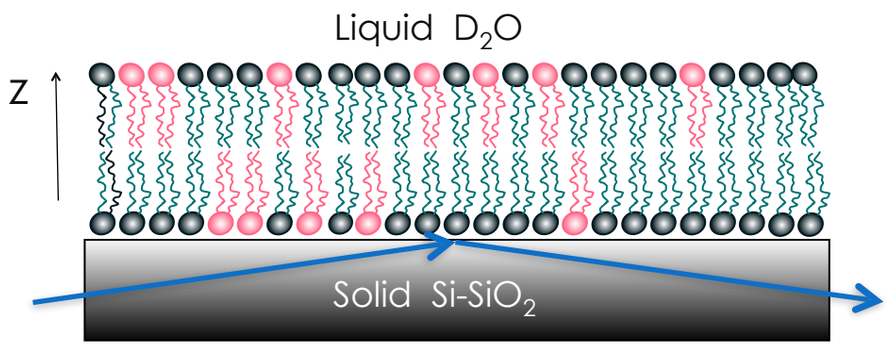

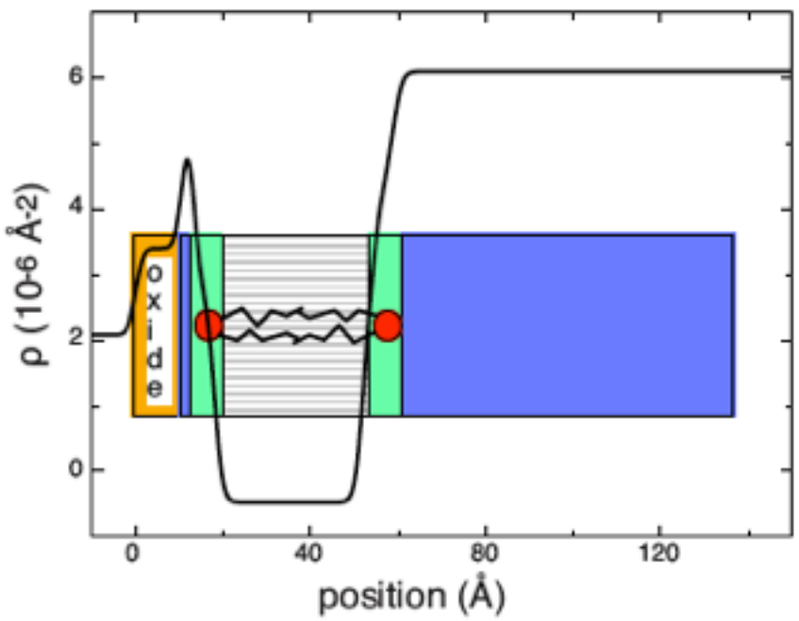

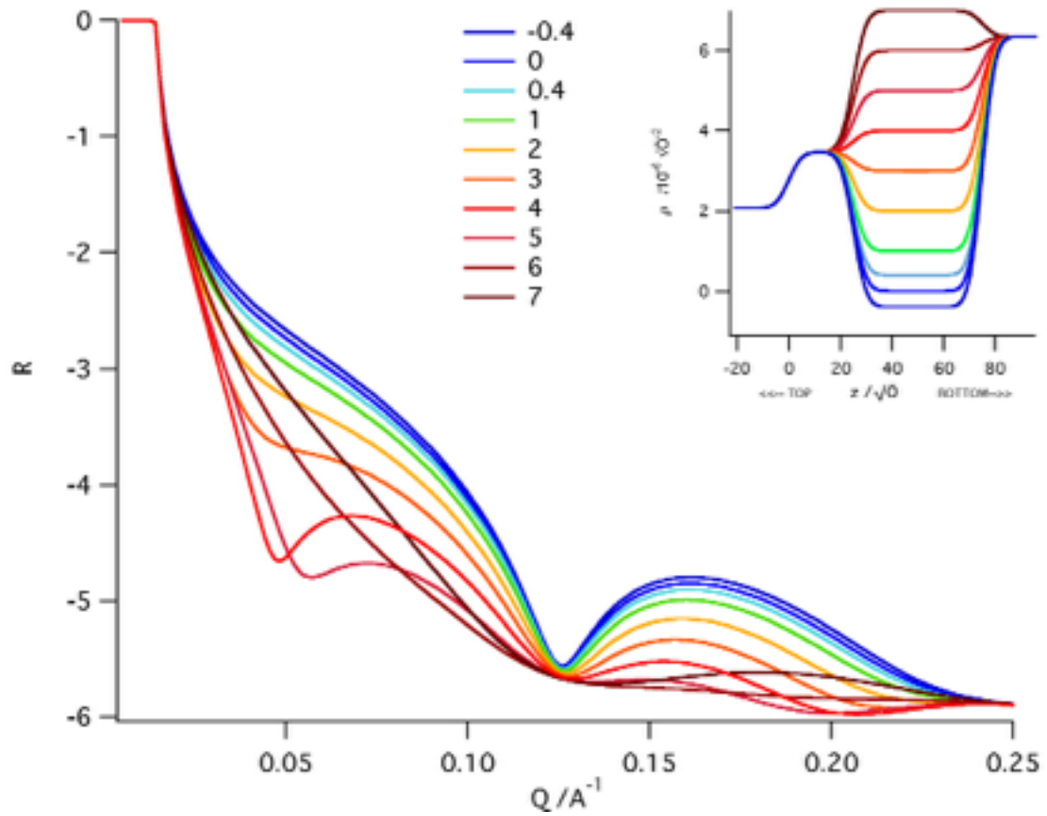

1675 - *Newton* realised that the colour of the light reflected by a thin film illuminated by a parallel beam of white light could be used to obtain a measure of the film thickness. Spectral colours develop as a result of interference between light reflected from the front and back surfaces of the film.

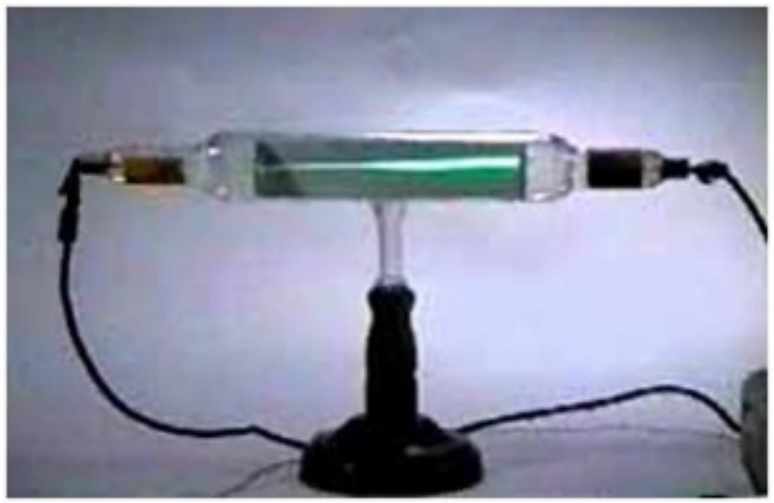

1922 - *Compton* showed that x-ray reflection is governed by the same laws as reflection of light but with different refractive indices depending on the number of electrons per unit volume.

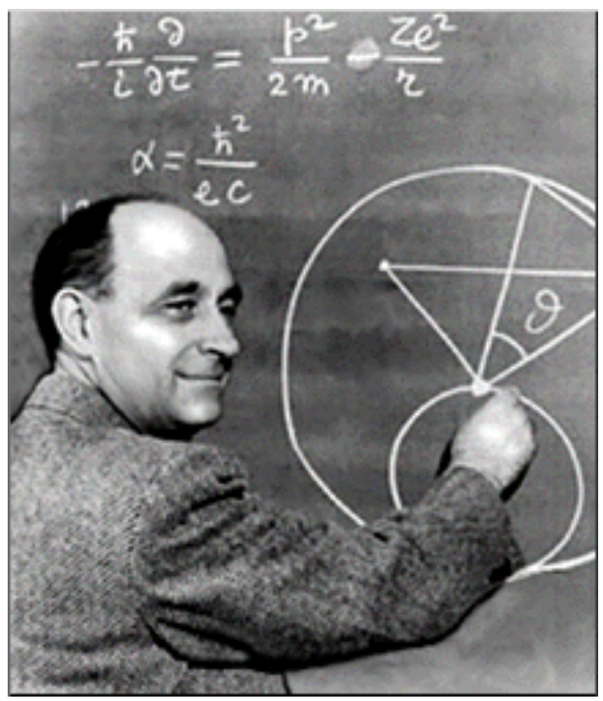

1944 - *Fermi* and ***Zinn*** first demonstrated the mirror reflection of neutrons. Again this follows the same fundamental equations as optical reflectivity but with different refractive indices.

For both kinds of radiation the refractive index is a function of the scattering length density and wavelength.

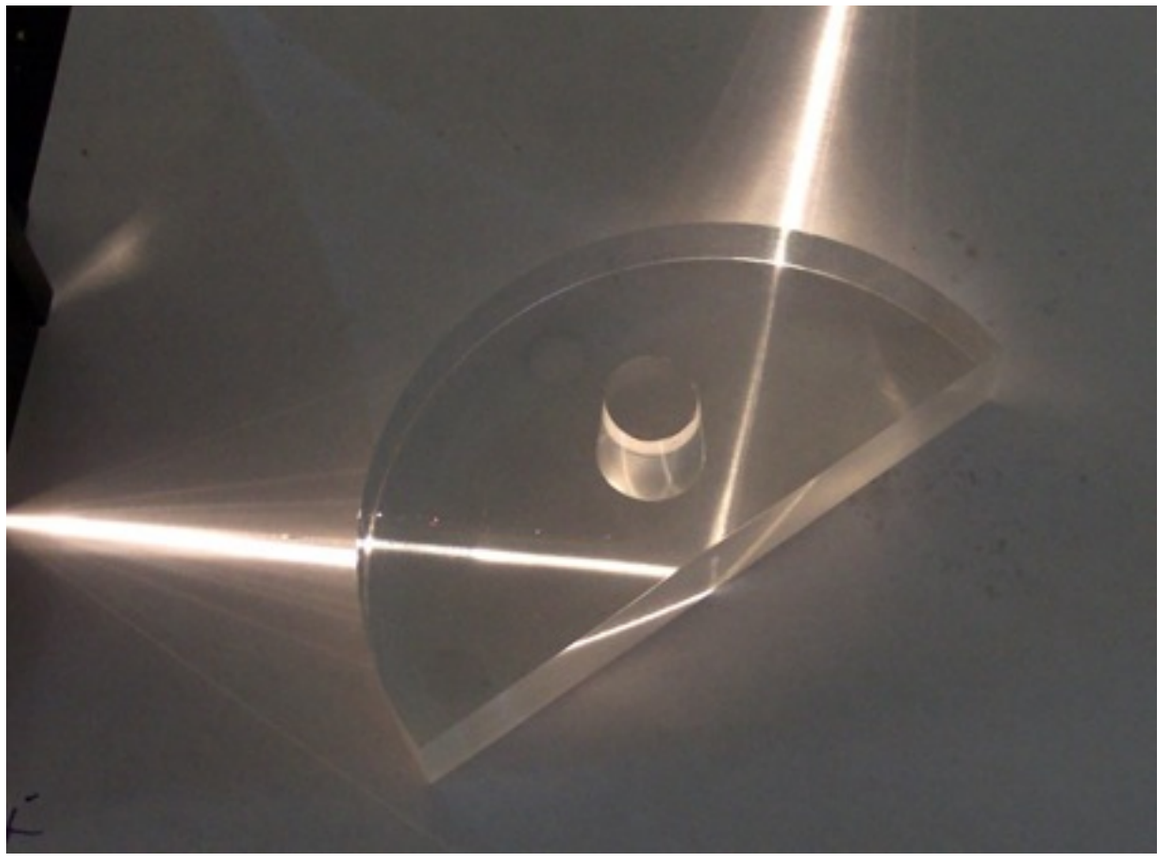

As with light, total reflection may occur when neutrons pass from a medium of higher refractive index to one of lower refractive index.

Optical Demonstrations

Reflection from a thin film

Newton's Rings

Courtesy of R. K. Thomas
http://rkt.chem.ox.ac.uk/techniques/nrmain.html

Basic Principles of Neutron Reflection Theory

neutron scattering
A PRIMER

by Roger Pynn

"Neutron man" personifies the neutron's dual nature, exhibiting wave and particle properties. Here he enters a crystal lattice as a plane wave (blue), interacts with the crystal lattice (green), and becomes, through interference effects, an outgoing plane wave (red) with a direction dictated by Bragg's law. His particle properties allow him to be absorbed by a helium atom in a neutron detector, and his time of flight is measured.

How can we determine the relative positions and motions of atoms in a bulk sample of solid or liquid? Somehow we need to see inside the material with a suitable magnifying glass. But seeing with light in an everyday sense will not suffice. First, we can only see inside the few materials that are transparent, and second, there is no microscope that will allow us to see individual atoms. These are not merely technical hurdles, like those of sending a man to the moon, but intrinsic limitations. We cannot make an opaque body transparent nor can we see detail on a scale finer than the wavelength of the radiation we are using to observe it. For observations with visible light this limits us to objects separated by about a micrometer (10^{-6} meter), which is more than a thousand times longer than the typical interatomic distance in a solid (about 10^{-10} meter or so).

X rays have wavelengths much shorter than those of visible light, so we might try using them to find atomic positions. For many crystalline materials this technique works quite well. The x rays are diffracted by the material, and one can work out the relative atomic positions from the pattern of spots the diffracted rays make on a photographic plate. However, not all atoms are equally "visible" to x rays:

"Neutron man" personifies the neutron's dual nature, exhibiting wave and particle properties. Here he enters a crystal lattice as a plane wave (blue), interacts with the crystal lattice (green), and becomes, through interference effects, an outgoing plane wave (red) with a direction dictated by Bragg's law. His particle properties allow him to be able to be absorbed by a He atom in a neutron detector, and his time of flight measured.

Neutrons can be treated as a wave:

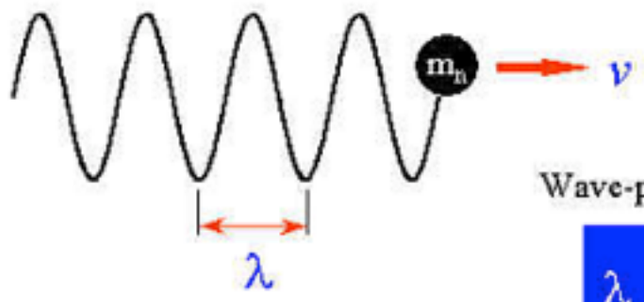

Wave-particle duality

$$\lambda = \frac{h}{m_n v}$$

de Broglie (1924)

$m_n = 1.674 \times 10^{-27}$ kg

Thus: $\lambda \sim 10^{-10}$ m

$E \sim k_B T$

The Schroedinger equation is analogous to the wave equation for light and leads to neutrons showing characteristic optical behaviour such as total reflection and refraction.

The Schroedinger equation may be written as:

$$-\frac{h^2}{8\pi^2 m_n}\nabla^2\Psi + V\Psi = E\Psi$$

Where *V* is the potential to which the neutron is subject and *E* its energy

V **represents the net effect of the interactions between the neutron and the scatterers in the medium through which it moves.**

$$V = \frac{h^2}{2\pi m_n} N_b$$

$$N_b = \frac{\sum_j b_j n_j}{Vol}$$

scattering length density

Coherent neutron scattering lengths [fm]

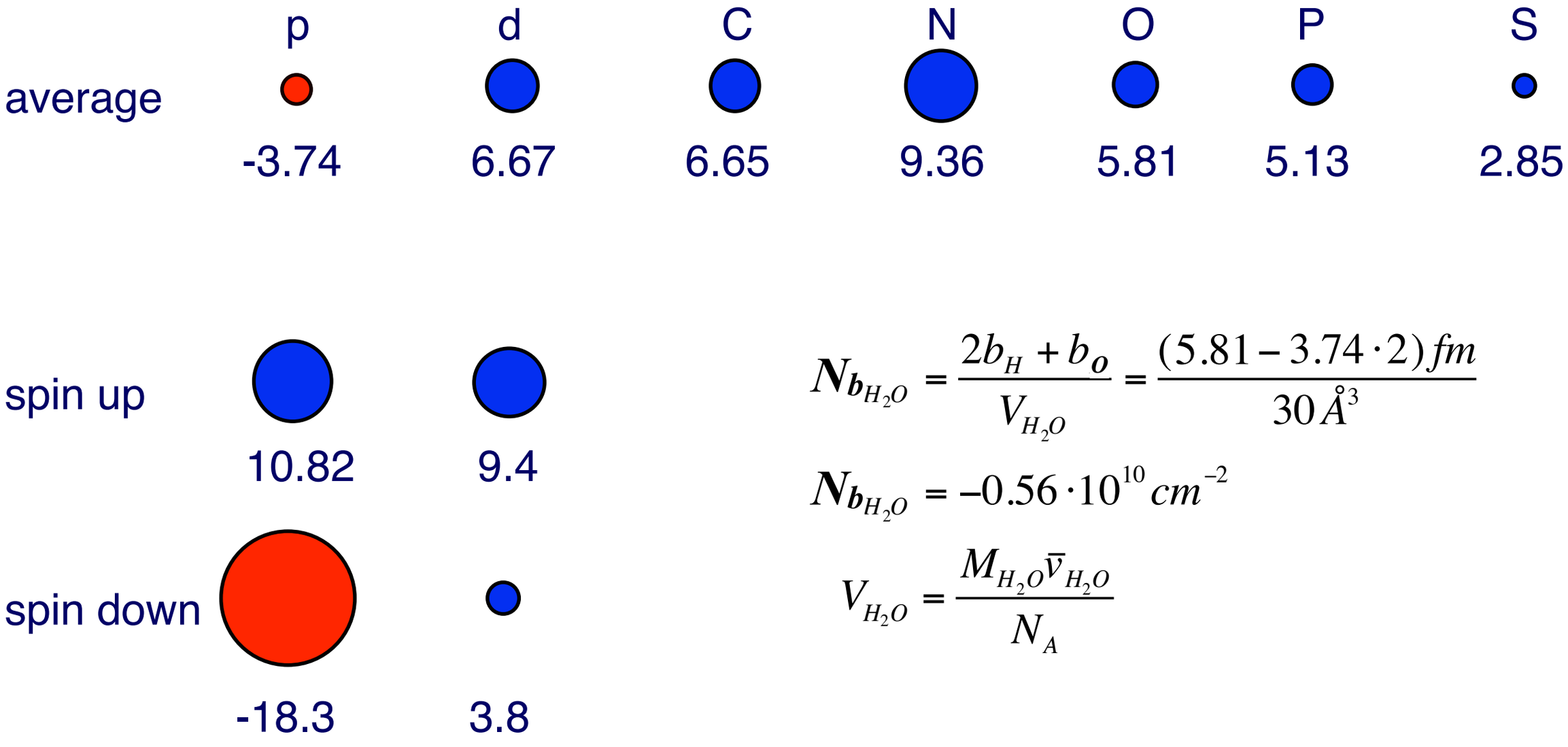

Spin-dependent scattering lengths

$$N_{\boldsymbol{b}_{H_2O}} = \frac{2b_H + b_O}{V_{H_2O}} = \frac{(5.81 - 3.74 \cdot 2)\,fm}{30\,\mathring{A}^3}$$

$$N_{\boldsymbol{b}_{H_2O}} = -0.56 \cdot 10^{10}\,cm^{-2}$$

$$V_{H_2O} = \frac{M_{H_2O}\bar{v}_{H_2O}}{N_A}$$

Calculation of the scattering length density

neutrons deflected from hydrogen are 180° out of phase relative to those deflected by the other elements

Let us consider *a beam approaching a surface with a bulk potential V*, infinitely deep

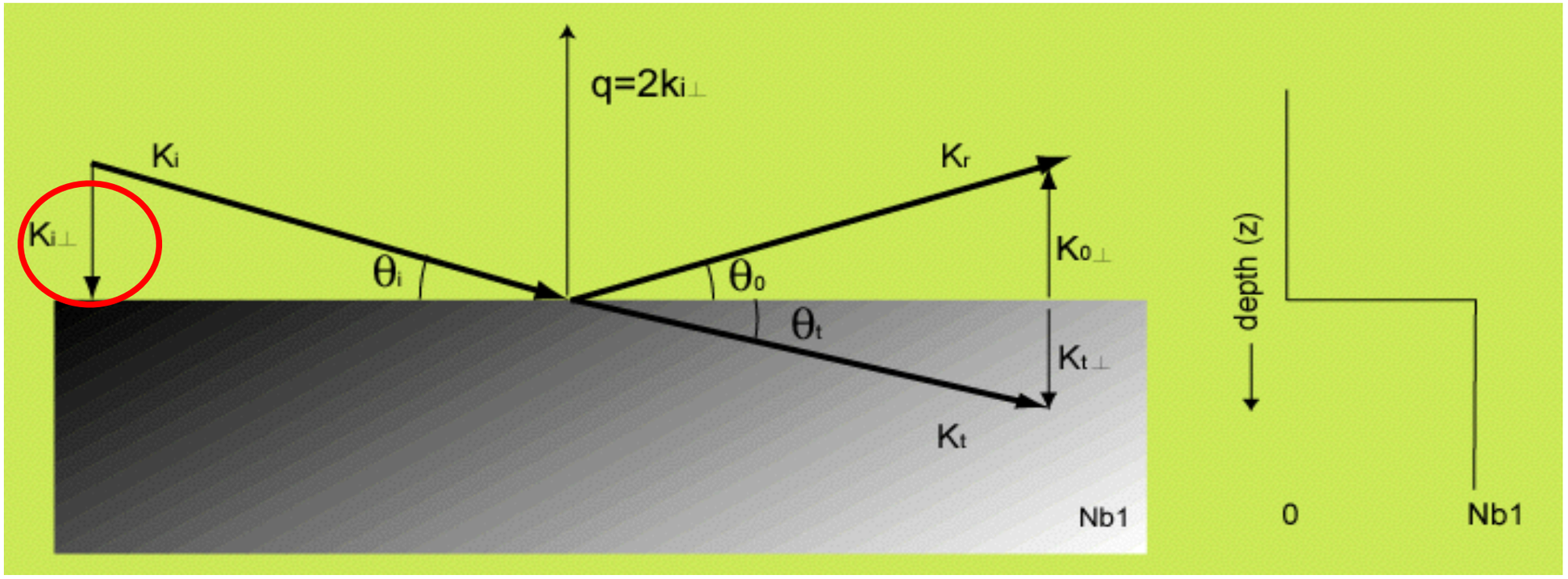

With no structure within the surface the only potential gradient and hence force is perpendicular to the surface.

Only the normal component of the incoming wave vector, k_i is altered by the barrier potential and it is the normal component of the kinetic energy $E_{i\perp}$ which determines whether the neutron is totally reflected from the barrier or not.

$$E_{i\perp} = \frac{(hk_i \sin\theta_i)^2}{8\pi^2 m_n}$$

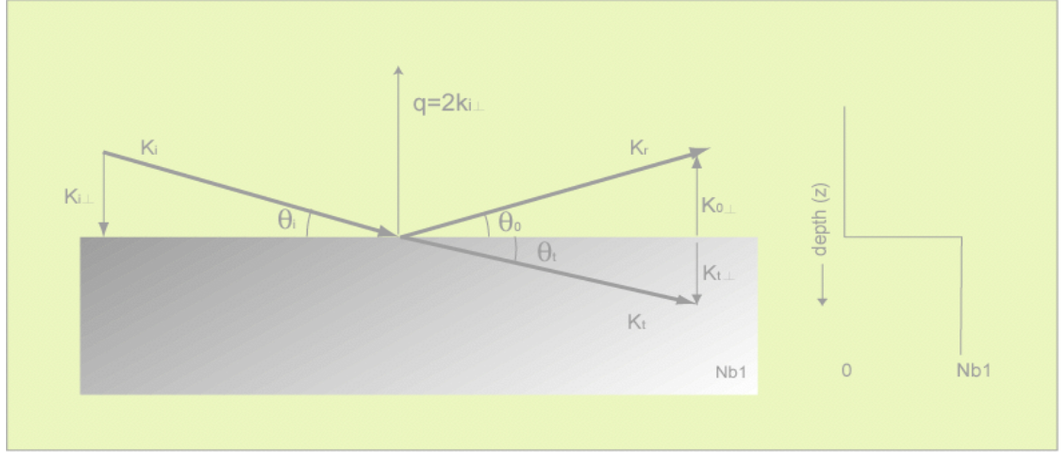

If $E_{i\perp}$<V then there is total reflection and when $E_{i\perp} = V = \frac{h^2}{2\pi m_n} N_b$

$$q_c = \sqrt{16\pi N_b} \quad \text{as} \quad q = 2k_i \sin\theta_i$$

If interaction is elastic then conservation of momentum and

$$\theta_i = \theta_o$$

***i.e.* the reflection is specular**

Provided the sample is static, any off specular reflection must be a result of potential gradients within the xy plane of the surface.

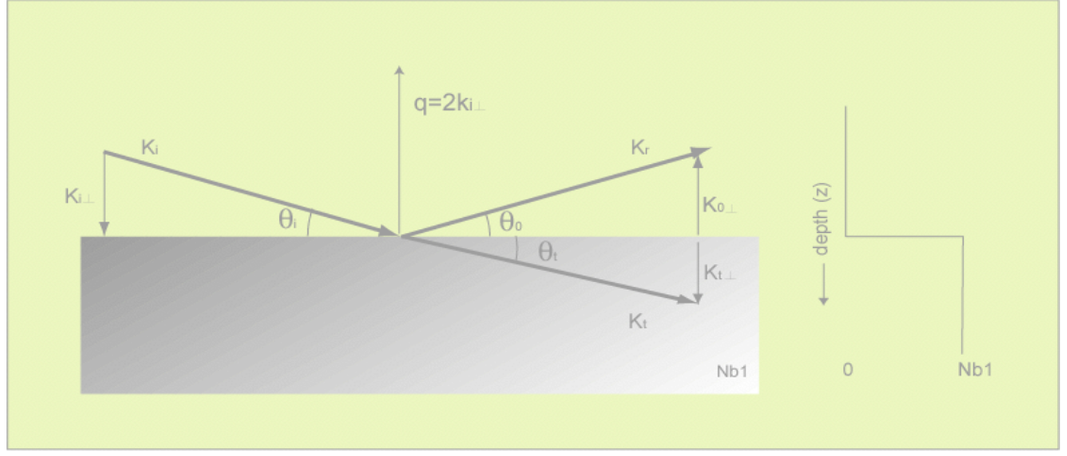

If $E_{i\perp}$>V, then the reflection is not total and the neutron can either be reflected or transmitted into the bulk of the material.

The transmitted beam, k_t with its normal component of kinetic energy reduced by the potential must change direction i.e. it is refracted.

The change in the normal wave vector is $$k_{t\perp}^2 = k_{i\perp}^2 - 4\pi N_b$$

$$n^2 = \frac{k_t^2}{k_i^2} = \frac{k_{i//}^2 + (k_{i\perp}^2 - 4\pi N_b)}{k_i^2} = 1 - \frac{4\pi N_b}{k_i^2} = 1 - \frac{\lambda^2 N_b}{\pi}$$

Values of Refractive Index

$$n = 1 - \delta - i\beta$$

X-RAYS

$$\delta = \frac{\lambda^2}{2\pi} r_e \rho$$

NEUTRONS

$$\delta = \frac{\lambda^2}{2\pi} N_b$$

- Small difference in refractive index mean that critical angles are small (less than 1 degree)
- As most n < 1, total external reflection is common. In optics n > 1
- Mixtures of isotopes can be used to match values of different materials
- β absorption coefficient small with neutrons

Quantum mechanical approach

The wavefunction describing the probability amplitude of a neutron near to the surface is:

$$\frac{\partial^2 \Psi_z}{\delta z^2} + k_\perp^2 = 0 \qquad \text{where} \qquad k_\perp^2 = \frac{2m_n}{\hbar^2}\left(E_i - V\right) - k_{//}^2$$

Solutions for this above and below the surface are:

$$\Psi_z = e^{ik_{i\perp}z} + re^{-ik_{i\perp}z} \qquad \& \qquad Y_z = te^{ik_{t\perp}z}$$

where r and t are the probability amplitudes for reflection and transmission.

Continuity of the wavefunction and its derivative gives the expressions:

$$1 + r = t \qquad\qquad k_{i\perp}\left(1 - r\right) = t\, k_{t\perp}$$

where the second relation only holds for $\mathbf{E_{i\perp} > V}$;

this leads directly to the classical ***Fresnel coefficients*** found in optics:

$$r = \frac{k_{i\perp} - k_{t\perp}}{k_{i\perp} + k_{t\perp}} \qquad \& \qquad t = \frac{2k_{i\perp}}{k_{i\perp} + k_{t\perp}}$$

Reflectivity is measured as a function of wavevector transfer or *q*

Note that what is measured is an intensity and thus is a function of the quantum mechanical probability amplitude squared.

$$R = r^2 = \left[\frac{q - \left(q^2 - q_c^2\right)^{1/2}}{q + \left(q^2 - q_c^2\right)^{1/2}} \right]^2$$

Fresnel reflectivity

$$q = \frac{4\pi}{\lambda} \sin\theta$$

Born Approximation

$q >> q_c$

Ignored double scattering processes because these are usually very weak

$$q_c = \sqrt{16\pi N_b}$$

$$R(q) = \frac{16\pi^2}{q^4}\left|N_b(q)\right|^2$$

$$N_b(q) = \int_{-\infty}^{+\infty} \exp(iqz)\frac{dN_b}{dz}dz$$

Scattering length density

$$N_b = \frac{\sum_i n_i b_i}{V}$$

$R = 1$ below q_{crit}

$\theta_c = \arccos(n_1/n_2)$

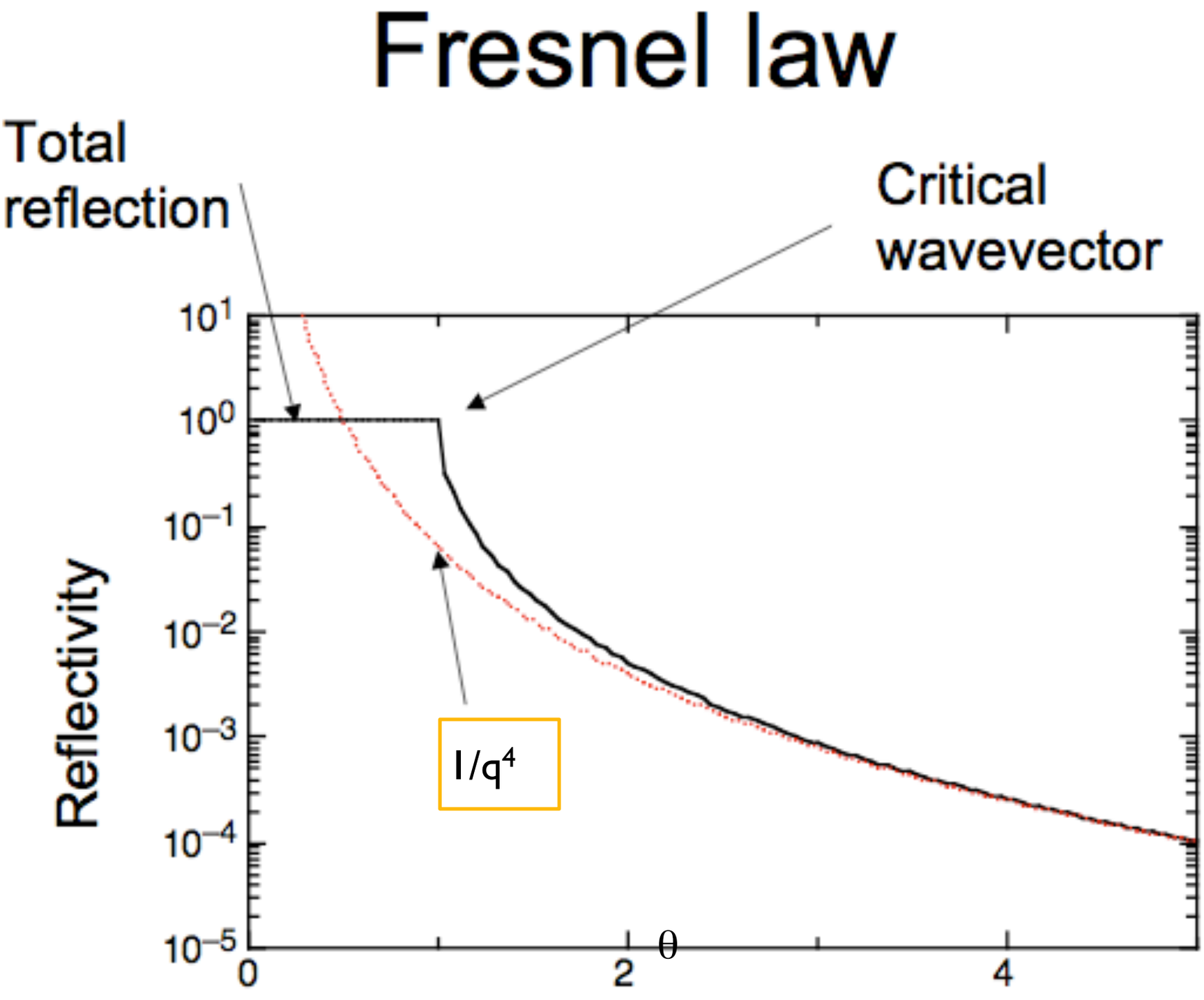

Roughness and Interdiffusion

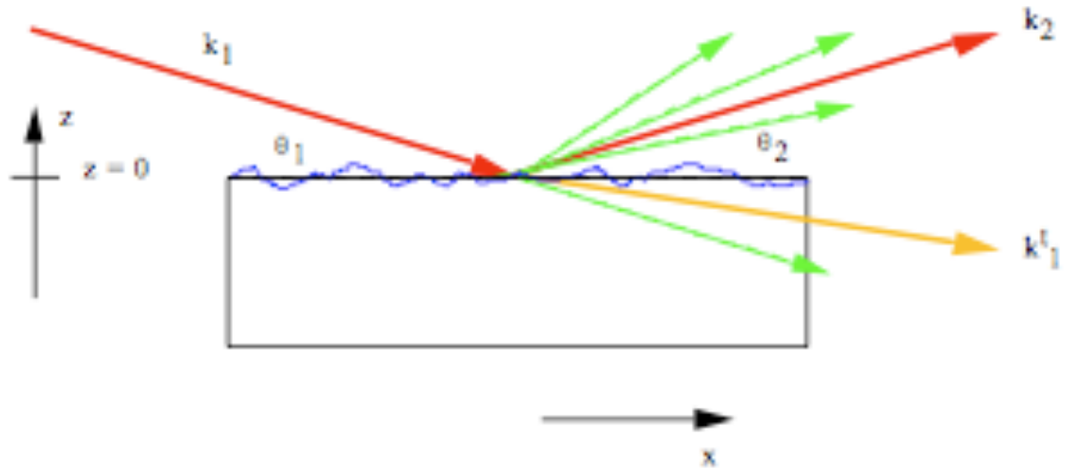

Both the rough and diffuse case the specular reflectivity is reduced by a factor very much like the Debye-Waller factor reduces scattered intensity from a crystal

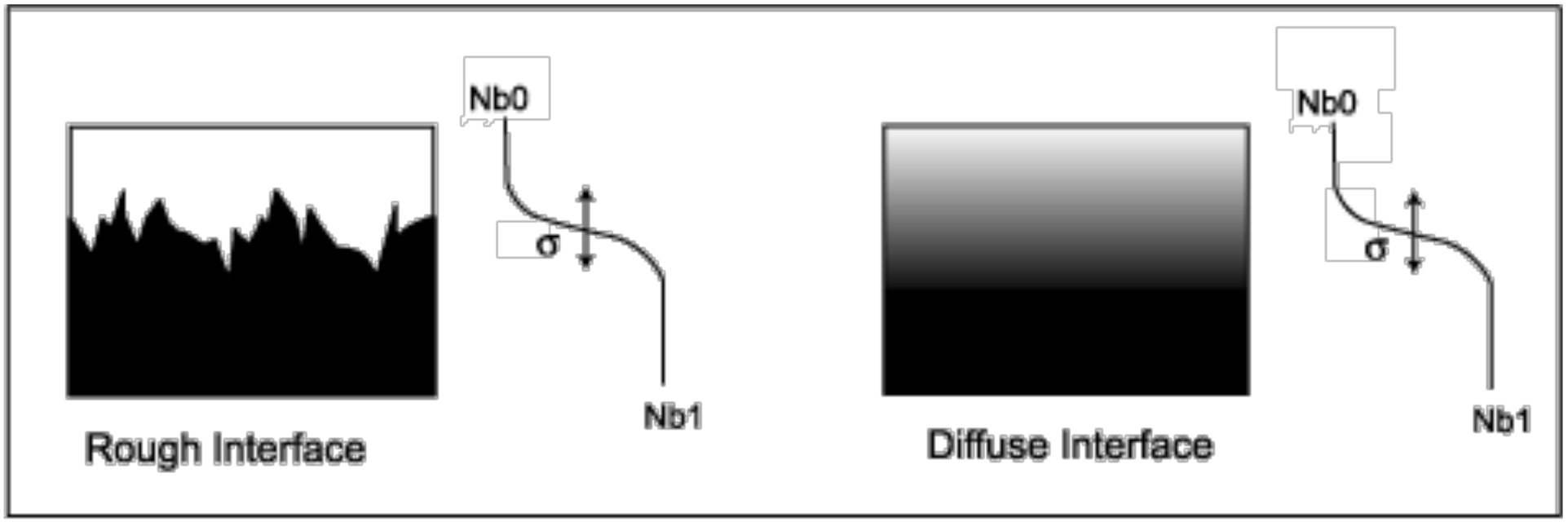

$$R \approx \left(\frac{16\pi^2}{q^4} N_b^2 \right) e^{-q_z^2 \sigma^2}$$

σ is a characteristic length scale of the layer imperfection

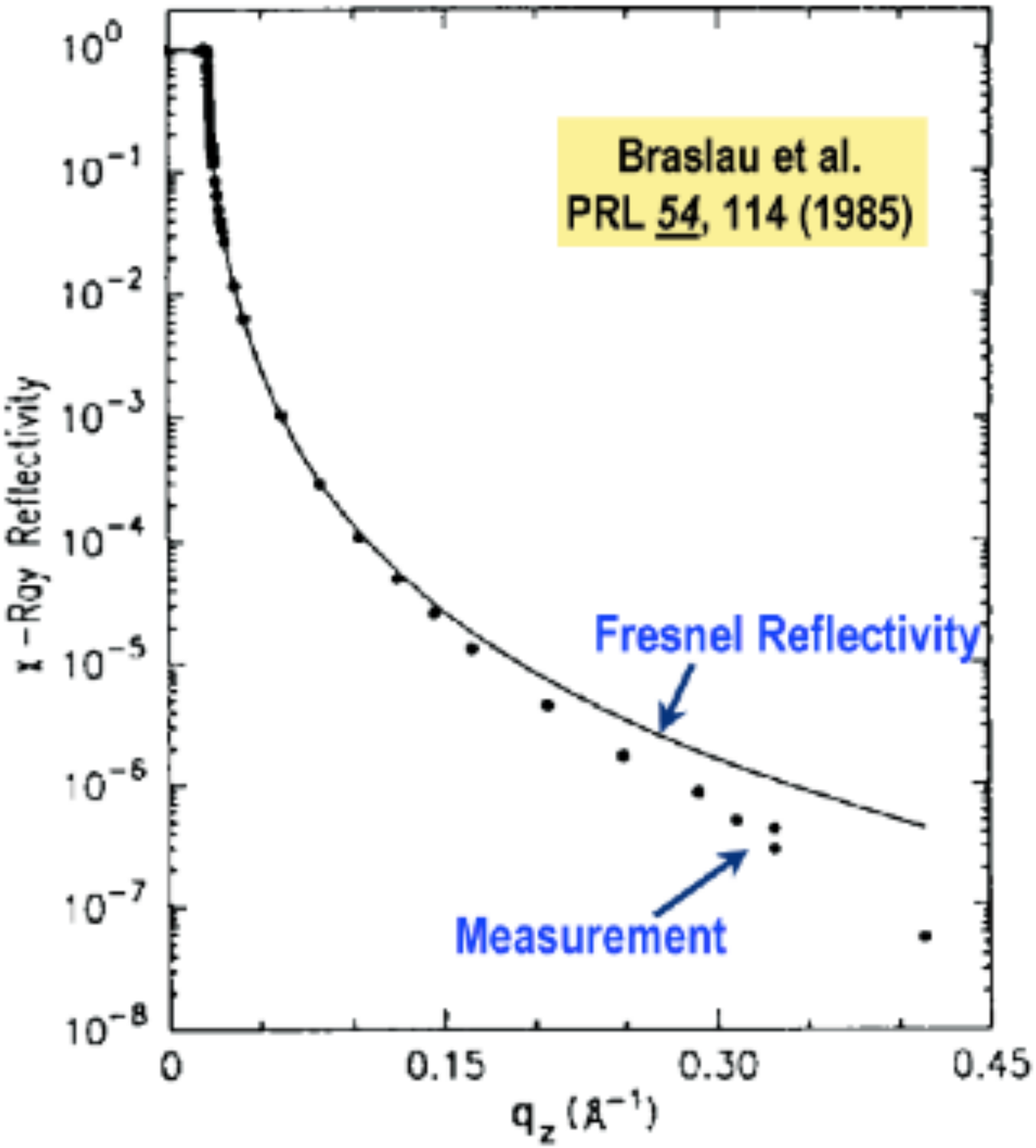
Braslau et al.
PRL 54, 114 (1985)
Fresnel Reflectivity
Measurement
X-Ray Reflectivity
10^{0}
10^{-1}
10^{-2}
10^{-3}
10^{-4}
10^{-5}
10^{-6}
10^{-7}
10^{-8}
0
0.15
0.30
0.45
q_z (Å^{-1})

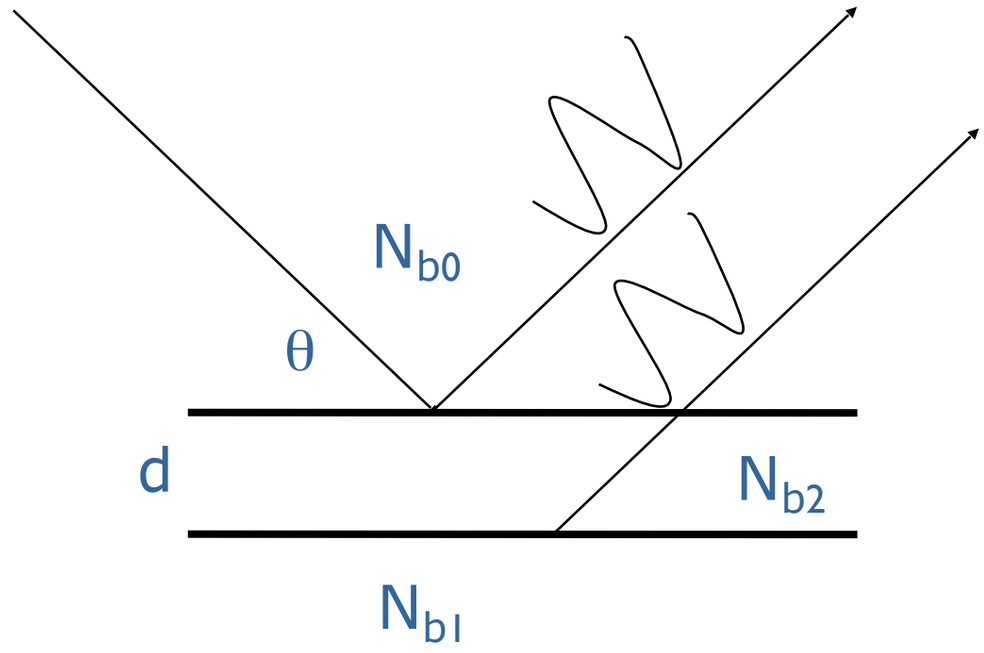

- Model calculation on smooth surface.
- Fringe spacing depends on thickness
- Fringe spacing ~ 2π/d

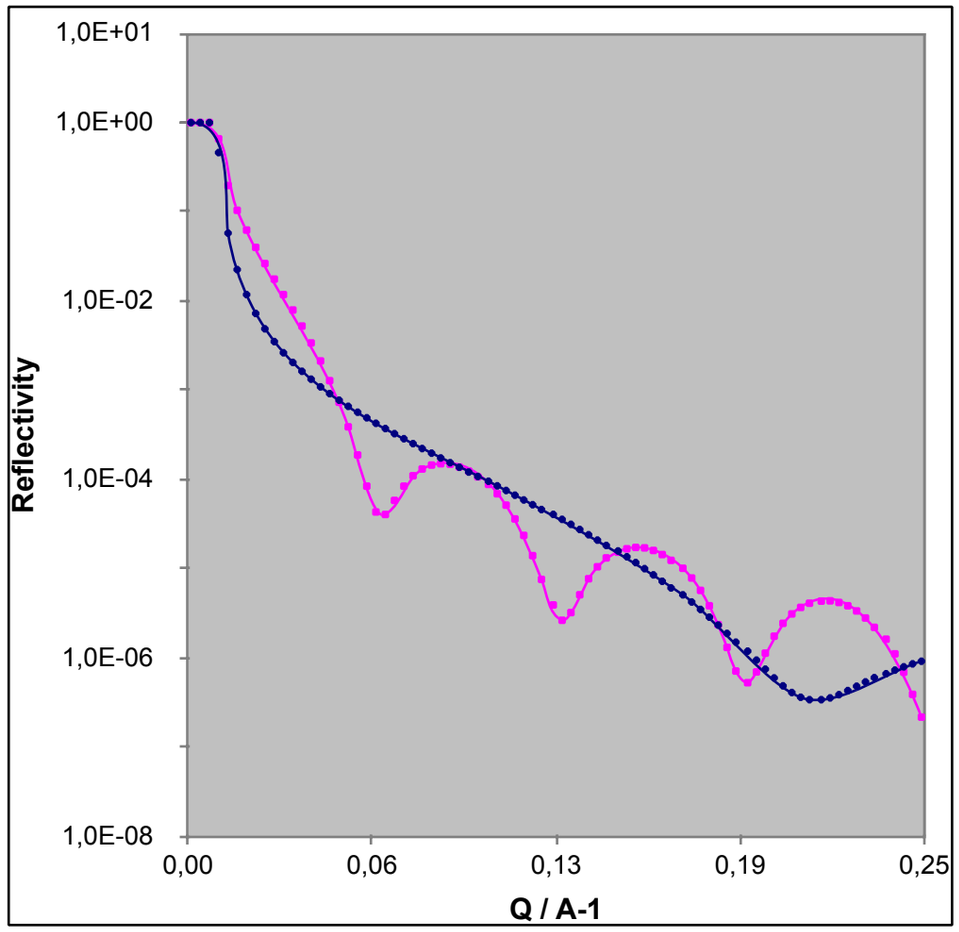

Model layer with ρ = 5 x 10^{-6} Å^2 on Si (2.07 10^{-6} Å $^{-2}$)
Blue 30 Å, Pink 100 Å. No roughness.

$$Rq^4 = [(N_{b2} - N_{b0})^2 + (N_{b1} - N_{b2})^2 + 2(N_{b2} - N_{b0})(N_{b1} - N_{b2})\cos(qd)]$$

Reflectivity from m layers

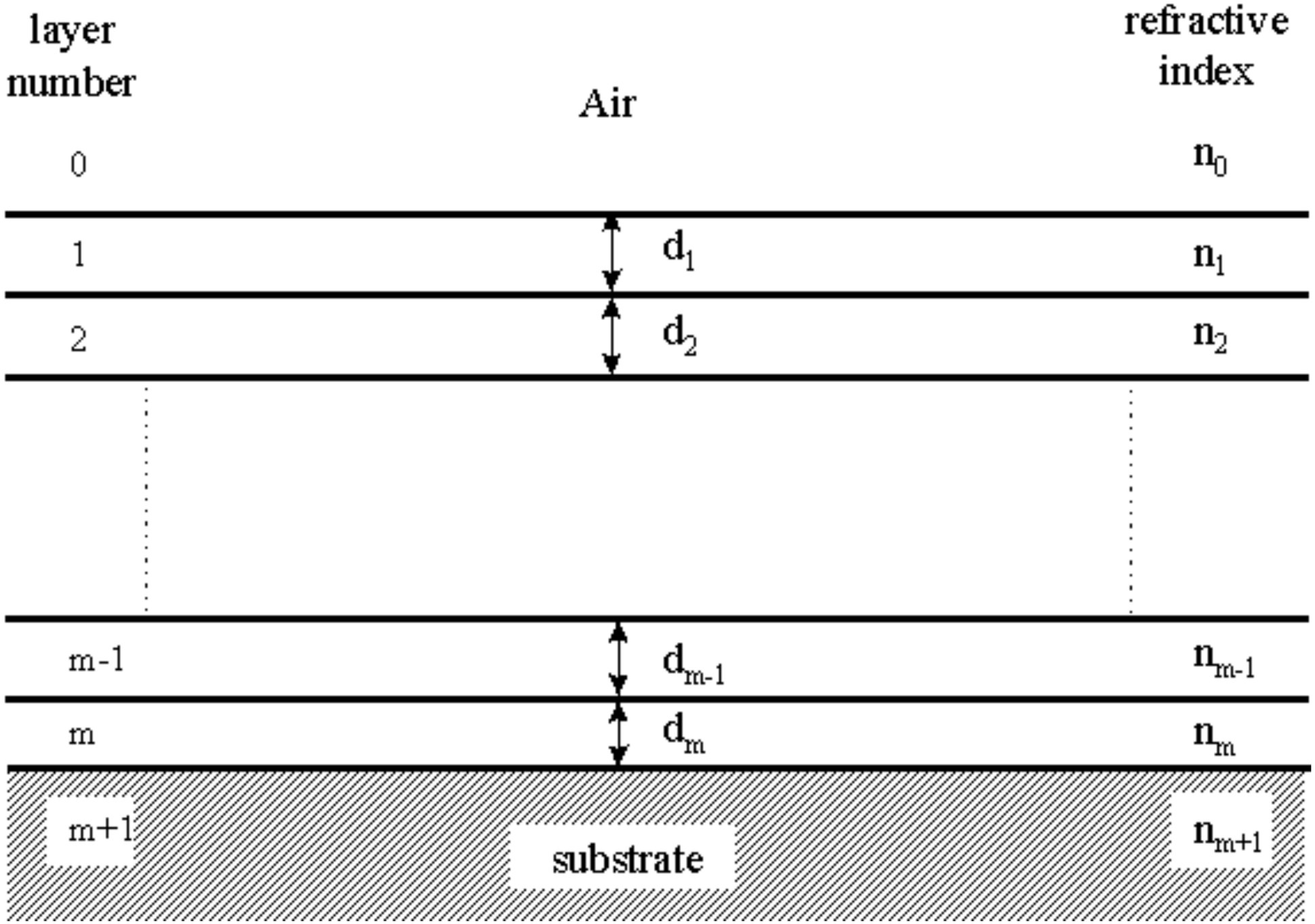

The reflection coefficient for the sample is calculated by firstly considering the coefficient between the substrate and the bottom layer, $r_{m,m+1}$, *i.e.* between the $(m+1)^{th}$ and m^{th} layers

$$r_{j,j+1} = \frac{n_j \sin\theta - n_{j+1} \sin\theta_{j+1}}{n_j \sin\theta + n_{j+1} \sin\theta_{j+1}}$$

The reflectivity coefficient between the (m-1)th and m^{th} is then given by:

$$r'_{m-1,m} = \frac{r_{m-1,m} - r_{m,m+1}\exp(2i\beta_m)}{r_{m-1,m} + r_{m,m+1}\exp(2i\beta_m)}$$

A phase factor, β_m, has also been introduced and represents an optical path length term for the mth layer, such that

$$\beta_m = (2\pi/\lambda) n_m d_m \sin\theta$$

where n_m and d_m are the refractive index and thickness respectively of layer m

This approach of calculating reflectivity is exact but extending it to multilayers is cumbersome.

A more general solution widely used is the **OPTICAL MATRIX METHOD** (Abeles).

$$c_m = \begin{bmatrix} \cos\beta_m & -(i/\kappa_m)\sin\beta_m \\ -i\kappa_m \sin\beta_m & \cos\beta_m \end{bmatrix}$$

An overall sample matrix is then defined as the product of the individual matrices:

$$M = \prod_{m=0}^{m} c_m = \begin{bmatrix} M_{11} & M_{12} \\ M_{21} & M_{22} \end{bmatrix}$$

The reflectivity is simply related to the matrix elements from M by:

$$R = \left| \frac{(M_{11} + M_{12}k_{m+1})k_0 - (M_{21} + M_{22})k_{m+1}}{(M_{11} + M_{12}k_{m+1})k_0 + (M_{21} + M_{22})k_{m+1}} \right|^2$$

where m+1 denotes the substrate and 0 the air

DATA ANALYSIS

Routine analysis of reflectivity data would ideally be solved by direct inversion of experimental data into either scattering length density, *Nb(z)*, or even volume fraction, f(z), profiles.

Generally, this cannot be achieved due to the loss of phase information, making this closely related to the phaseless Fourier problem.

Fitting data

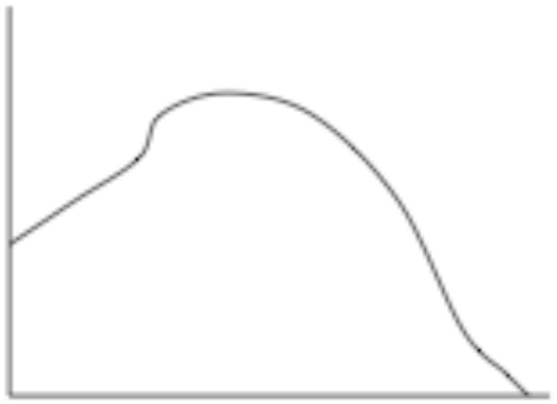

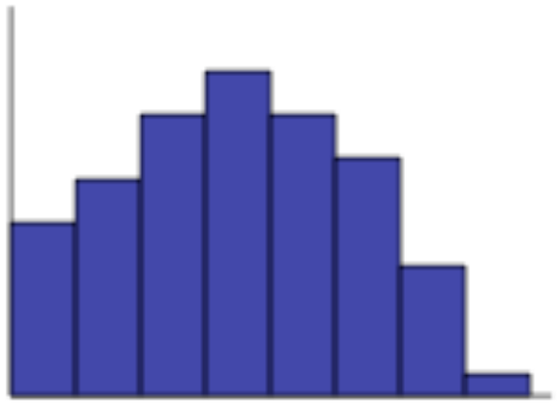

Model

Layers

Calculated reflectivity

Goodness of fit (χ^2)

Best fit

New parameters

Data (+errors)

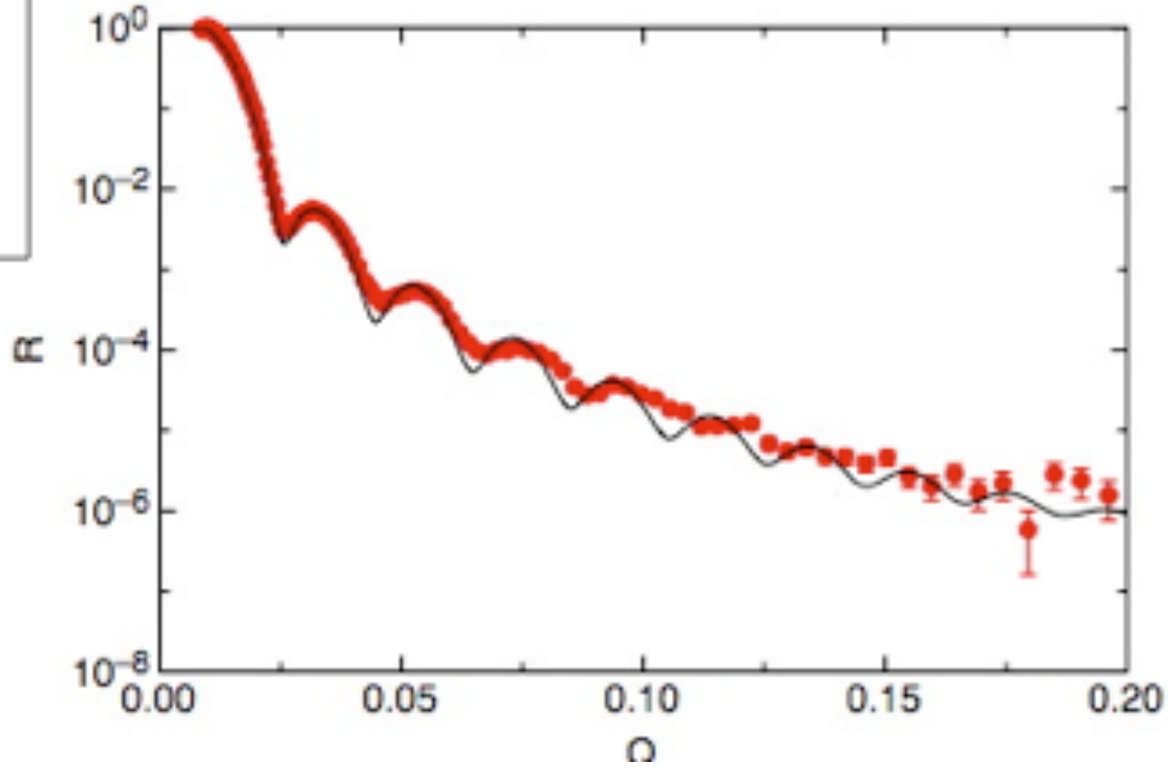

Courtesy R. Jones

Contrast variation

More than one model of $N_b(z)$ may give the same reflectivity profile – phase information is lost

Measurement with multiple ‘contrasts’ normally resolves ambiguity

Physical knowledge of system may define a unique model

Data modelling

Contrast variation
Multiple Contrasts

Courtesy of R. K. Thomas
http://rkt.chem.ox.ac.uk/techniques/nrmain.html

The Goal of Reflectivity Measurements Is to Infer a Density Profile Perpendicular to a Flat Interface

In general the results are not unique, but independent knowledge of the system often makes them very reliable

Frequently, layer models are used to fit the data

Advantages of neutrons include:

– Contrast variation (using H and D, for example)
– Low absorption –probe buried interfaces, solid/liquid interfaces etc
– Non-destructive
– Sensitive to magnetism
– Thickness length scale <5 Å – 5000 Å

- Issues include:

– Generally no unique solution for the SLD profile (use prior knowledge)
– Large samples (~10 cm^2) with good scattering contrast are needed

Some useful references:

- V. F. Sears 'Neutron Optics', Oxford Press, Oxford (1989)
- Lekner J 1987 in: "*Theory of Reflection*" Martinus Nijhoff Dordrecht
- Born M and Wolfe E 1989 in: "*Principles of Optics*" Pergamon Press Eds. Oxford
- Penfold J and Thomas R K 1990 *J. Phys. Condens. Matter* **2** 1369
- Russell T. P. 1990 *Mat. Sci. Rep.* **5** 171
- Felcher G P 1981 *Phys. Rev. B* **24** 1995
- Sinha S K, Sirota E B, Garoff S and Stanley H B 1998 *Phys. Rev. B* **38** 2297
- Zhou X-L and Chen S-H 1995 *Phys. Rep.* **257** 223
- W. Williams 'Polarized Neutrons' , Oxford Press, Oxford (1989)
- Névot L and Croce P 1990 *Rev. de Phys. Appl.* **15** 761
- Daillant J and Gibaud A 1999 in:

"*X-ray and Neutron Reflectivity: Principles and Applications*" Springer Eds.

- Heavens O S 1955 in: "*Optical Properties of Thin Films*", Butterworths Eds. London

Web-sites:

http://www.mrl.ucsb.edu/~pynn/ (Roger Pynn)
http://www.pcl.ox.ac.uk/~rkt/ (Bob Thomas)

***Ref for this talk*:** Cubitt R. and Fragneto G. 2002 "*Neutron Reflection: Principles and Examples of Applications*", in *Scattering*, p. 1198-1208, Academic Press eds.

Basic Principles of Neutron Reflection Measurement

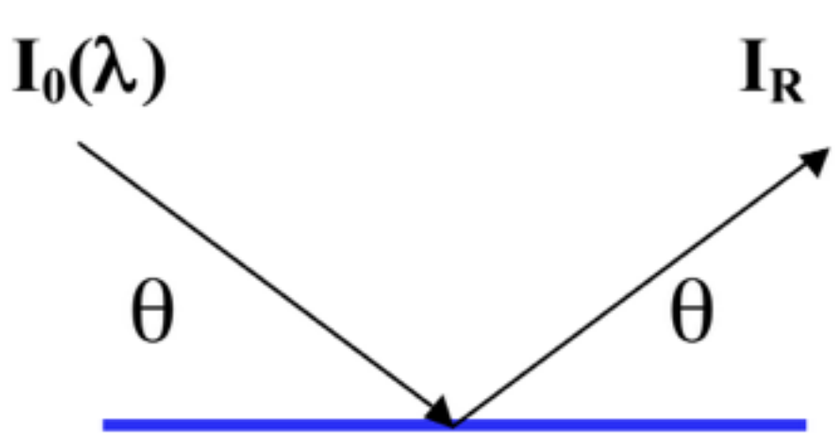

Reflected beam deflected: 2θ

Reflectivity

$R(\theta, \lambda) = I_R/I_0(\lambda)$

Momentum transfer

$q = (4\pi/\lambda) \sin \theta$

Measurement can be done by:

varying θ at constant λ

measuring the TOF ($\Rightarrow\lambda$) at constant θ

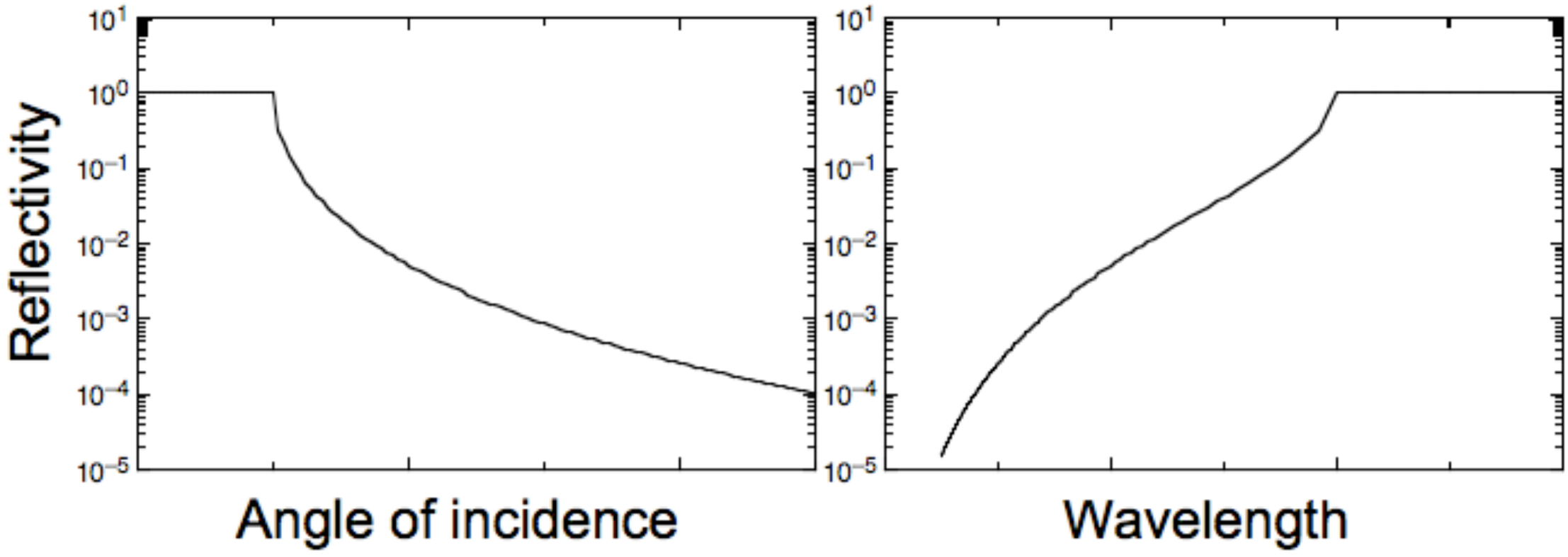

For the same resolution TOF is less efficient (flux at min and max λ up to two orders of magnitude smaller than at peak flux) *but* better for kinetics

Classes of Interface

Air/Liquid Air/Solid	Samples can be limited by smoothness and by flatness (capillary waves amplitude is 0.3 nm)
Liquid/Solid Solid/Solid Liquid/Liquid	Constrained by passage through one phase. Signal can be limited by absorption or scattering background

Neutron reflection is an ideal tool to study buried interfaces because neutrons can penetrate solids (i.e. in solid/liquid systems), are not destructive, allow to gain information in the fraction of nanometer scale

Fate of a Neutron at an Interface

- Reflected
- Scattered/Diffracted from surface
- Absorbed
- Scattered from bulk (either side of surface)
- Other accidents

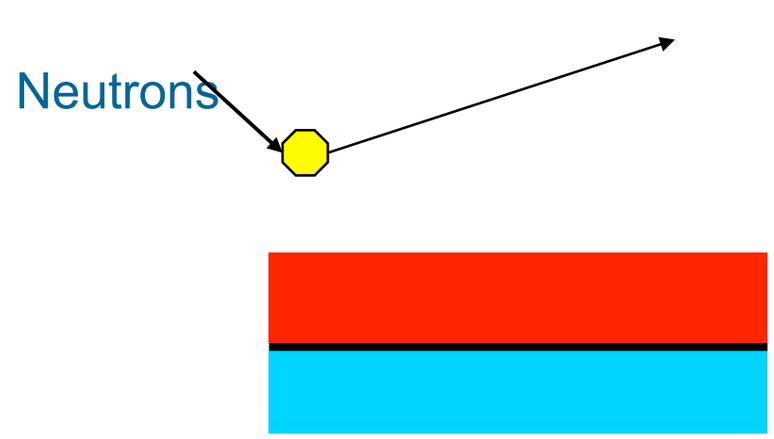

Practical Issues

- Reflectivity drops quickly with increasing Q (or angle). Signal is easily ‘lost’ in background.

- To observe fringes it will be necessary to measure over an appropriate range of Q and to have sufficient resolution (ΔQ small enough).

$$\left(\frac{\Delta Q}{Q}\right)^2 = \left(\frac{\Delta\lambda}{\lambda}\right)^2 + \left(\frac{\Delta\theta}{\theta}\right)^2$$

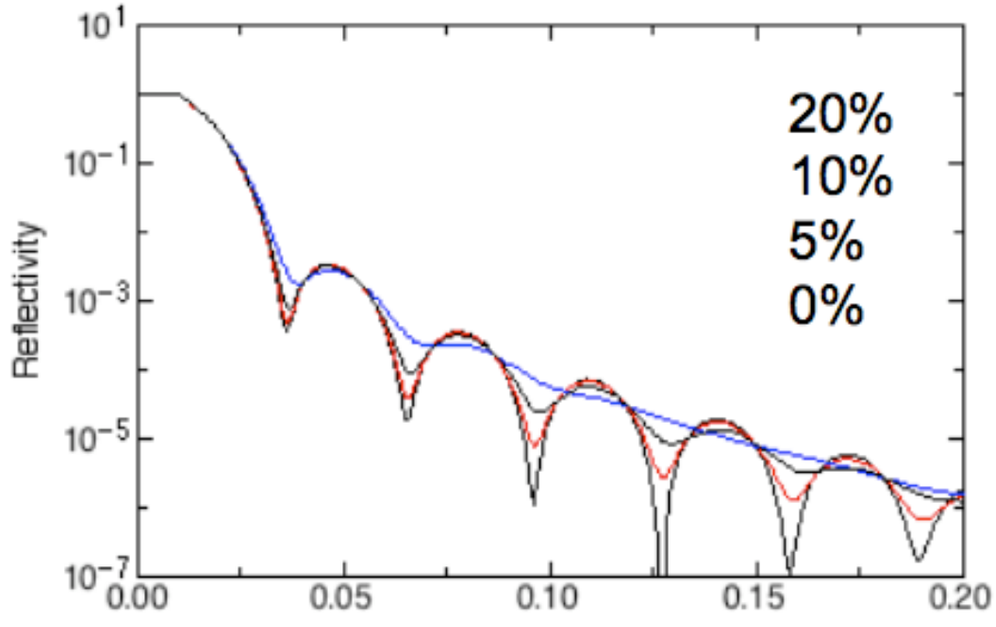

- Attenuation by reduced transmission (caused by scattering or absorption) may be significant

Sources of background:

Electronics (negligible)

Scattering from other parts of the instrument (can be efficiently shielded with B4C, Cd, etc.)

Sample:

off-specular from roughness, inhomogeneities (can be measured and removed)

incoherent scattering (liquids)

*The **coherence length** is essentially the separation distance on the specimen from which neutrons or x-rays emerging will interfere coherently at the detector*

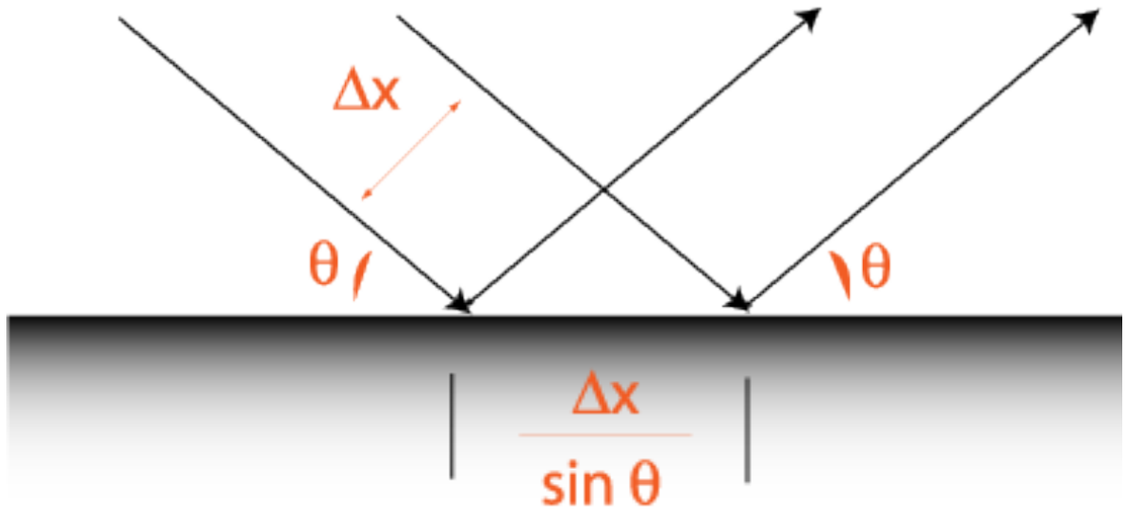

0.1 nm neutrons or x-rays
source divergence 0.005 deg

$\Delta k \Delta x = 2\pi$ $\Delta x = 600$ nm

$\theta = 1$
coherence length~30000 nm

The coherence length will depend on factors including:

- wavelength of the incident radiation
- angle of incidence
- and beam divergence (instrument dependent)

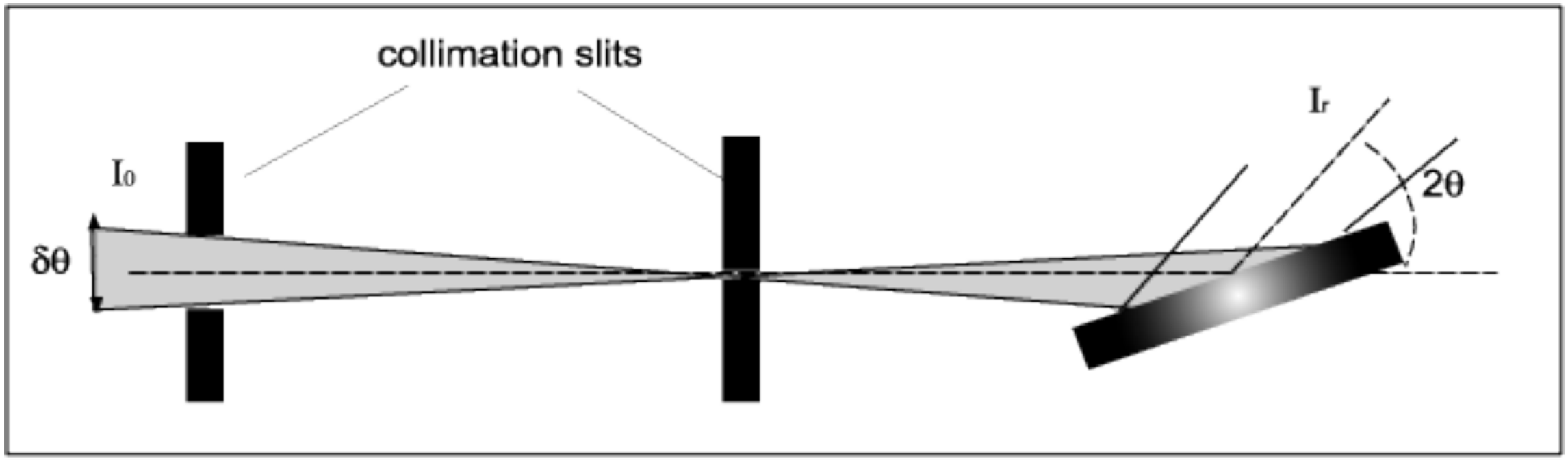

Usually a slit defines the incident beam with good resolution in one dimension and poor normal to this

Inhomogeneous sample

lateral coherence length of wave>>dimensions of regions A and B

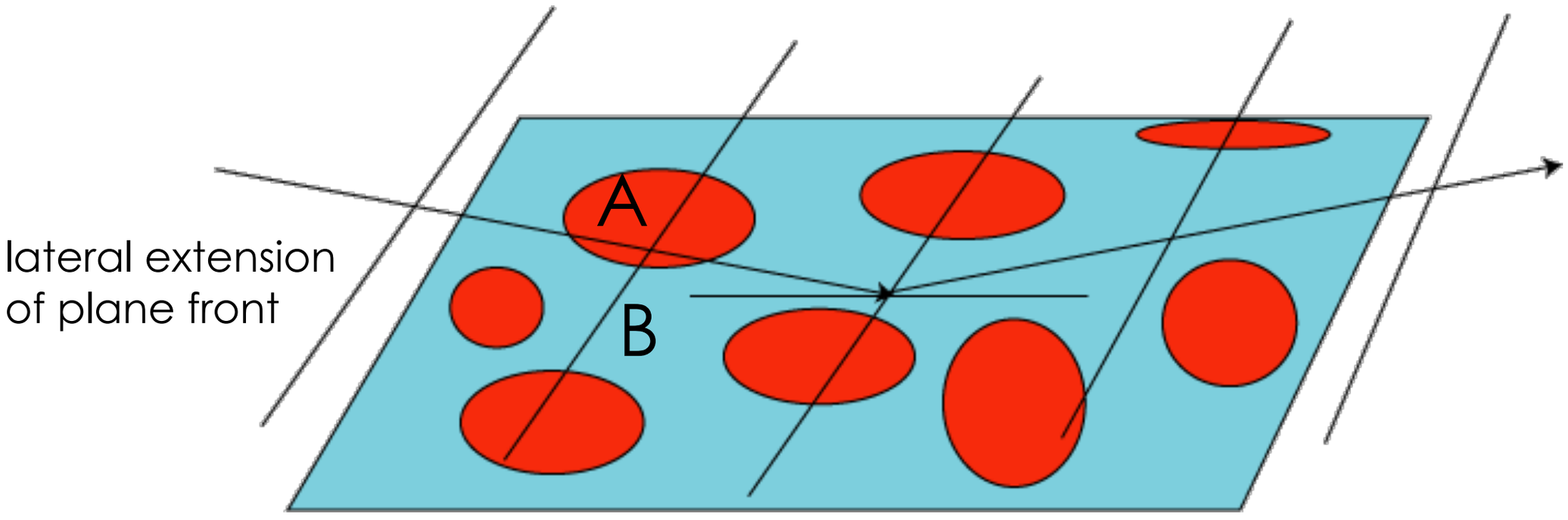

$$|r|^2_{observed} = \left| \frac{4\pi}{iq} \int_0^L \Psi(z)\left[f_A N b_A(z) + f_B N b_B(z) \Psi_0 dz \right] \right|^2$$

Inhomogeneous sample

lateral coherence length of wave<<dimensions of regions A and B

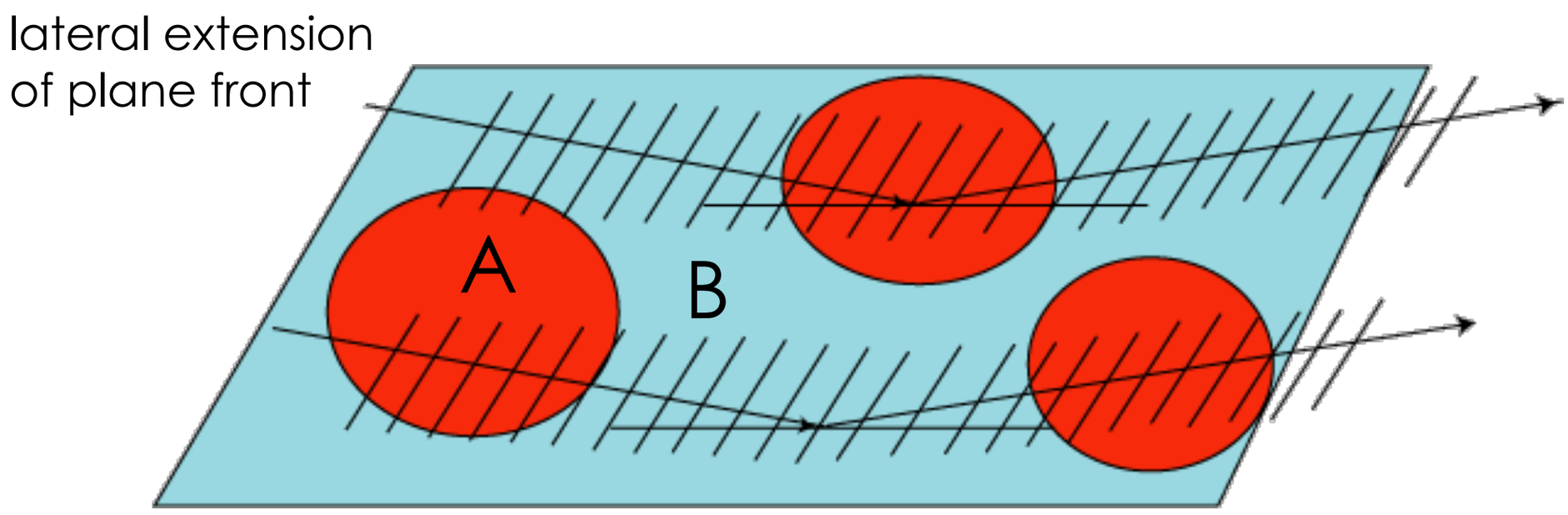

$$|r|^2_{observed} = f_A|r|^2_A + f_B|r|^2_B$$

Rafts in membranes: can we see them with reflectometry?

Lateral coherence length of neutron beam ~10*th* microns

>>

Domain size ~100*th* nanometers

Signal will come from the averaged structure on the surface

Need to use GISANS

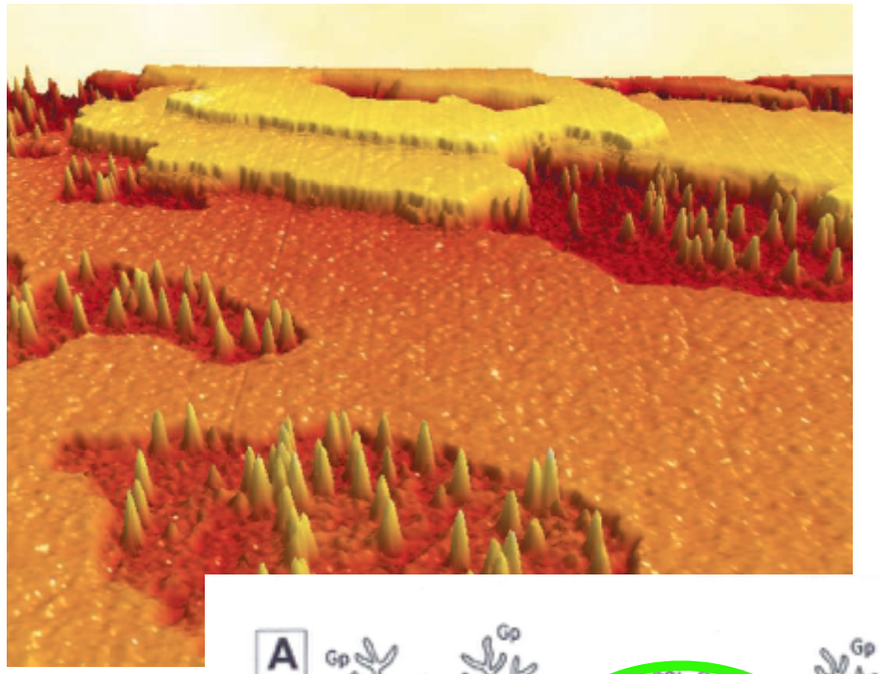

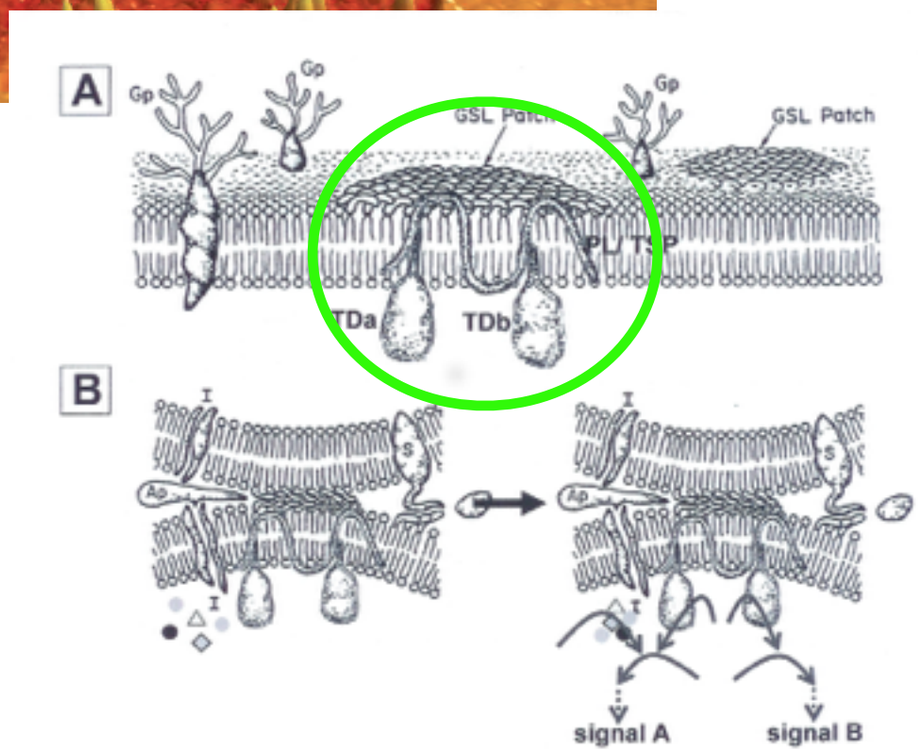

Example of reflectometer TOF mode:

The reflectometer FIGARO at the ILL

Fluid Interfaces Grazing Angles ReflectOmeter

Figaro

Fluid Interfaces Grazing Angles Reflectometer

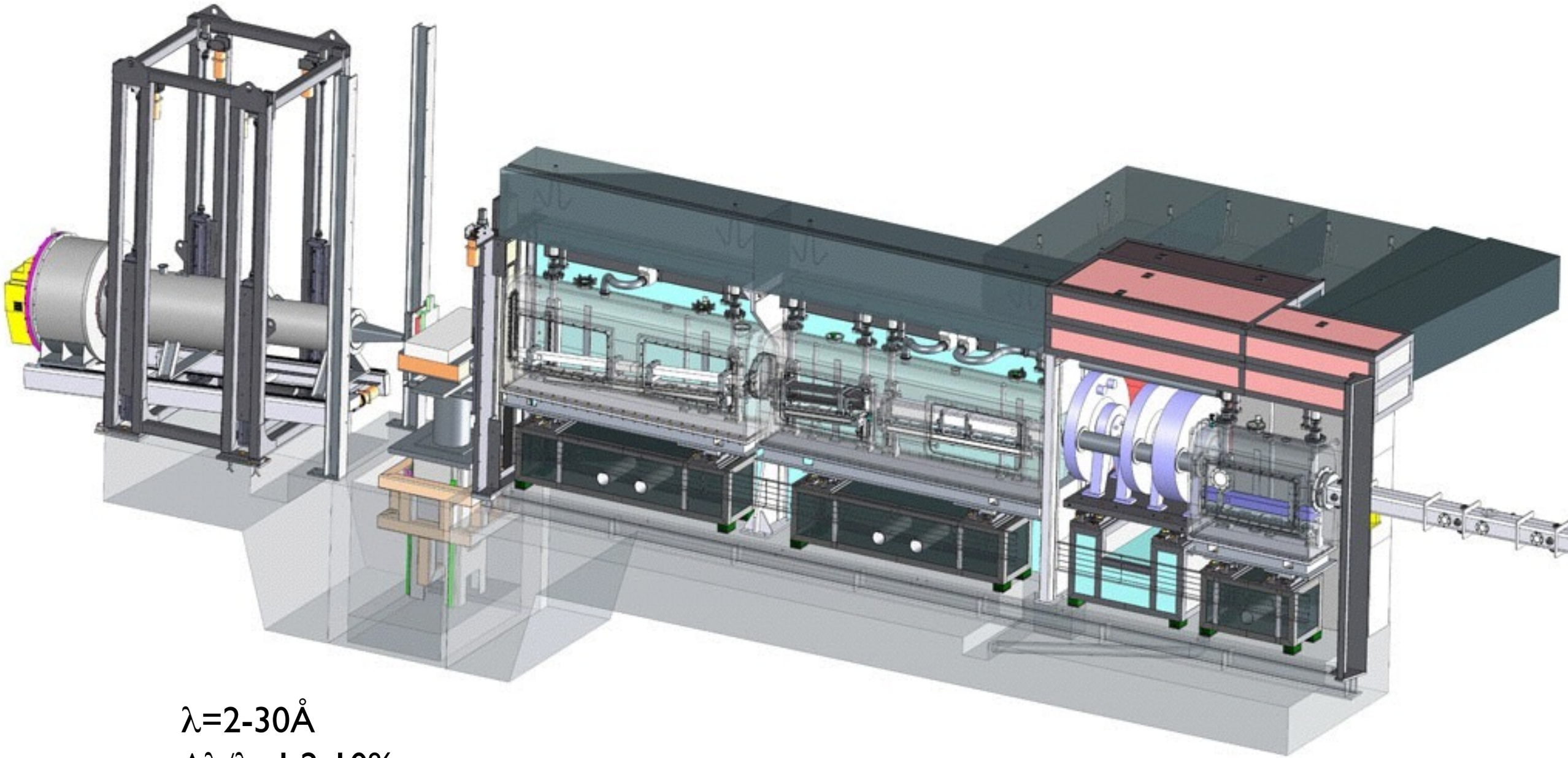

λ=2-30Å

Δλ/λ 1.2-10%

Beam strikes both sides of interfaces

Figaro

Fluid Interfaces Grazing Angles Reflectometer

Loose resolution allows high flux and measurements of thin films and liquid/ liquid interfaces

$$\frac{\delta t}{t} = \frac{D'}{D} + \frac{\phi}{2\pi} \frac{q}{q_{min}}$$

Δλ/λ	Disc Numbers	Disc separation (mm)
10 %	1 & 4	800
8.8%	2 & 4	700
4.2%	1 & 3	350
3.0%	2 & 3	250
5.4%	3 & 4	450

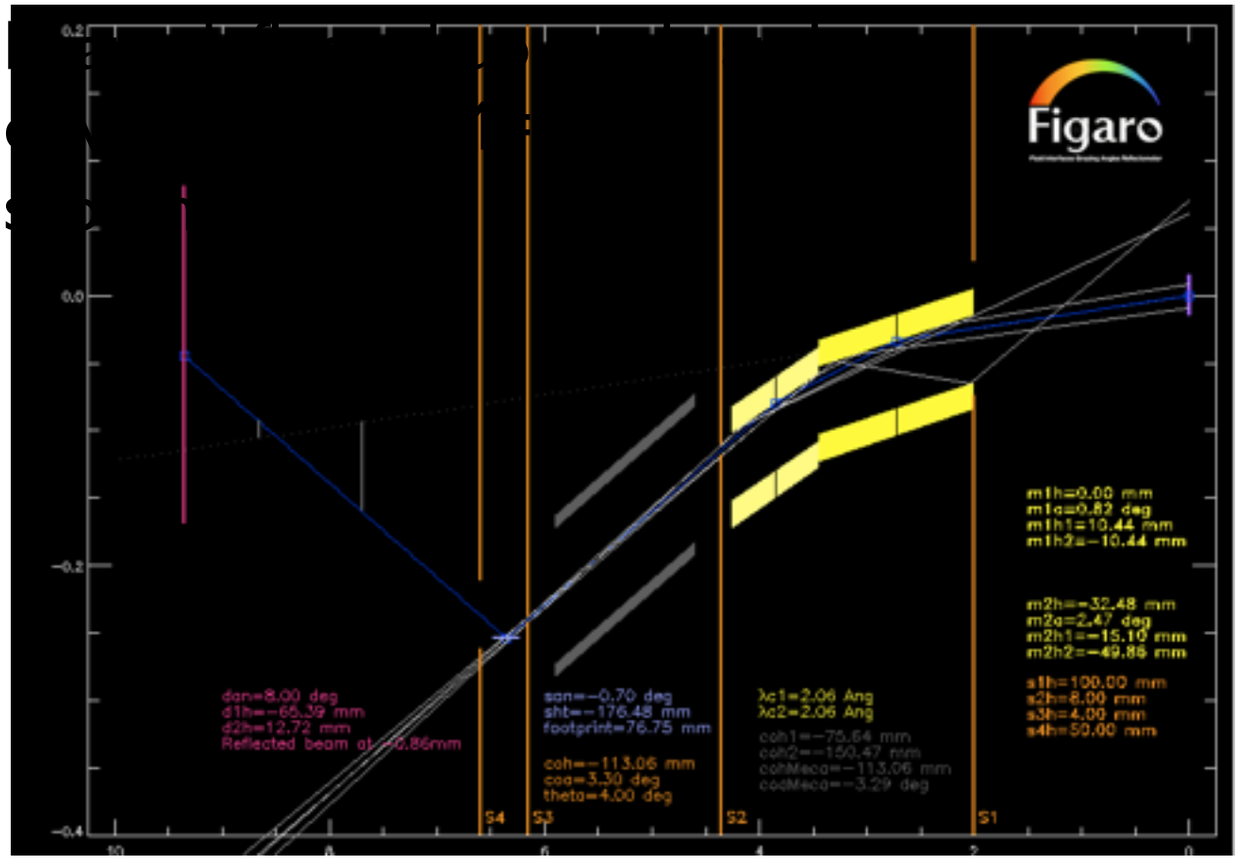
Figaro
dan=8.00 deg
d1h=-65.39 mm
d2h=12.72 mm
Reflected beam at -0.86mm
san=-0.70 deg
sht=-176.48 mm
footprint=76.75 mm
coh=-113.06 mm
coa=3.30 deg
theta=4.00 deg
λc1=2.06 Ang
λc2=2.06 Ang
coh1=-75.64 mm
coh2=-150.47 mm
cohMeca=-113.06 mm
coaMeca=-3.29 deg
m1h=0.00 mm
m1a=0.82 deg
m1h1=10.44 mm
m1h2=-10.44 mm
m2h=-32.48 mm
m2a=2.47 deg
m2h1=-15.10 mm
m2h2=-49.86 mm
s1h=100.00 mm
s2h=8.00 mm
s3h=4.00 mm
s4h=50.00 mm
S4
S3
S2
S1

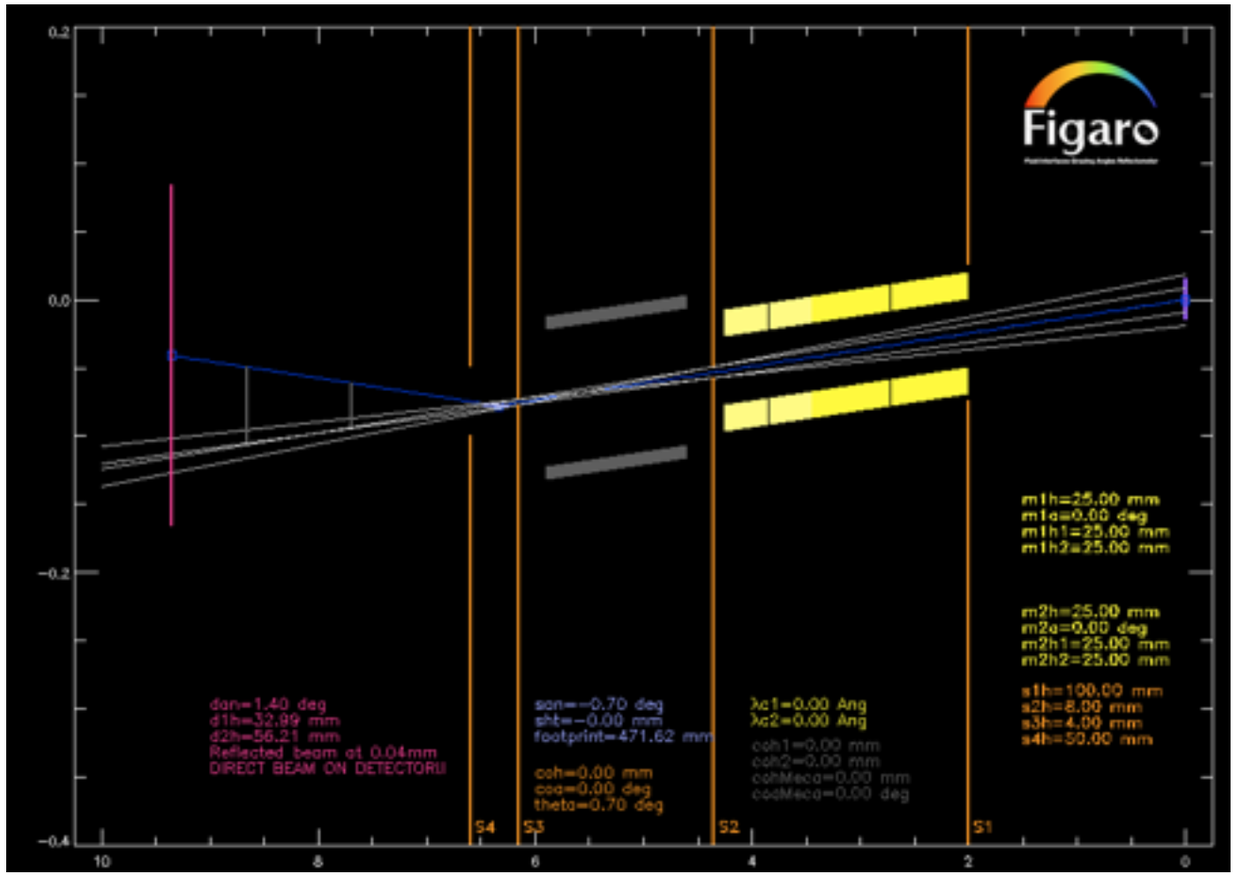
Figaro
dan=1.40 deg
d1h=32.99 mm
d2h=56.21 mm
Reflected beam at 0.04mm
DIRECT BEAM ON DETECTOR!!
san=-0.70 deg
sht=-0.00 mm
footprint=471.62 mm
coh=0.00 mm
coa=0.00 deg
theta=0.70 deg
λc1=0.00 Ang
λc2=0.00 Ang
coh1=0.00 mm
coh2=0.00 mm
cohMeca=0.00 mm
coaMeca=0.00 deg
m1h=25.00 mm
m1a=0.00 deg
m1h1=25.00 mm
m1h2=25.00 mm
m2h=25.00 mm
m2a=0.00 deg
m2h1=25.00 mm
m2h2=25.00 mm
s1h=100.00 mm
s2h=8.00 mm
s3h=4.00 mm
s4h=50.00 mm
S4
S3
S2
S1

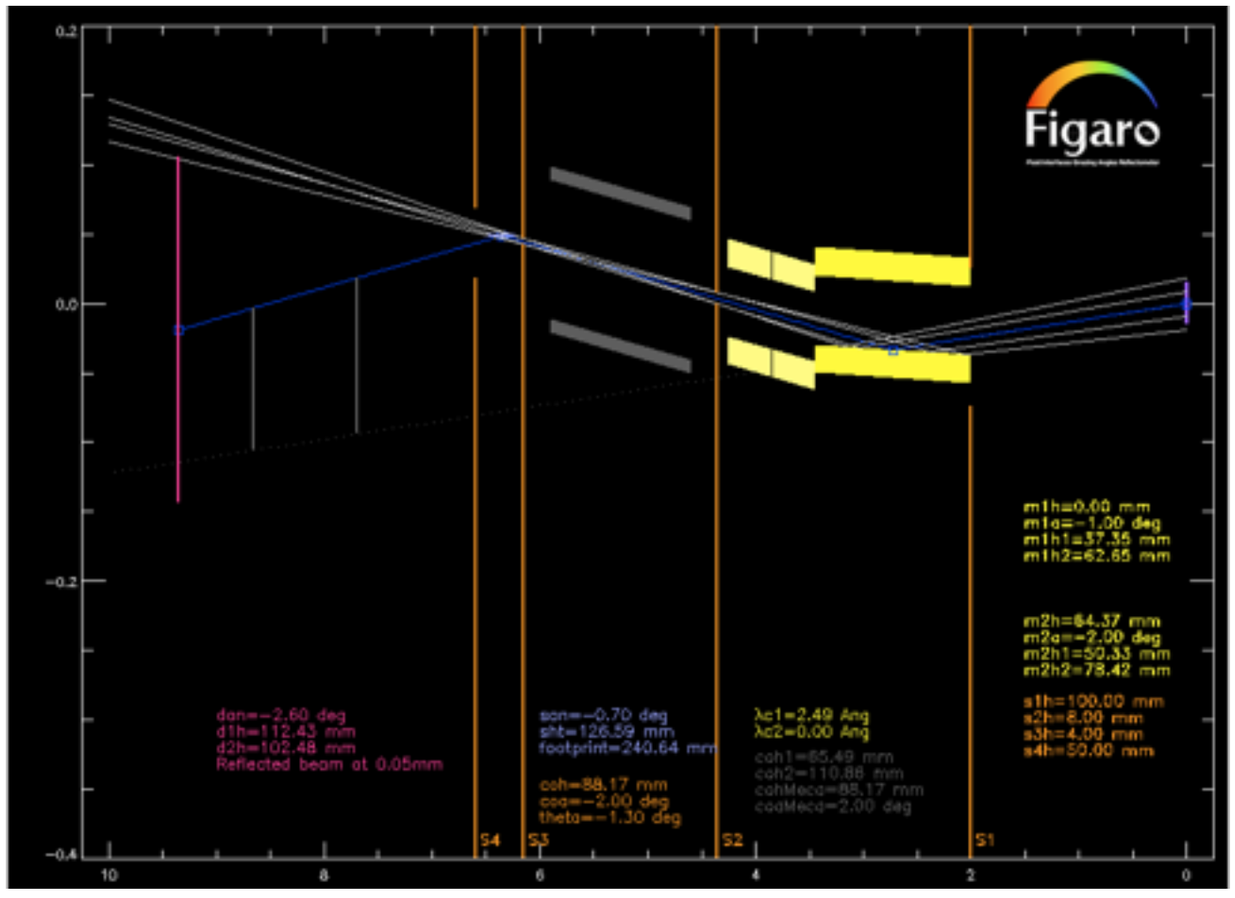
Figaro
dan=-2.60 deg
d1h=112.43 mm
d2h=102.48 mm
Reflected beam at 0.05mm
san=-0.70 deg
sht=126.59 mm
footprint=240.64 mm
coh=88.17 mm
coa=-2.00 deg
theta=-1.30 deg
λc1=2.49 Ang
λc2=0.00 Ang
coh1=65.49 mm
coh2=110.86 mm
cohMeca=88.17 mm
coaMeca=2.00 deg
m1h=0.00 mm
m1a=-1.00 deg
m1h1=37.35 mm
m1h2=62.65 mm
m2h=64.37 mm
m2a=-2.00 deg
m2h1=50.33 mm
m2h2=78.42 mm
s1h=100.00 mm
s2h=8.00 mm
s3h=4.00 mm
s4h=50.00 mm
S4
S3
S2
S1

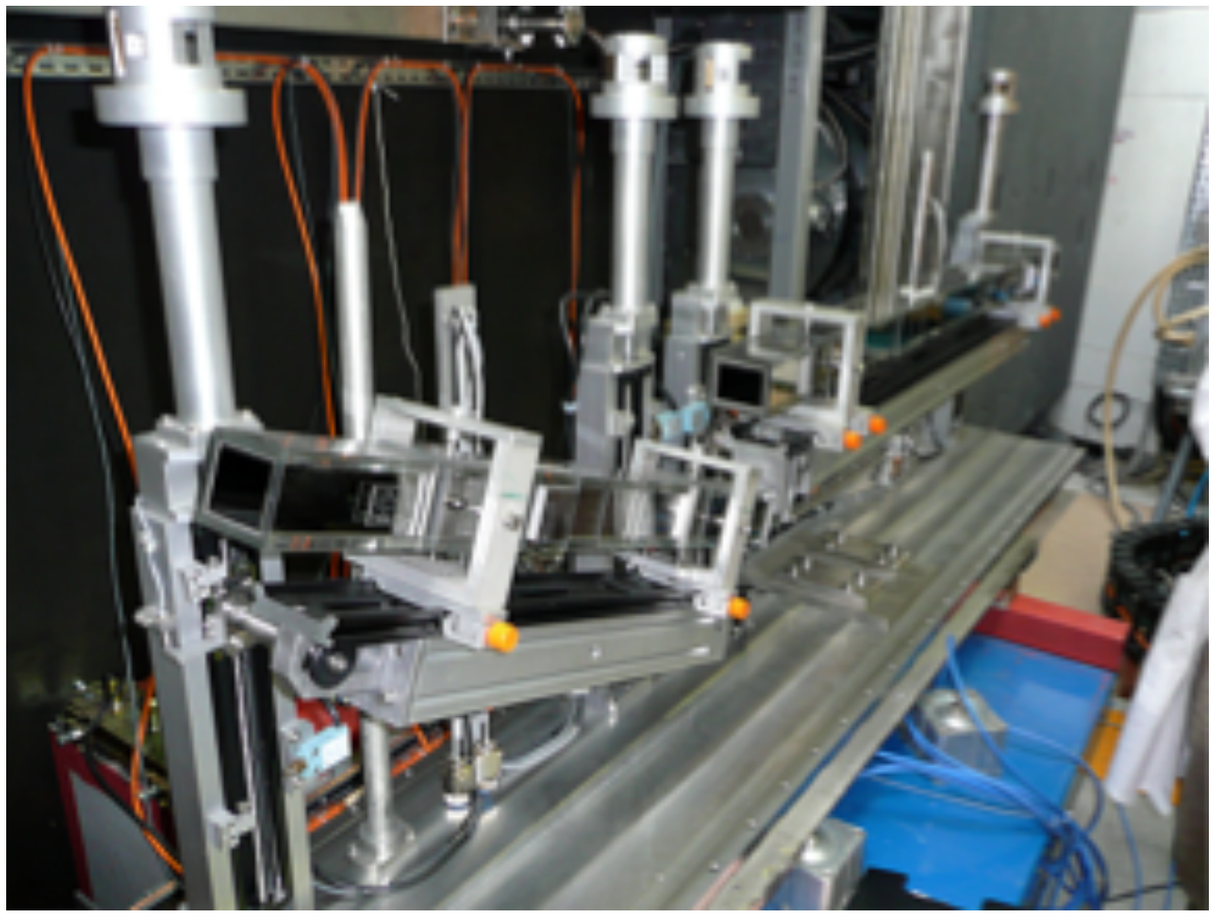

SAMPLE ENVIRONMENT

Adsorption troughs for adsorption from solution

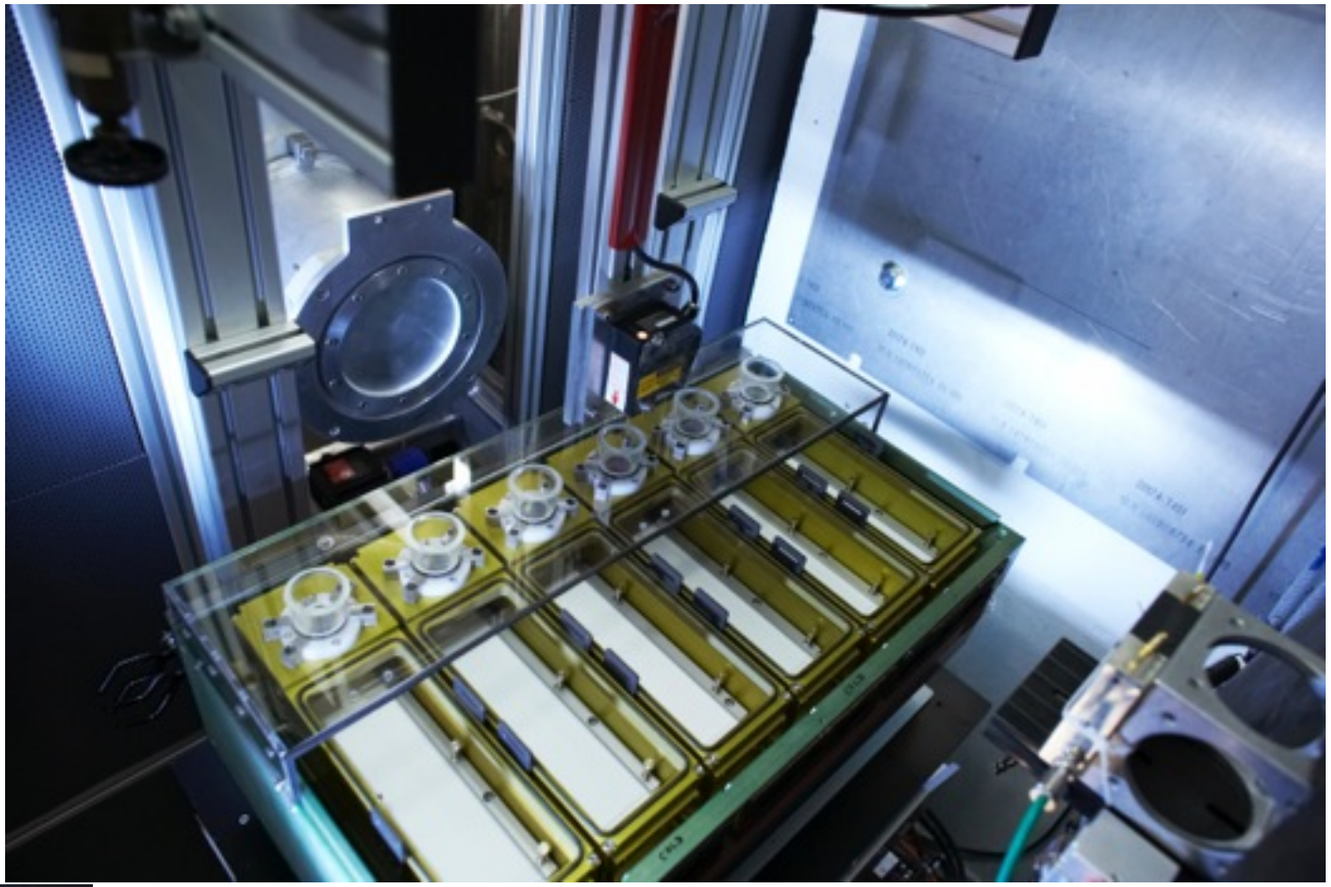

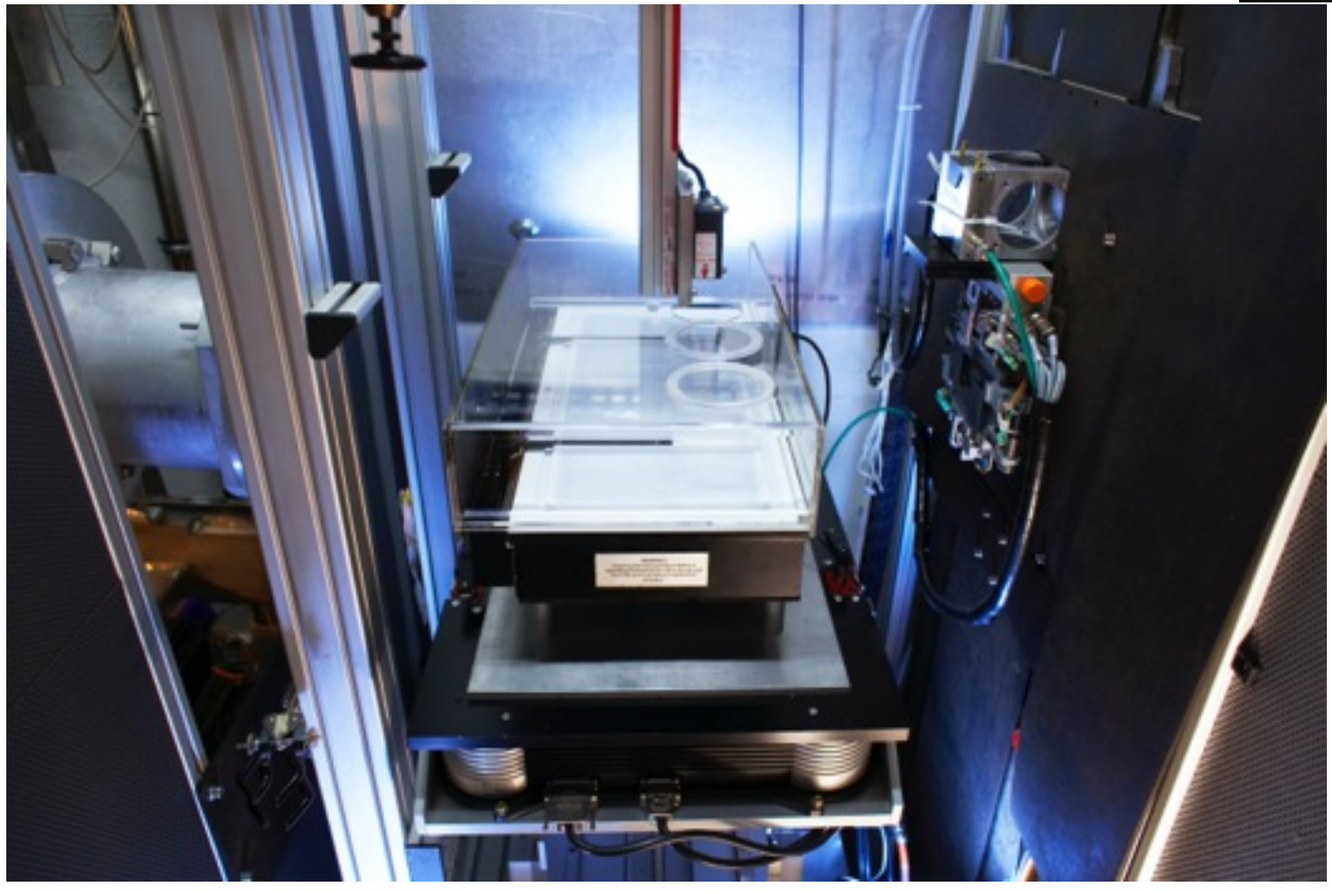

Langmuir trough for insoluble monolayers

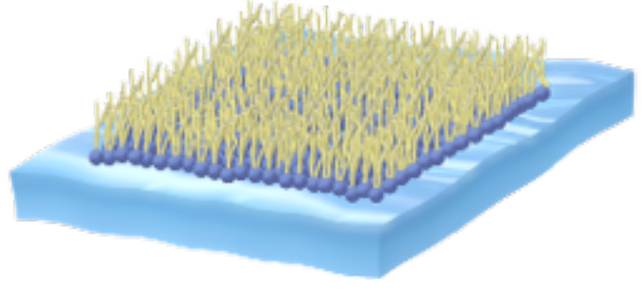

SAMPLE ENVIRONMENT

Solid/liquid cell for adsorption on surfaces

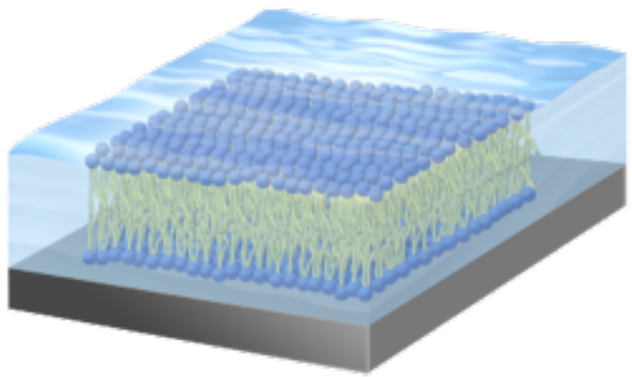

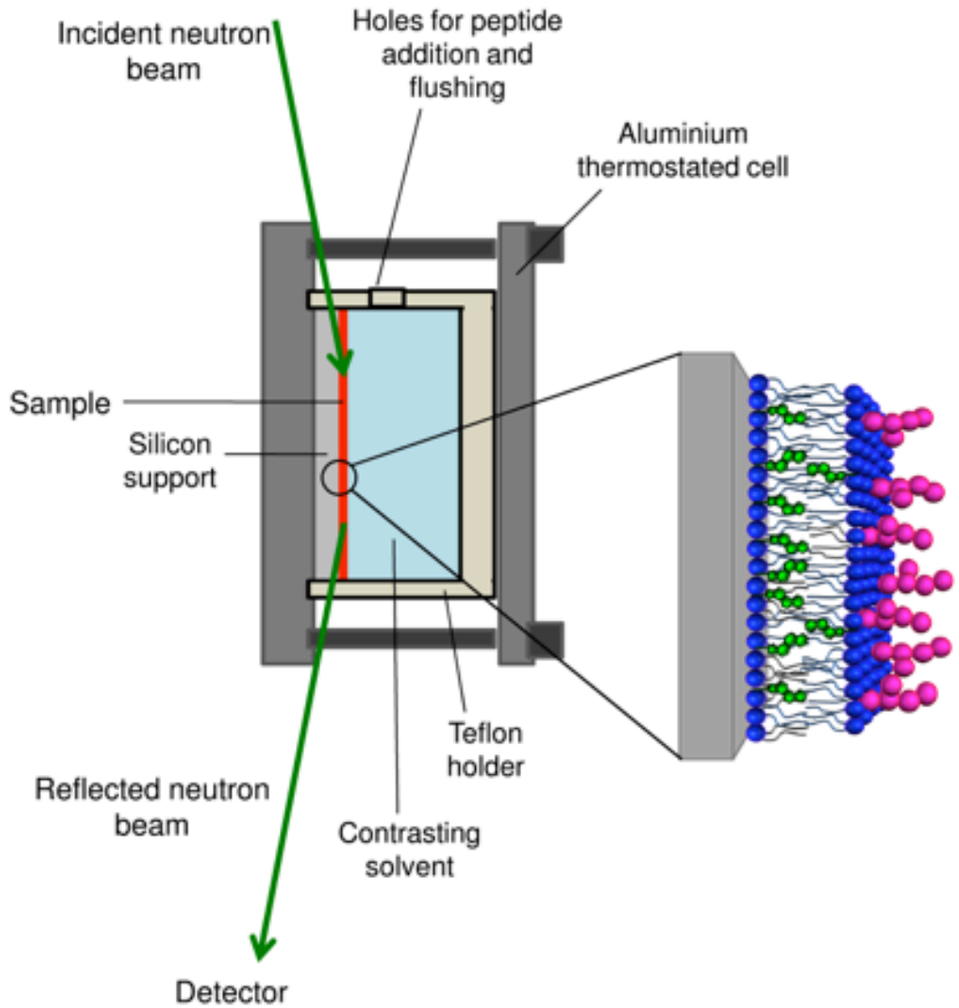

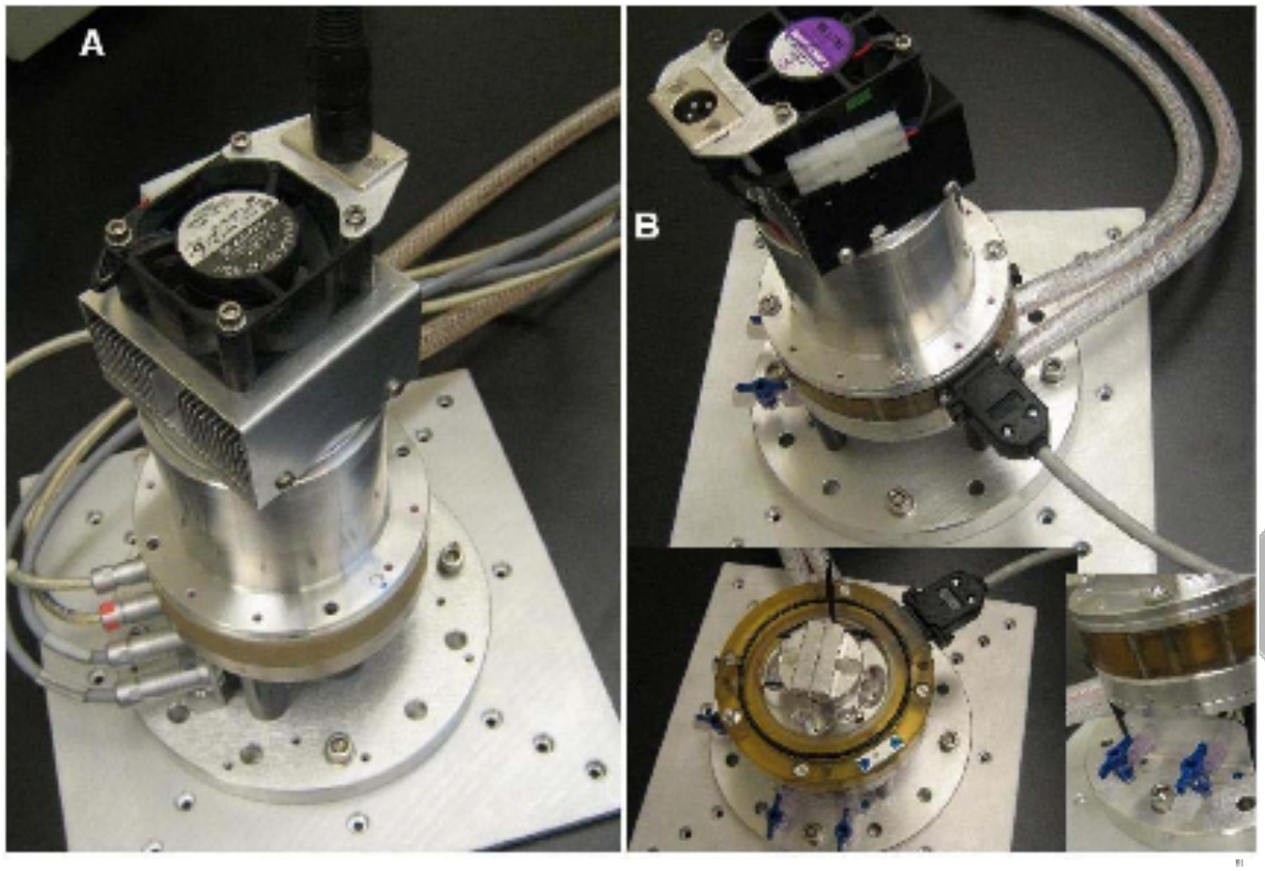

Humidity chamber

$r.h.=100p(T_w)/p(T_s)$

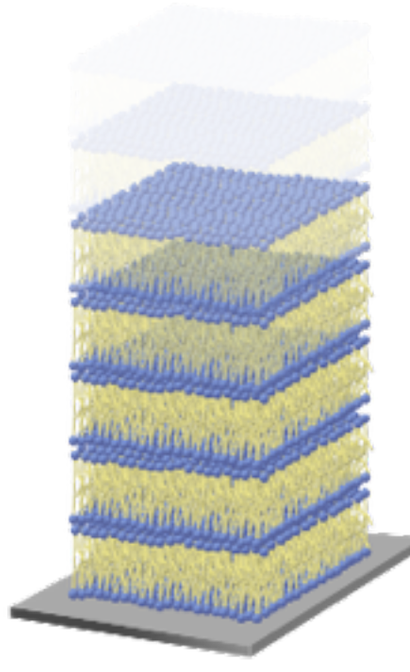

2-D DETECTOR: simultaneous access to off-specular/GISANS *(the latter after optimisation of instrument settings)*

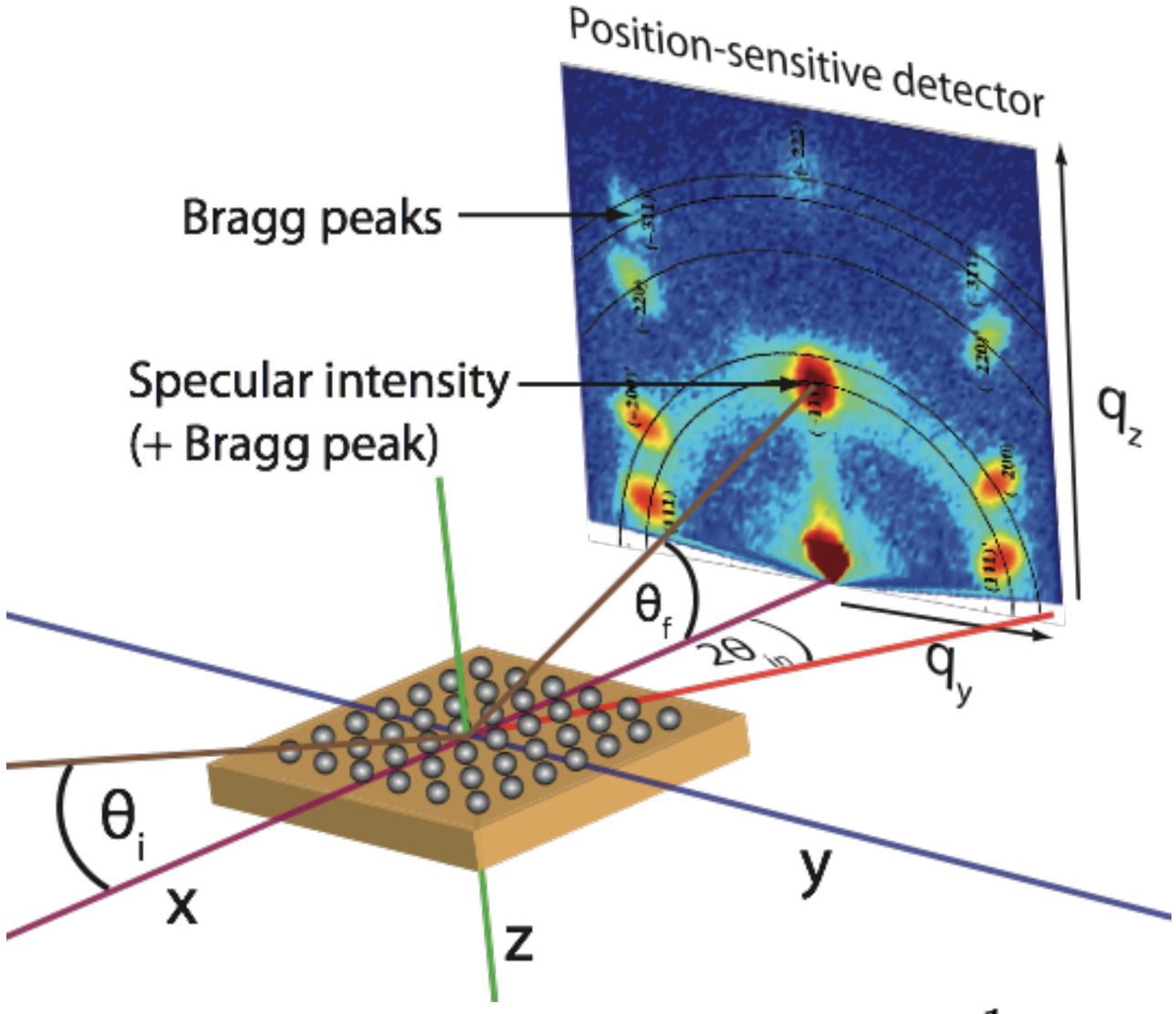

$$q_x = \frac{2\pi}{\lambda}(\cos\theta_f \cos 2\theta_{in} - \cos\theta_i)$$

$$q_y = \frac{2\pi}{\lambda}(\cos\theta_f \sin 2\theta_{in})$$

$$q_z = \frac{2\pi}{\lambda}(\sin\theta_i + \sin\theta_f)$$

$$10^{-5}\,\text{Å}^{-1} \leq q_x \leq 10^{-3}\,\text{Å}^{-1} \equiv 1 - 100\,\mu m$$

$$10^{-3}\,\text{Å}^{-1} \leq q_y \leq 10\,\text{Å}^{-1} \equiv 1 - 10000\,\text{Å}$$

$$10^{-3}\,\text{Å}^{-1} \leq q_z \leq 1\,\text{Å}^{-1} \equiv 10 - 10000\,\text{Å}$$

courtesy P. Gutfreund

Planning a Reflectivity Measurement

- **Simulation of reflectivity profiles is essential**

– Can you see the effect you want to see?

– What is the best substrate? Which materials should be deuterated?

- **If your sample involves free liquid surface you will need to use a reflectometer with a vertical scattering plane**

- **If you want to follow a changes with time (kinetics) better to use a time-of-flight instrument.**

- **Preparing good (i.e. low surface roughness) samples is key**

– Beware of large islands

- **Layer thicknesses between <10 Å and 5000 Å**

– But don't mix extremes of thickness

For a list of neutron reflectometers and programs to analyze the data:

http://material.fysik.uu.se/Group_members/adrian/reflect.htm#Instruments
by Adrian Rennie (Uppsala University)

Examples:

✤ Ganglioside/cholesterol pair **(V. Rondelli, L. Cantù, et al.)**

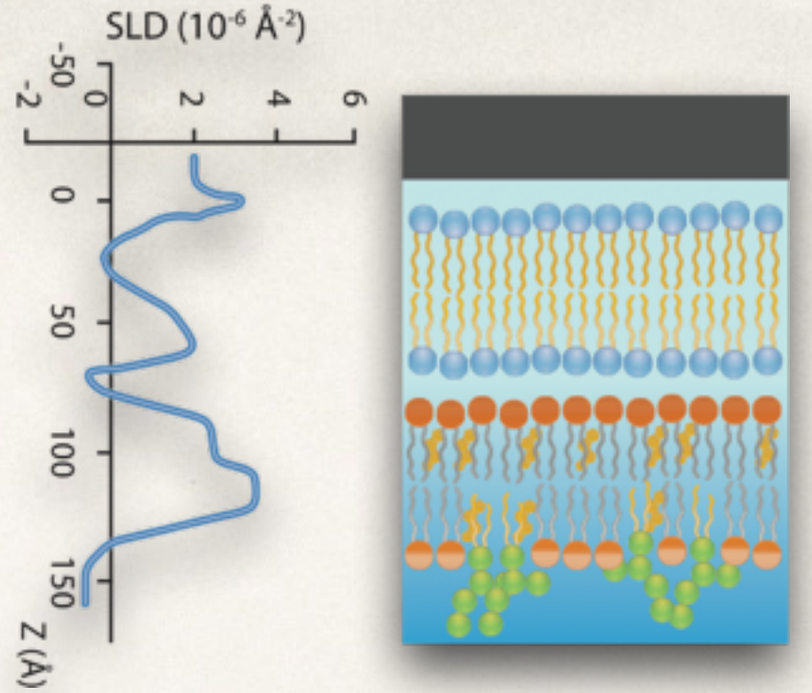

✤ Interaction of antibiotic with natural membranes **(A. de Ghellinck, H. Wacklin, M. Sferrazza, J. Jouhet, D-Lab, et al.)**

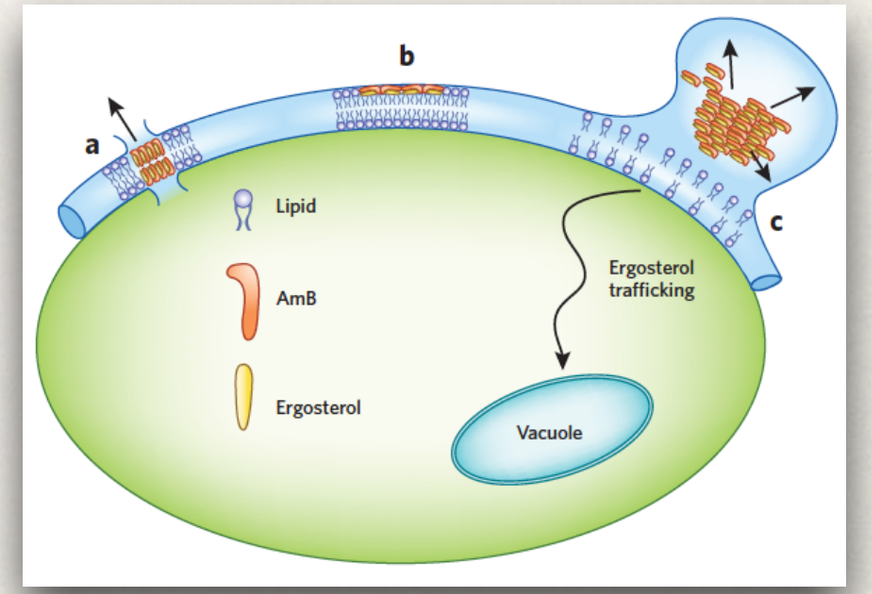

✤ Neutron reflectometry and deuteriation to probe density profiles of proteins adsorbed onto polymer brushes **(E. Schneck, A. Schollier, A. Halperin, M. Sferrazza, D-Lab)**

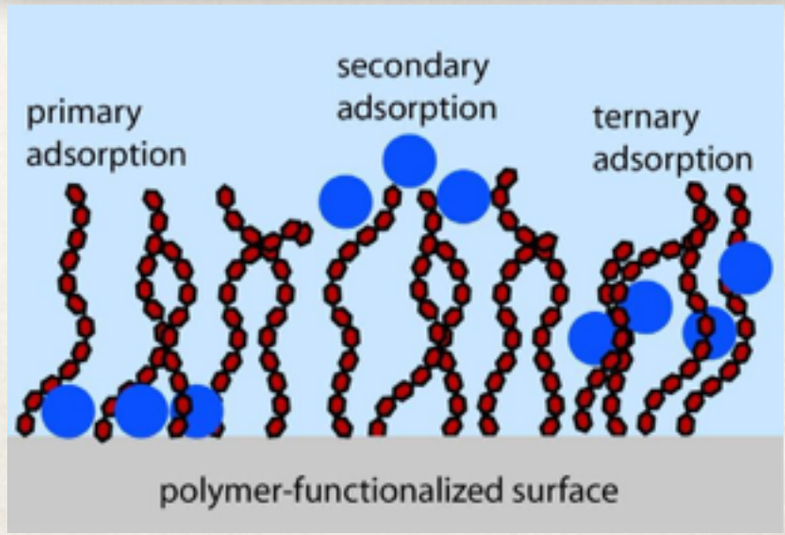

Examples:

✤ Ganglioside/cholesterol pair **(V. Rondelli, L. Cantù, et al.)**

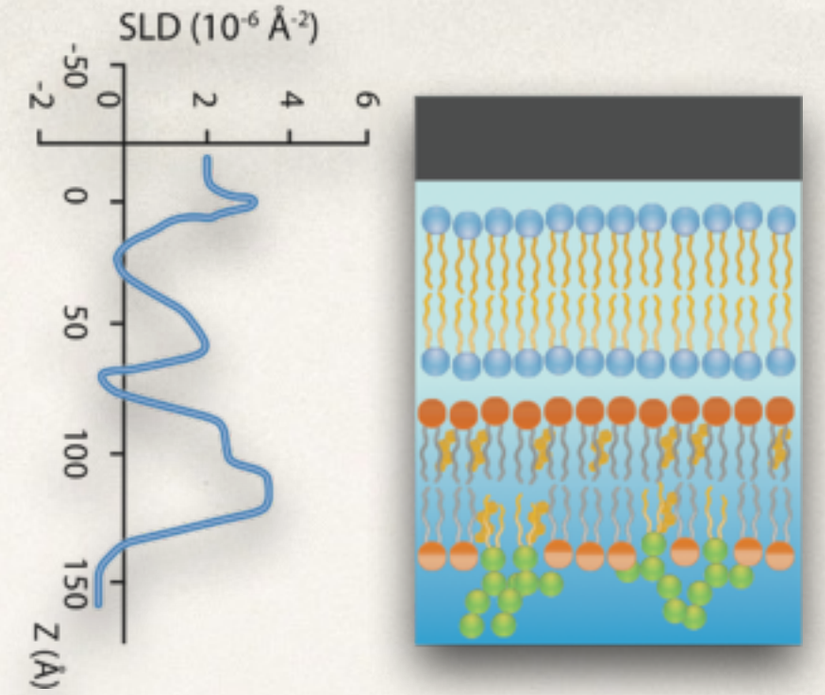

✤ Interaction of antibiotic with natural membranes **(A. de Ghellinck, H. Wacklin, M. Sferrazza, J. Jouhet, D-Lab)**

✤Neutron reflectometry and deuteriation to probe density profiles of proteins adsorbed onto polymer brushes **(E. Schneck, A. Schollier, A. Halperin, M. Sferrazza, D-Lab)**

Towards structural dynamics in complex biomimetic membranes

Valeria Rondelli, Laura Cantù, Elena Motta, Elena DelFavero, Paola Brocca, Sandro Sonnino

Università degli Studi di Milano

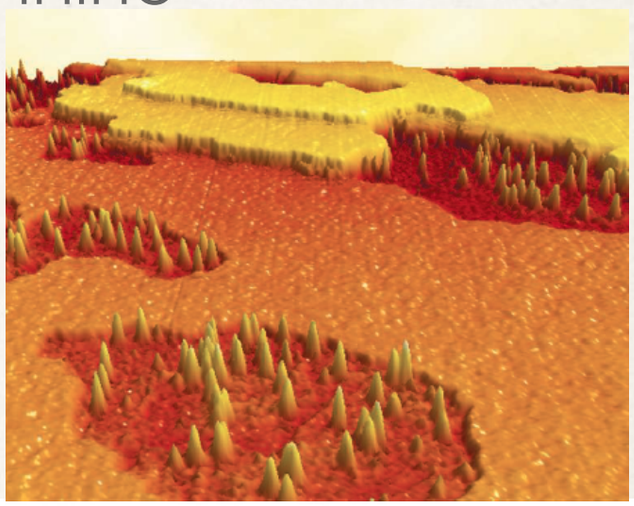

Phospholipid

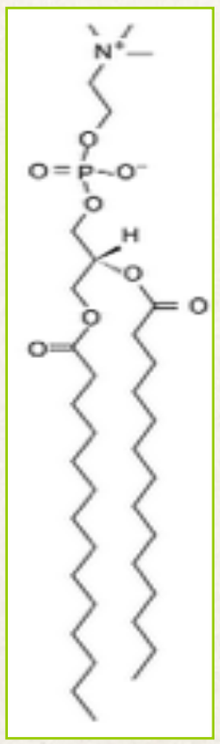

Cholesterol

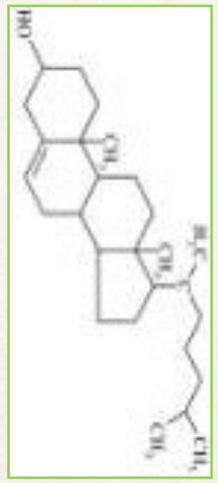

Glycolipid

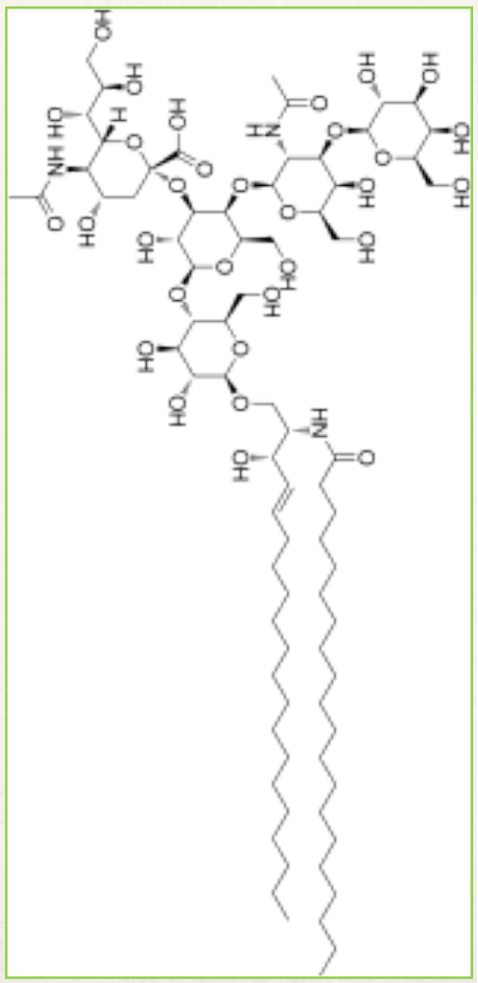

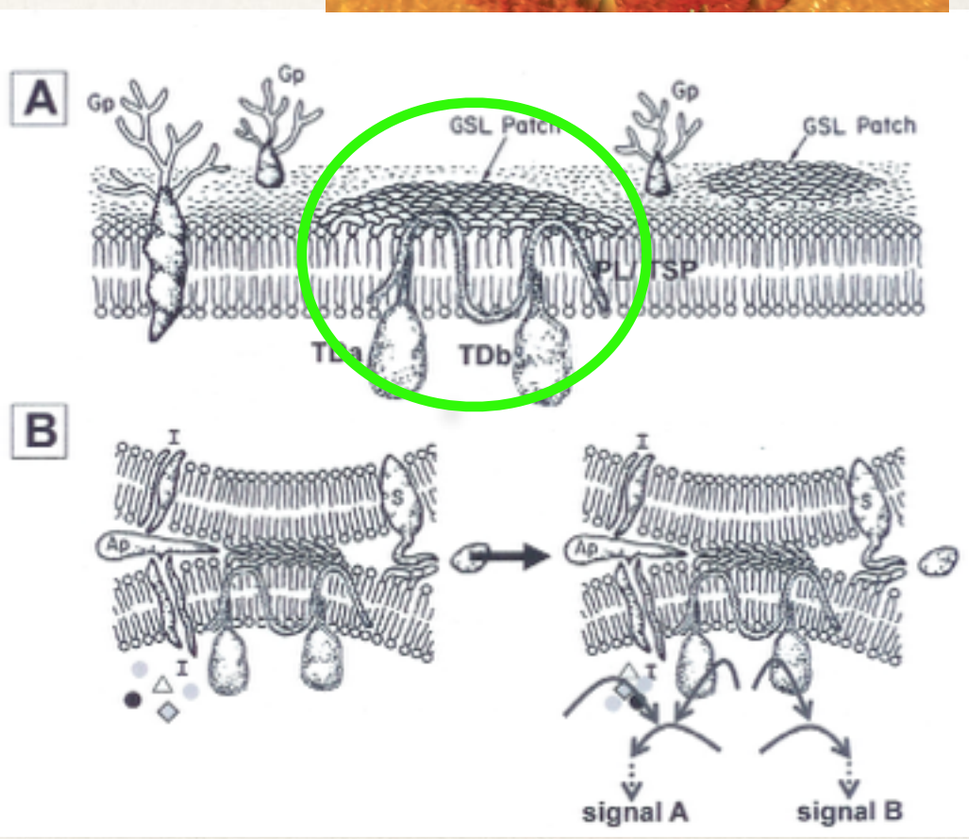

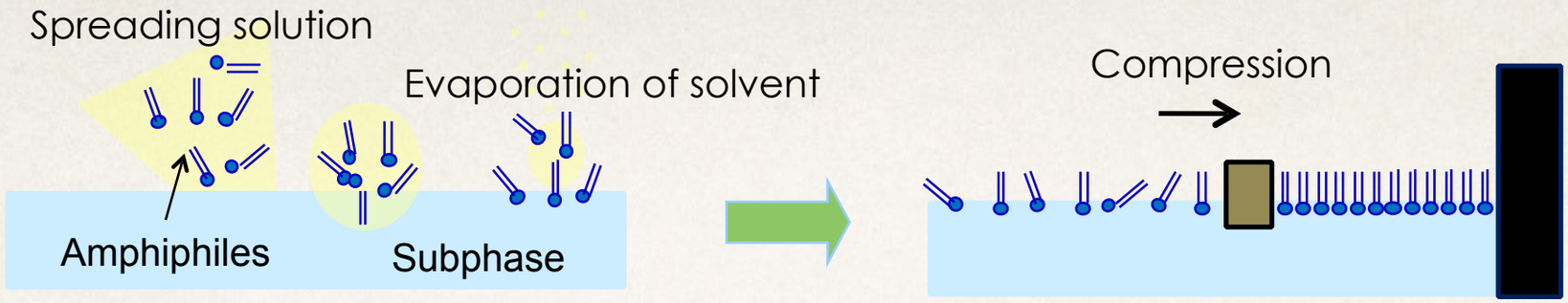

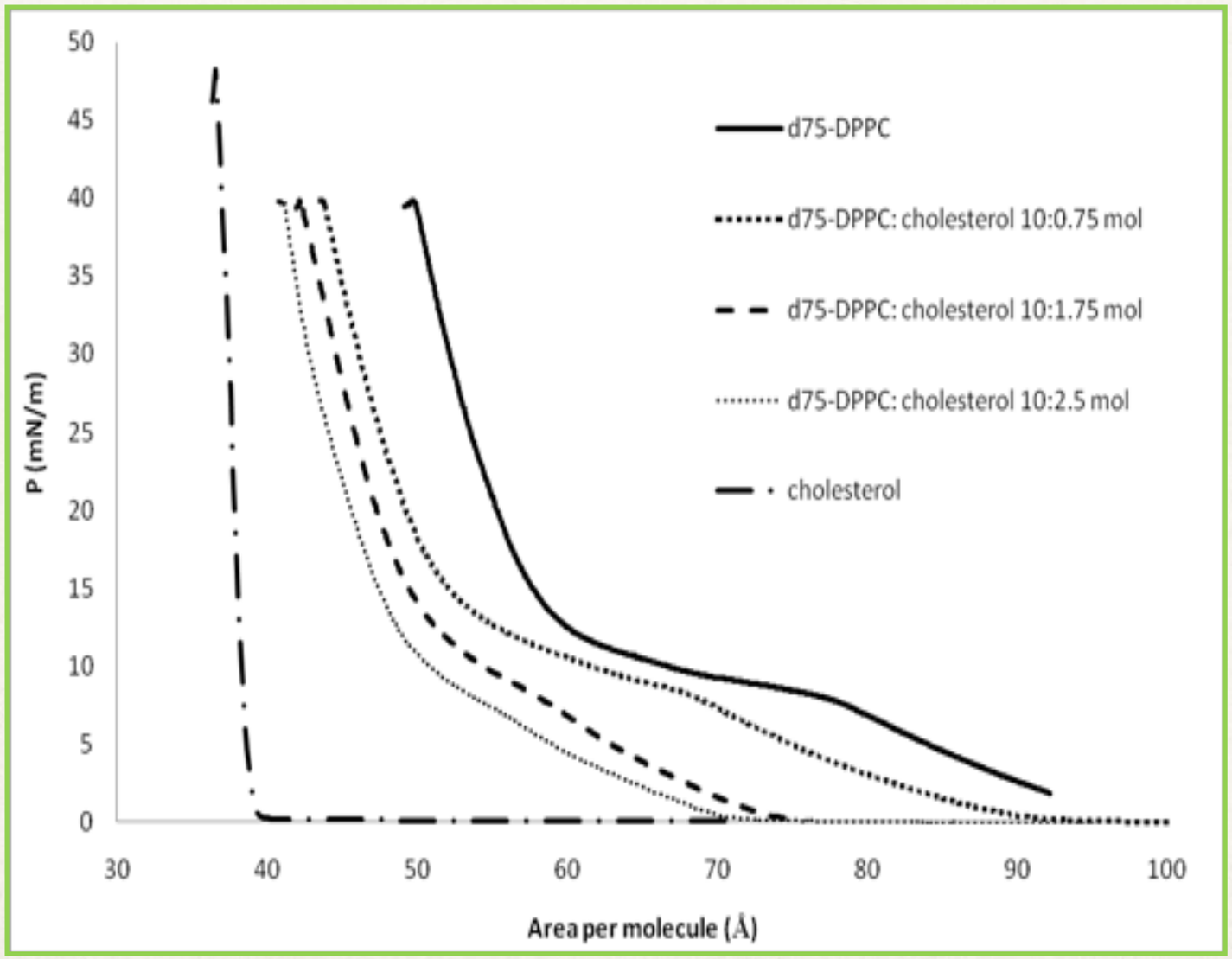

Rondelli et al., J. Phys. 2014

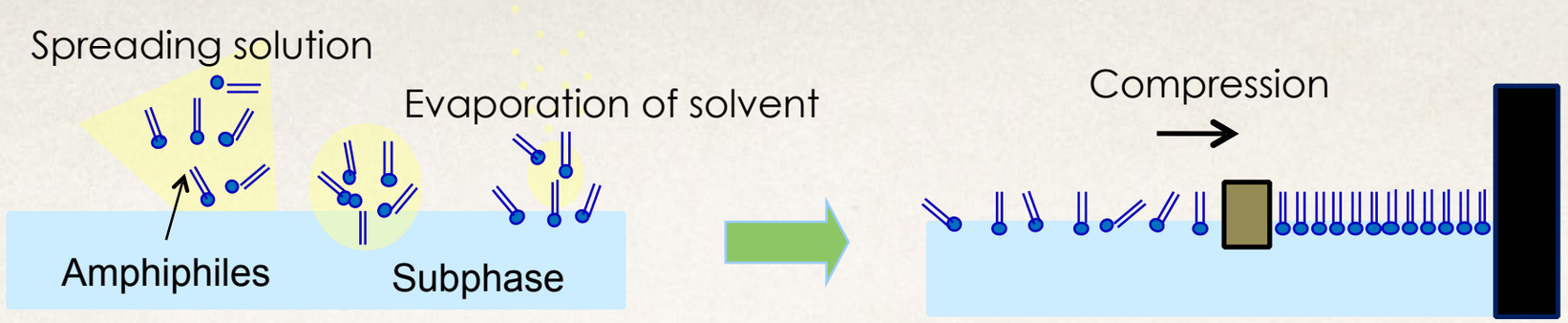

Langmuir Blodgett – Langmuir Schaefer technique

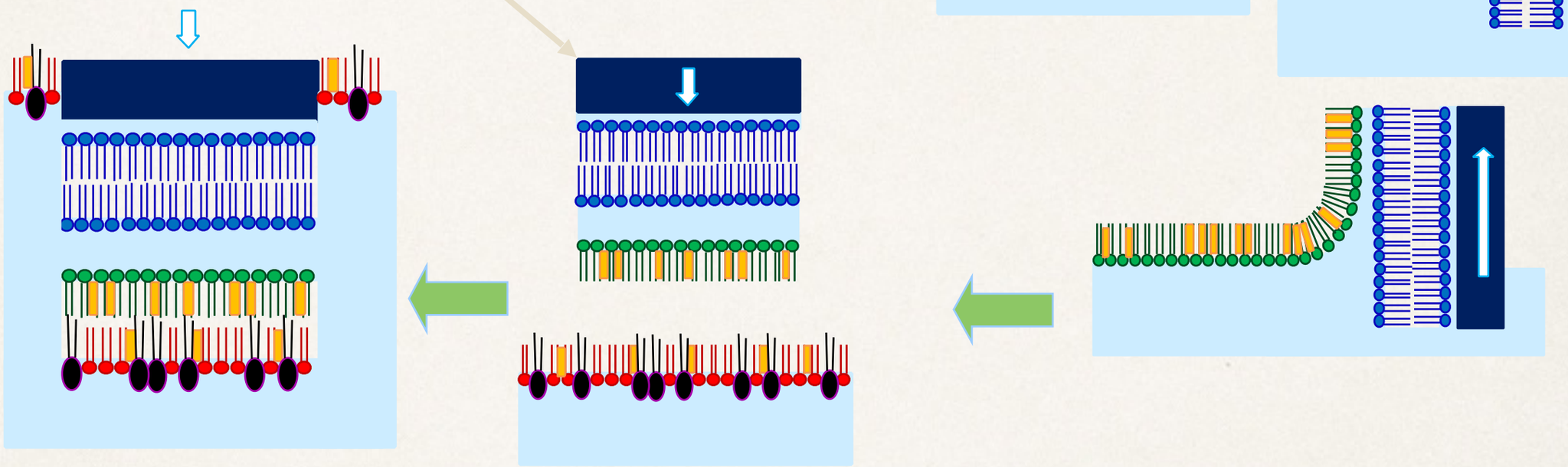

PRECISE CONTROL OF NUMBER OF LAYERS

HOMOGENEOUS DEPOSITION OVER **LARGE AREAS**

MULTILAYER STRUCTURES WITH **VARYING COMPOSITION LAYER BY LAYER**

Lipids exchange

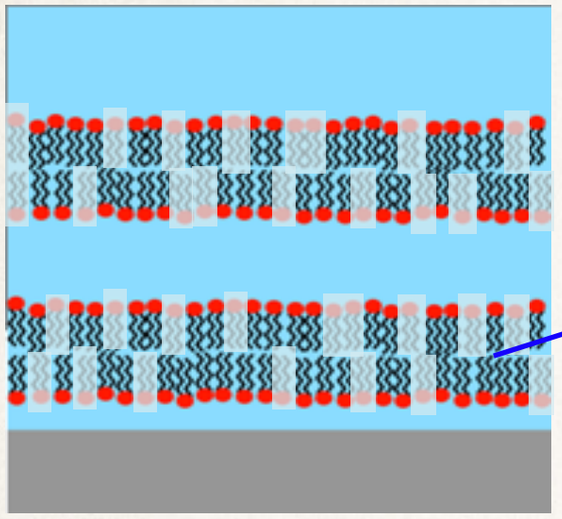

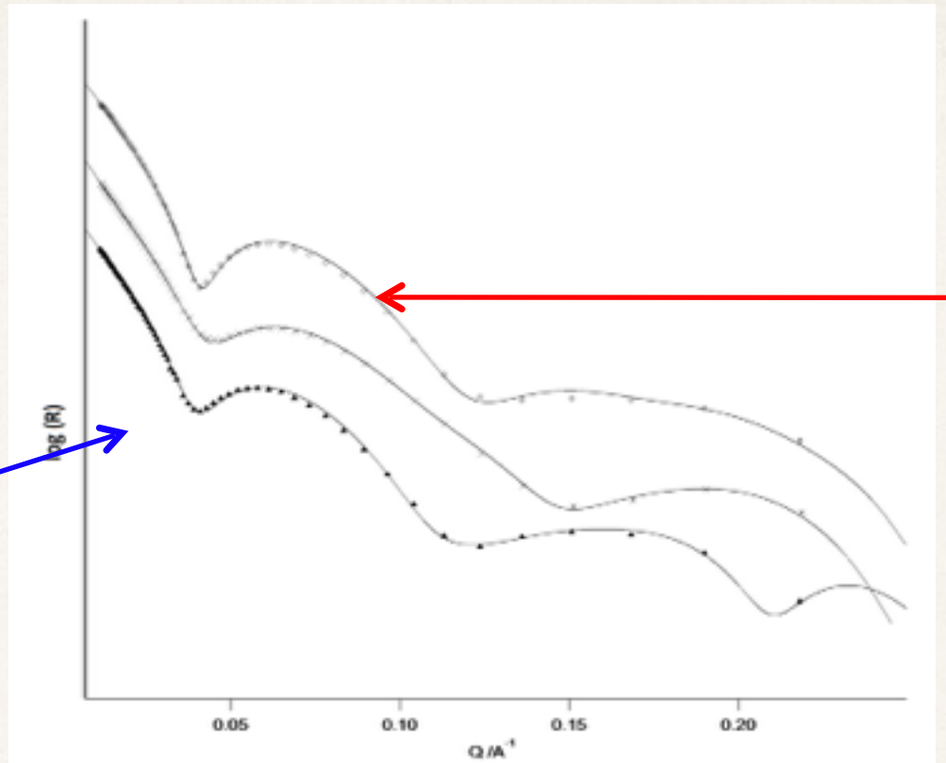

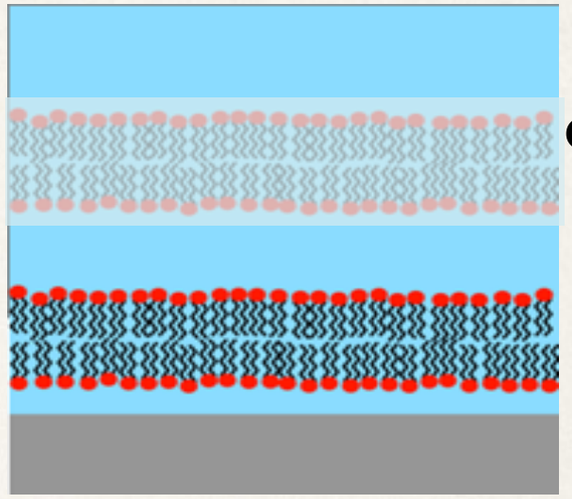

dDPPC

DSPC

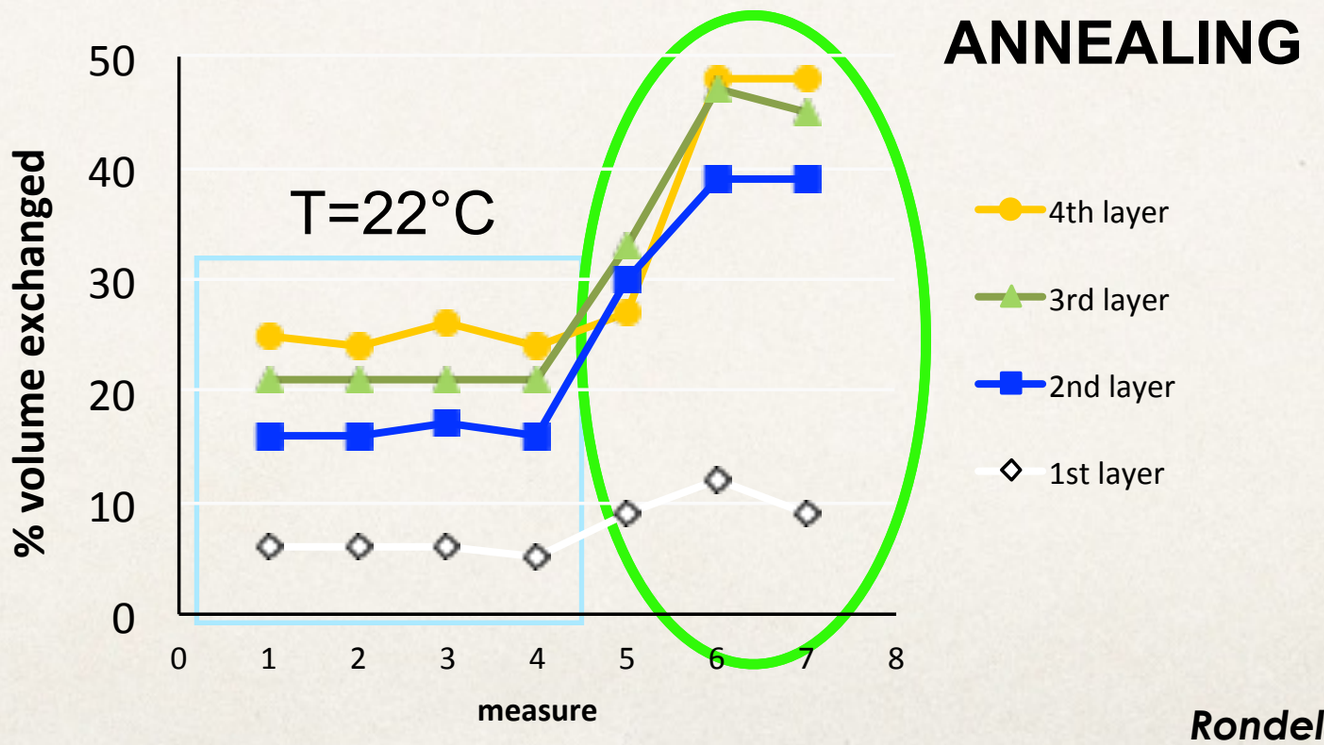

ANNEALING

Rondelli et al., J. Phys. 2014

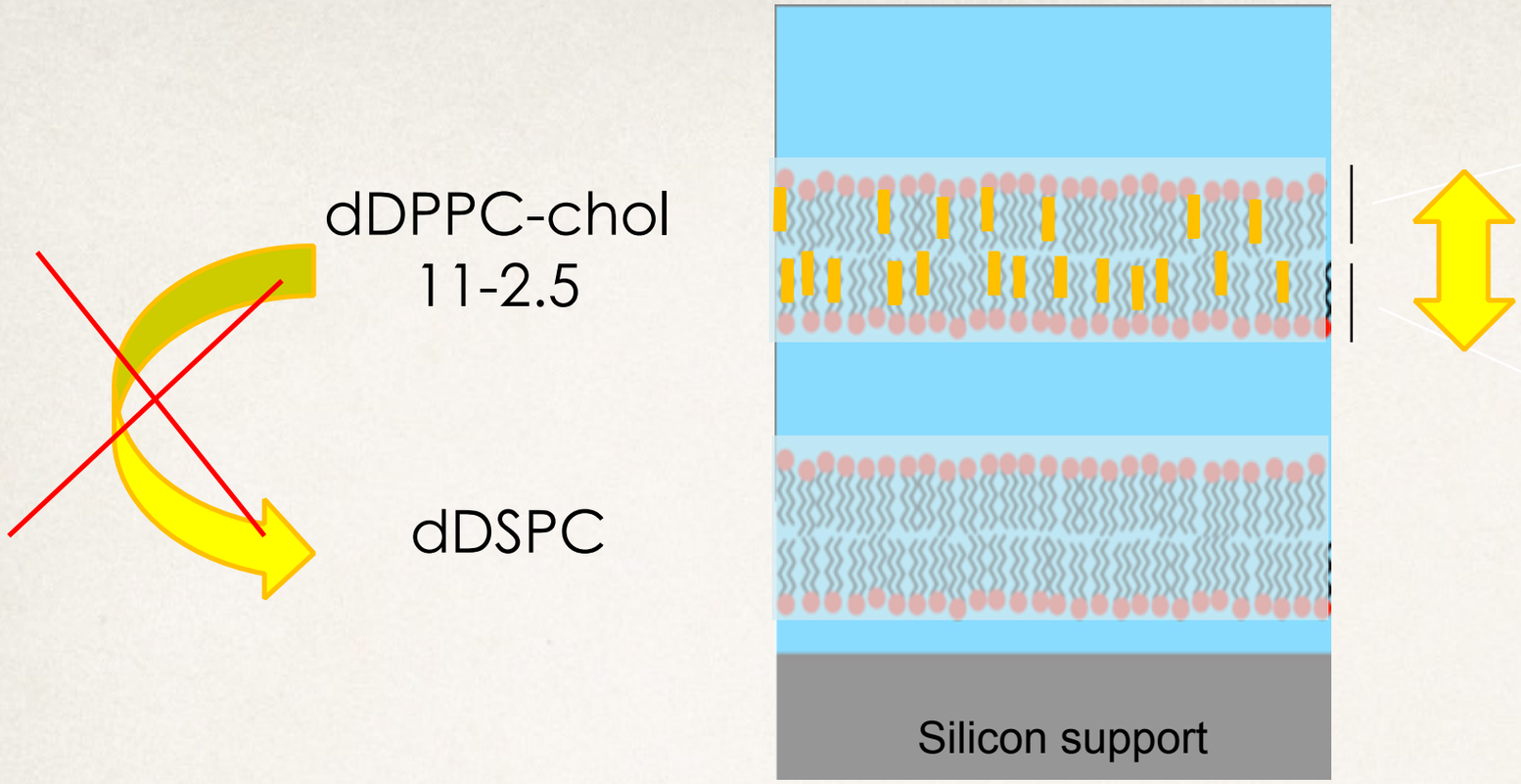

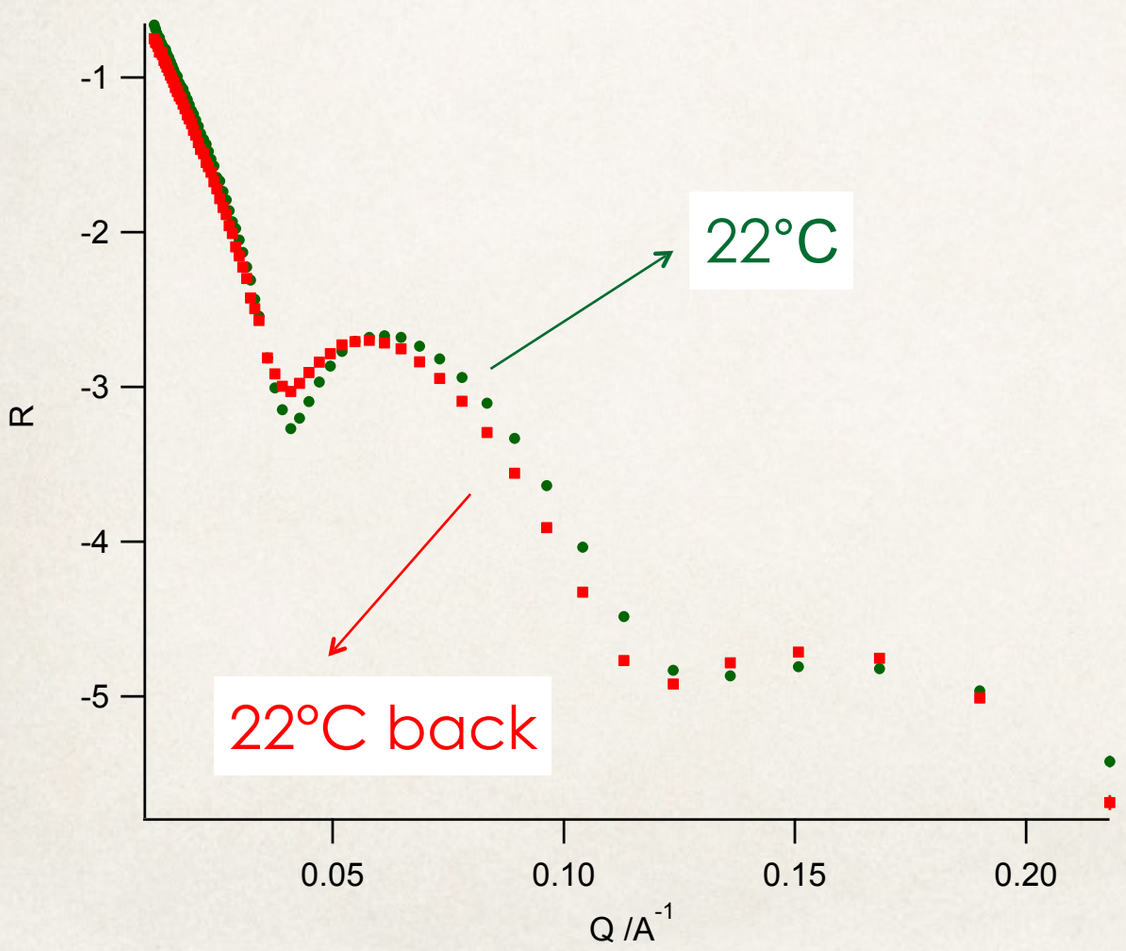

After annealing cholesterol was found to become **symmetrically** distributed in the hydrophobic region of the floating bilayer

Effect of ganglioside: co-deposition

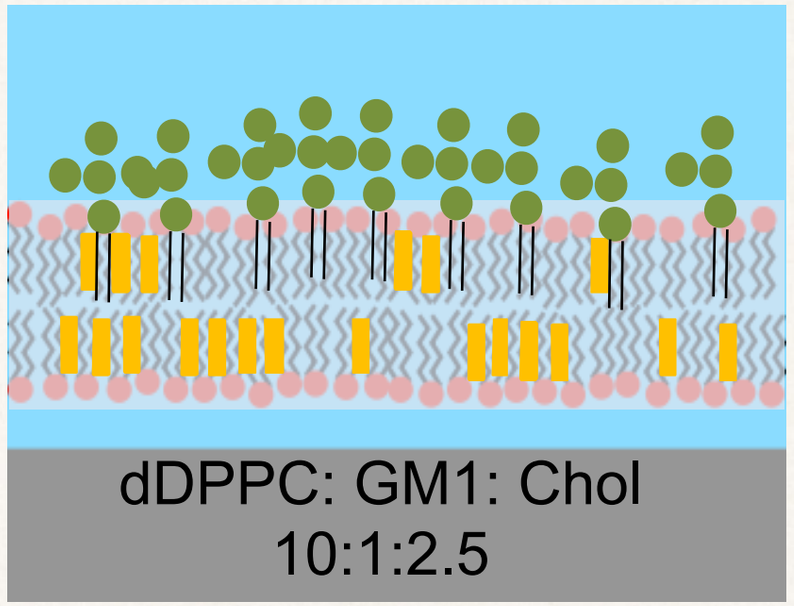

GM1
+
30%of the total
amount of cholesterol

70%of the total
amount of cholesterol

	bilayer thickness(Å)	%chol 1	%chol 2	solvent penetration (%vol)
22 °C	57	**74**	**26**	16
51 °C	56	67	33	8
22 °C back	60	63	37	27.5

Effect of ganglioside: micelles in solution

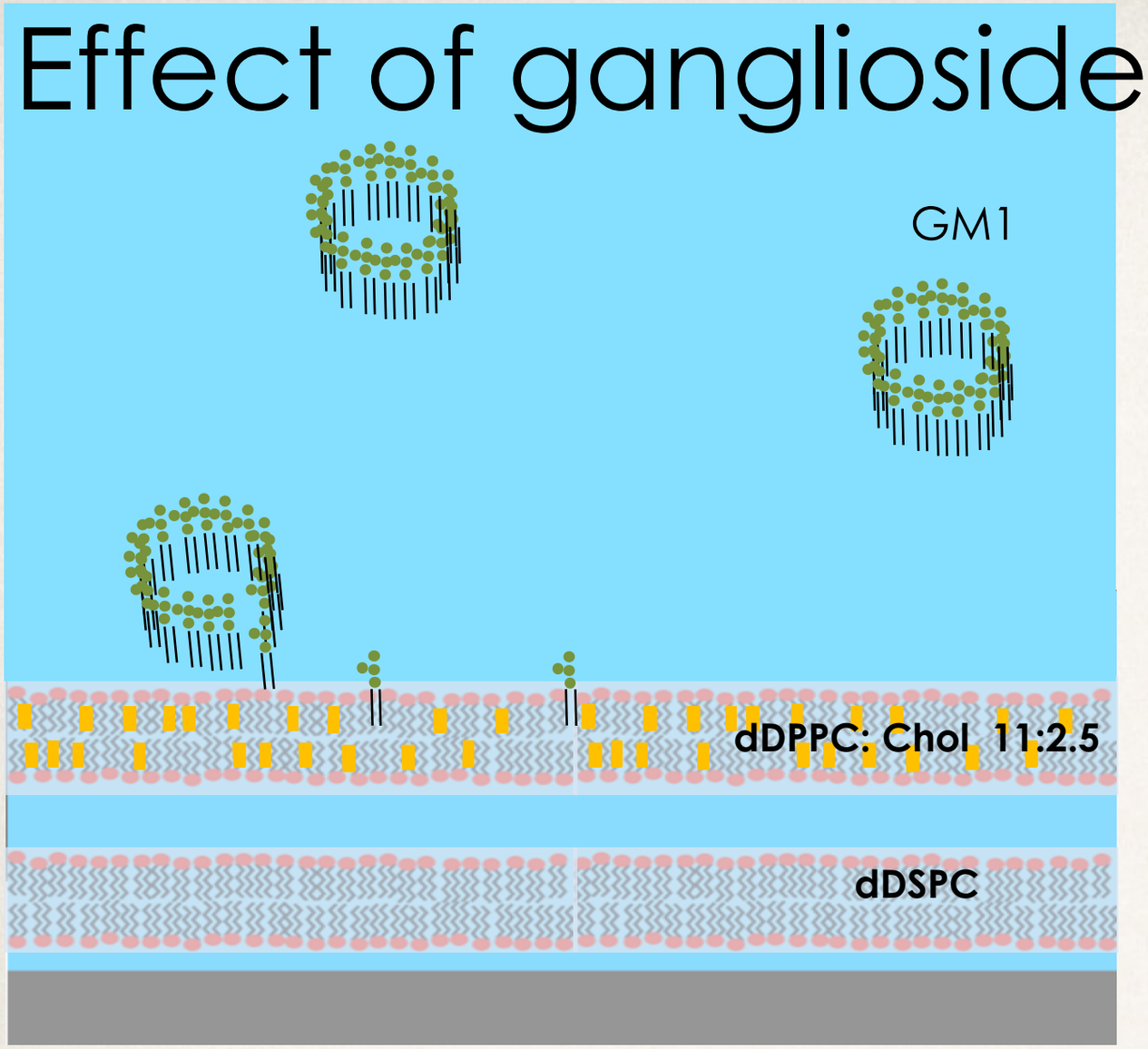

GM1 enters the membrane

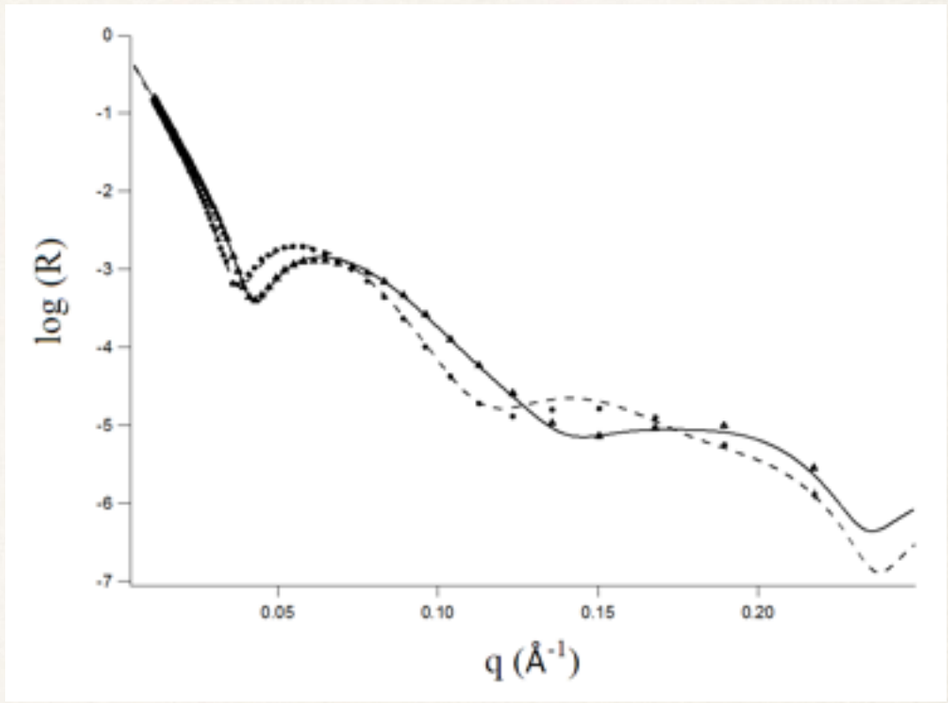

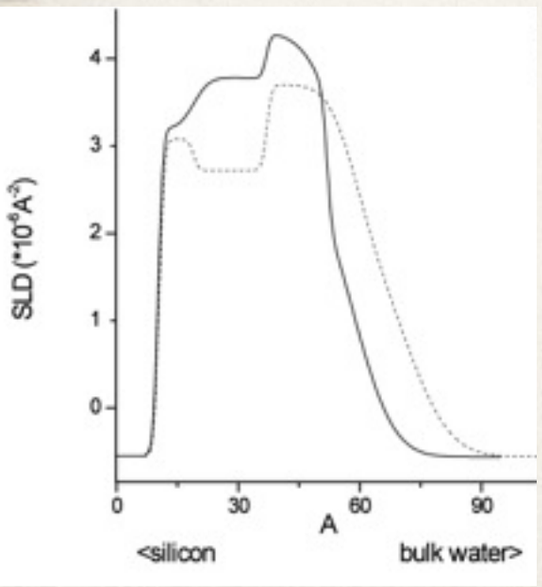

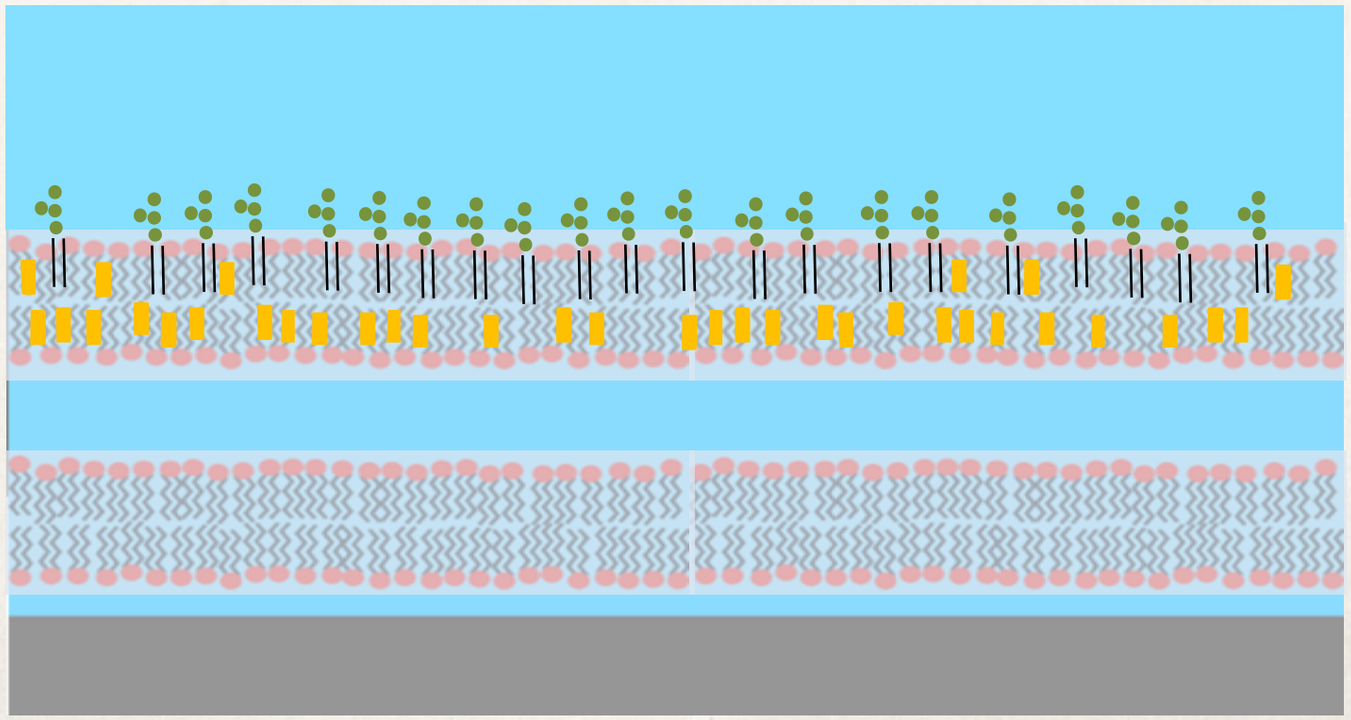

Cholesterol goes in the inner leaflet

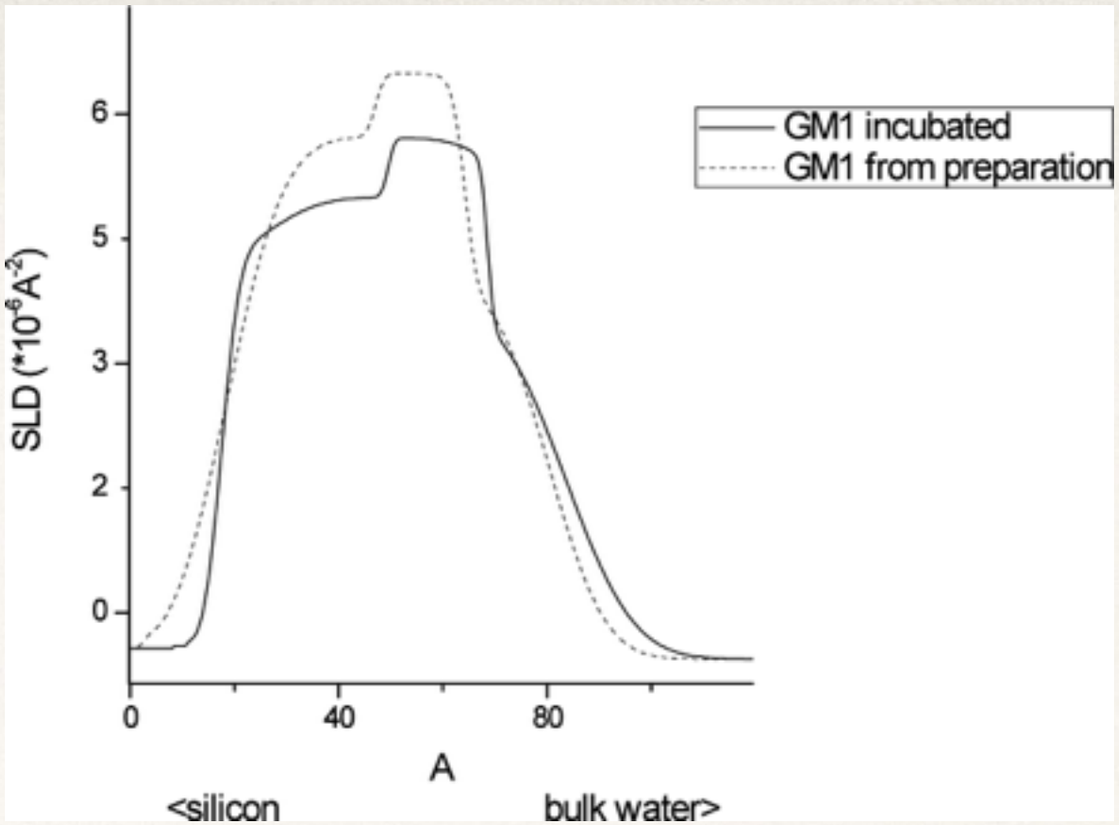
GM1 incubated
GM1 from preparation
SLD (*10-6A-2)
6
5
3
2
0
0
40
80
A
<silicon
bulk water>

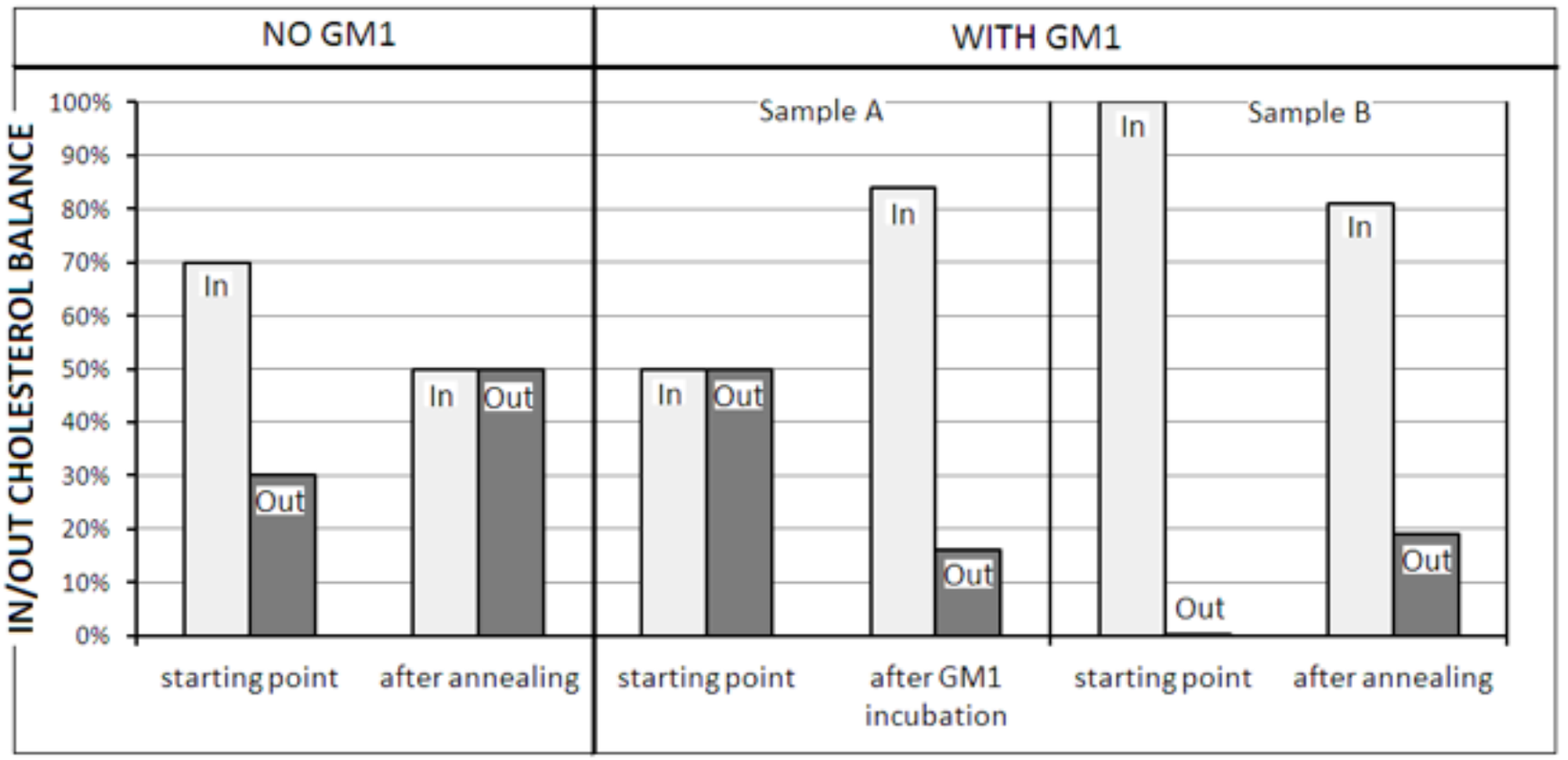
NO GM1
WITH GM1
IN/OUT CHOLESTEROL BALANCE
100%
90%
80%
70%
60%
50%
40%
30%
20%
10%
0%
Sample A
Sample B
In
Out
starting point
after annealing
after GM1 incubation

The presence of GM1 **forces asymmetry** in cholesterol distribution, opposite to what happens for a GM1-free membrane where a full symmetrisation of cholesterol distribution is observed.

A ***preferential*** **asymmetric distribution of GM1 and cholesterol** is attained revealing that a **true *coupling*** between the two molecules occurs.

GM1 GANGLIOSIDE AND **CHOLESTEROL** FORM A PAIR

KEY ROLE FOR MEMBRANE FUNCTIONALITY

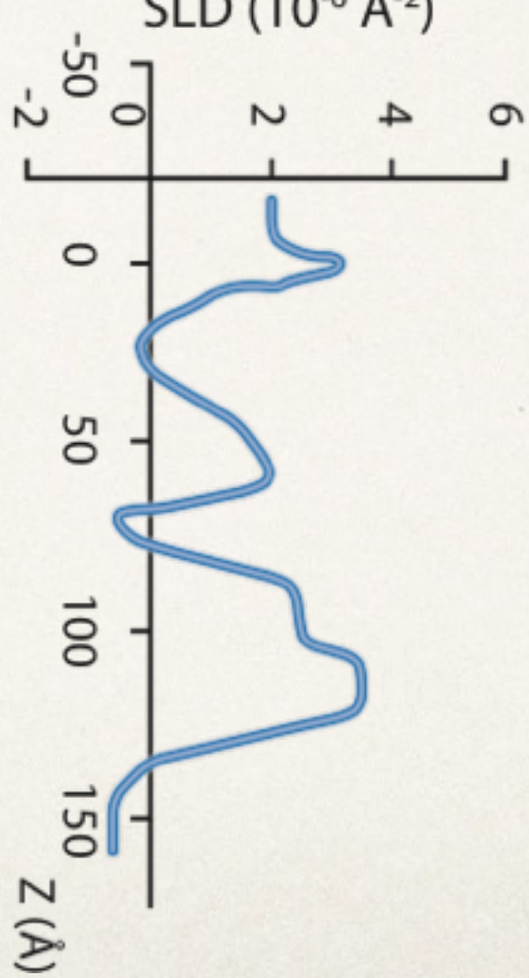

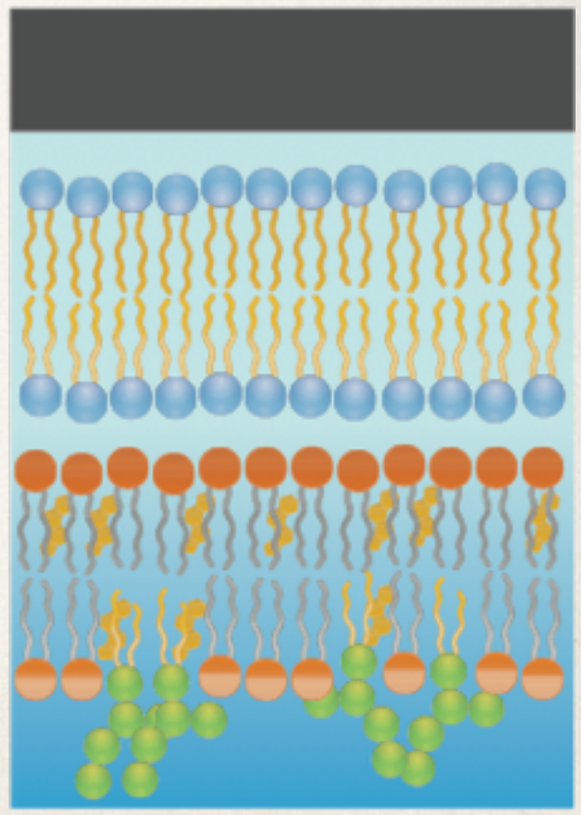

Effect of enzyme sialidase

SAXS measurements (ID02/ESRF) on gangliosides containing vesicles, after the addition of the enzyme **sialidase**

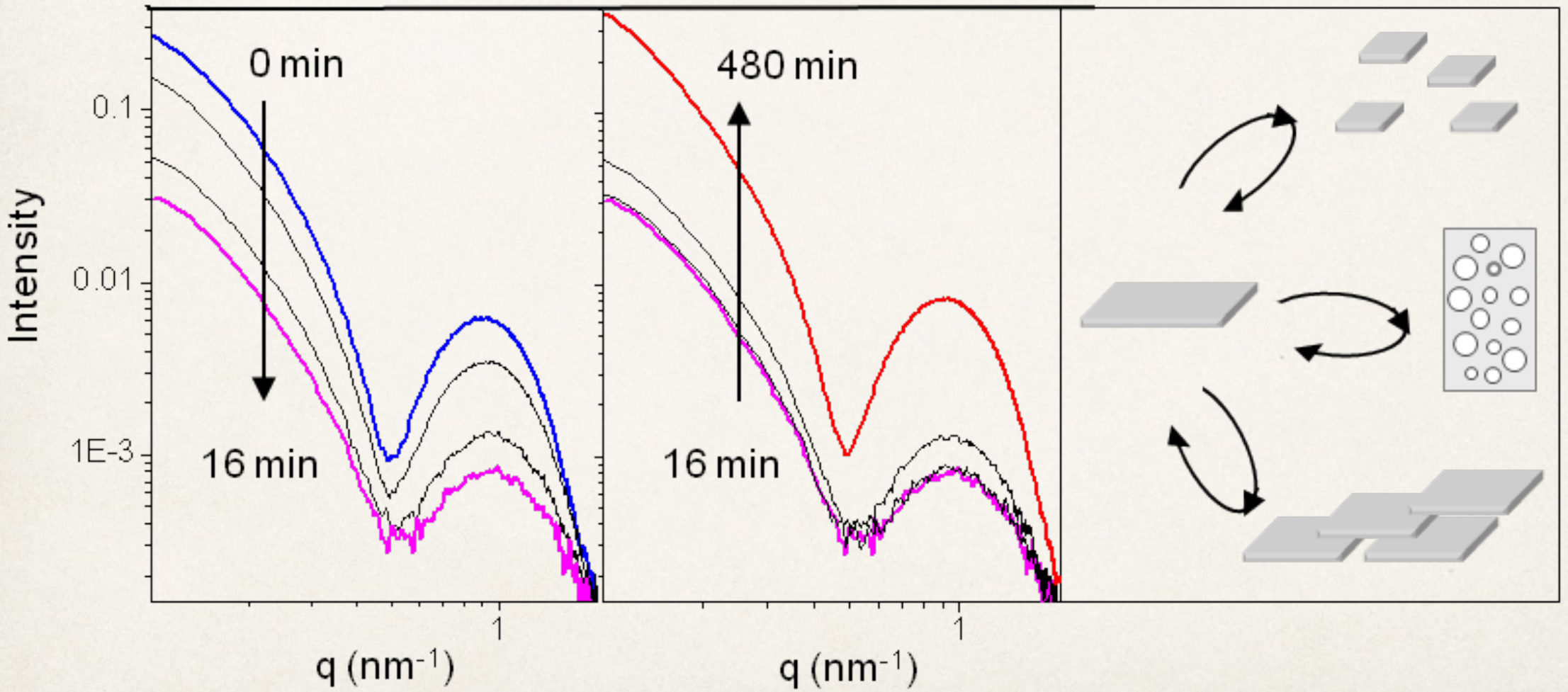

Courtesy L. Cantú, in preparation

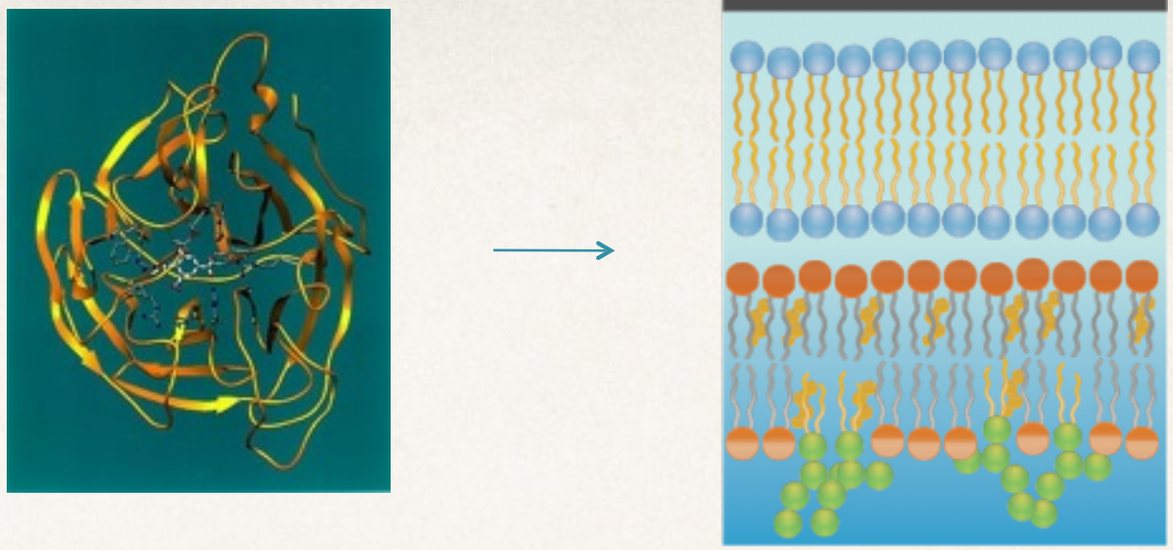

Interaction with enzyme sialidase, detectable with synchrotron radiation but not with neutrons (biggest effect at q>0.3Å^{-1})

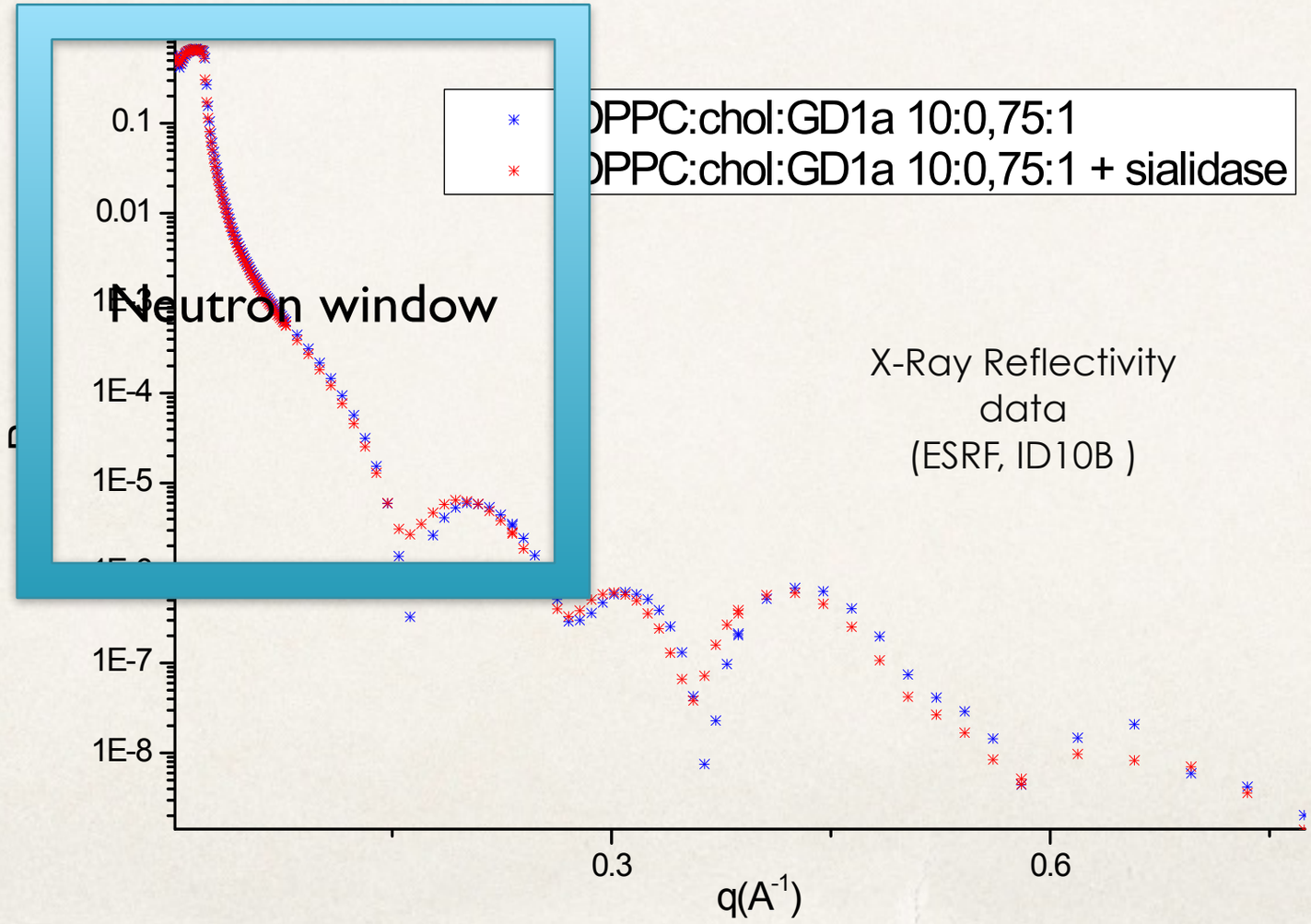

X-Ray Reflectivity data (ESRF, ID10B)

Analysis of specular and off-specular data is in progress

Examples:

- Ganglioside/cholesterol pair **(V. Rondelli, L. Cantù, et al.)**

- Interaction of antibiotic with natural membranes **(A. de Ghellinck, H. Wacklin, M. Sferrazza, J. Jouhet, M. Haertlein, …)**

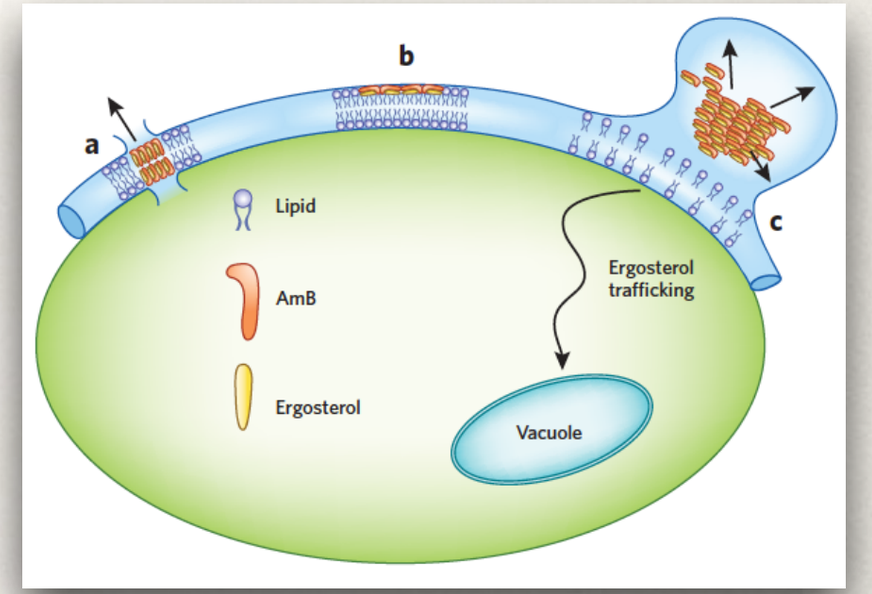

- Neutron reflectometry and deuteriation to probe density profiles of proteins adsorbed onto polymer brushes **(E. Schneck, A. Schollier, A. Halperin, M. Sferrazza)**

Production of natural deuterated lipids

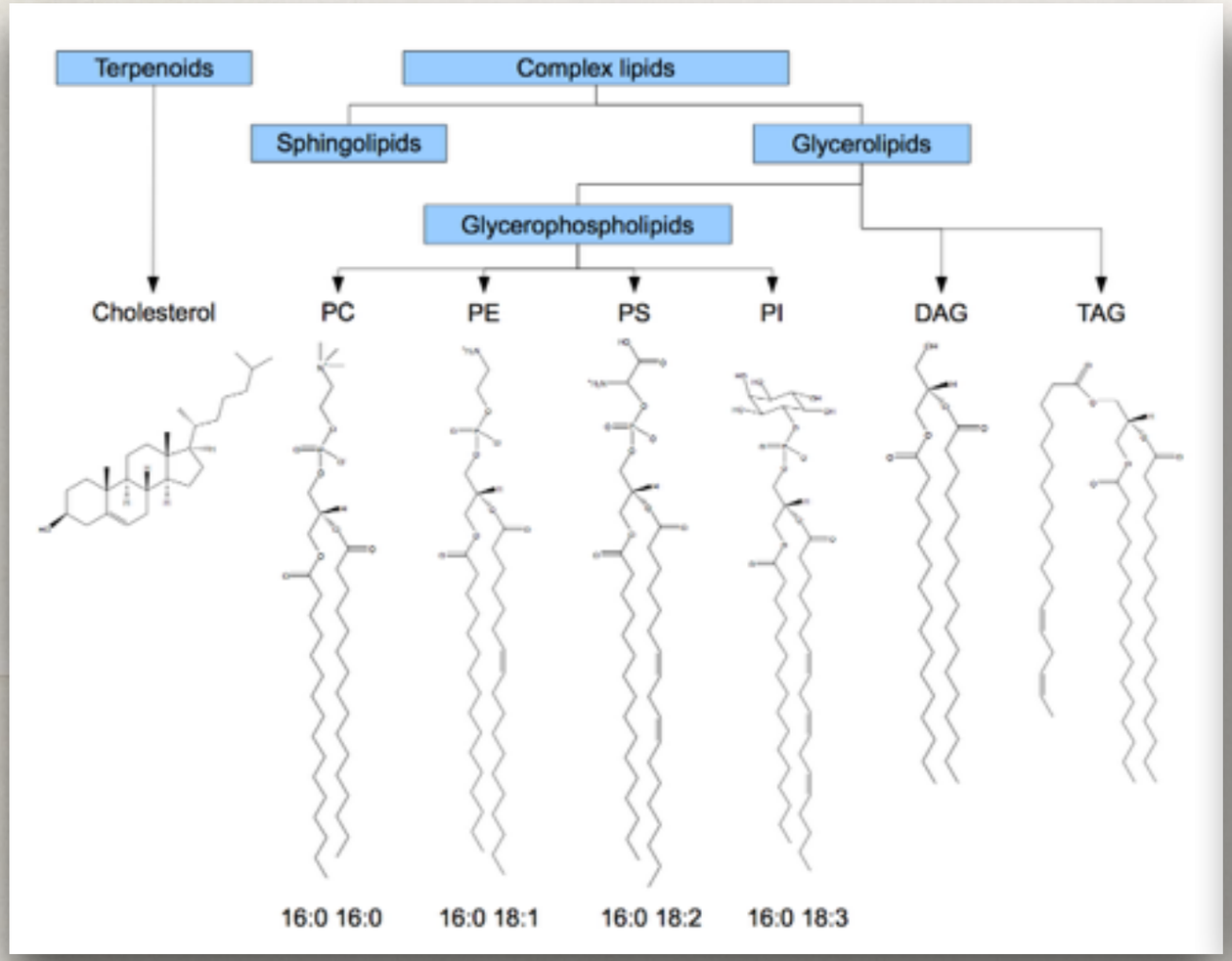

Unsaturation crucial for the fluidity of the membrane

Unsaturated deuterated lipids not commercially available

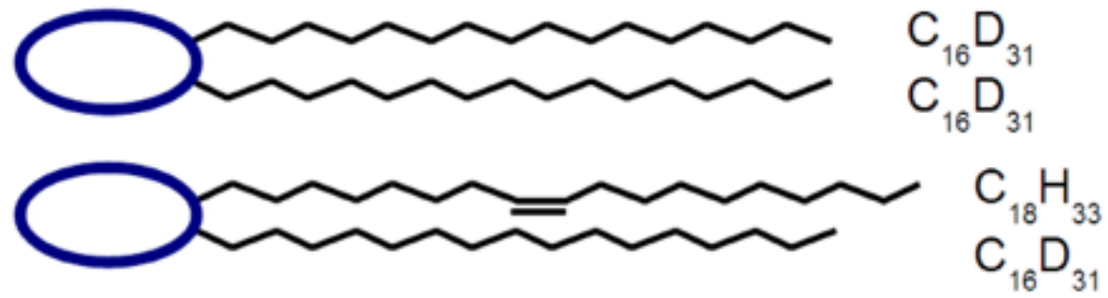

D-lab at the ILL uses yeast cells to produce d-proteins by biosynthesis

Yeast: a tool to produce lipids as well

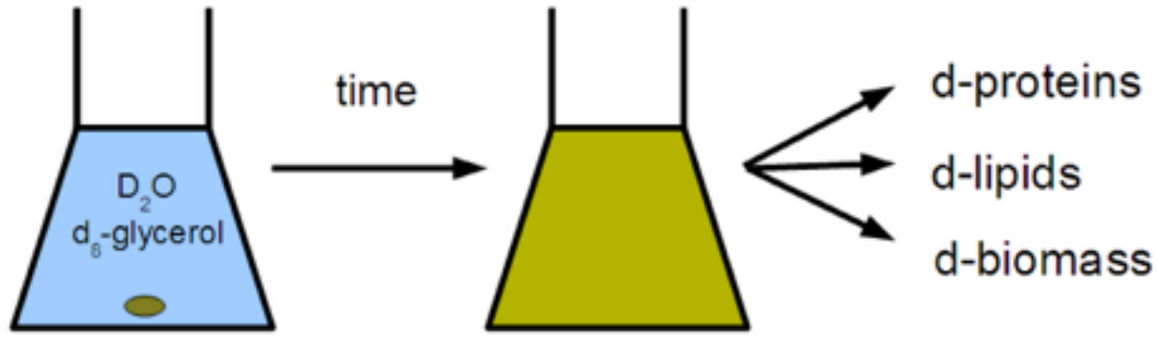

OPEN ACCESS Freely available online

PLOS | ONE

Production and Analysis of Perdeuterated Lipids from *Pichia pastoris* Cells

Alexis de Ghellinck[1,2], Hubert Schaller[3], Valérie Laux[1], Michael Haertlein[1], Michele Sferrazza[2], Eric Maréchal[4], Hanna Wacklin[5,6], Juliette Jouhet[4]*, Giovanna Fragneto[1]

1. Yeast cells are grown in H or D environment
2. Lipids are extracted according to the Folch method
3. Separation by 2D-TLC
4. Separated lipids are analysed by GC

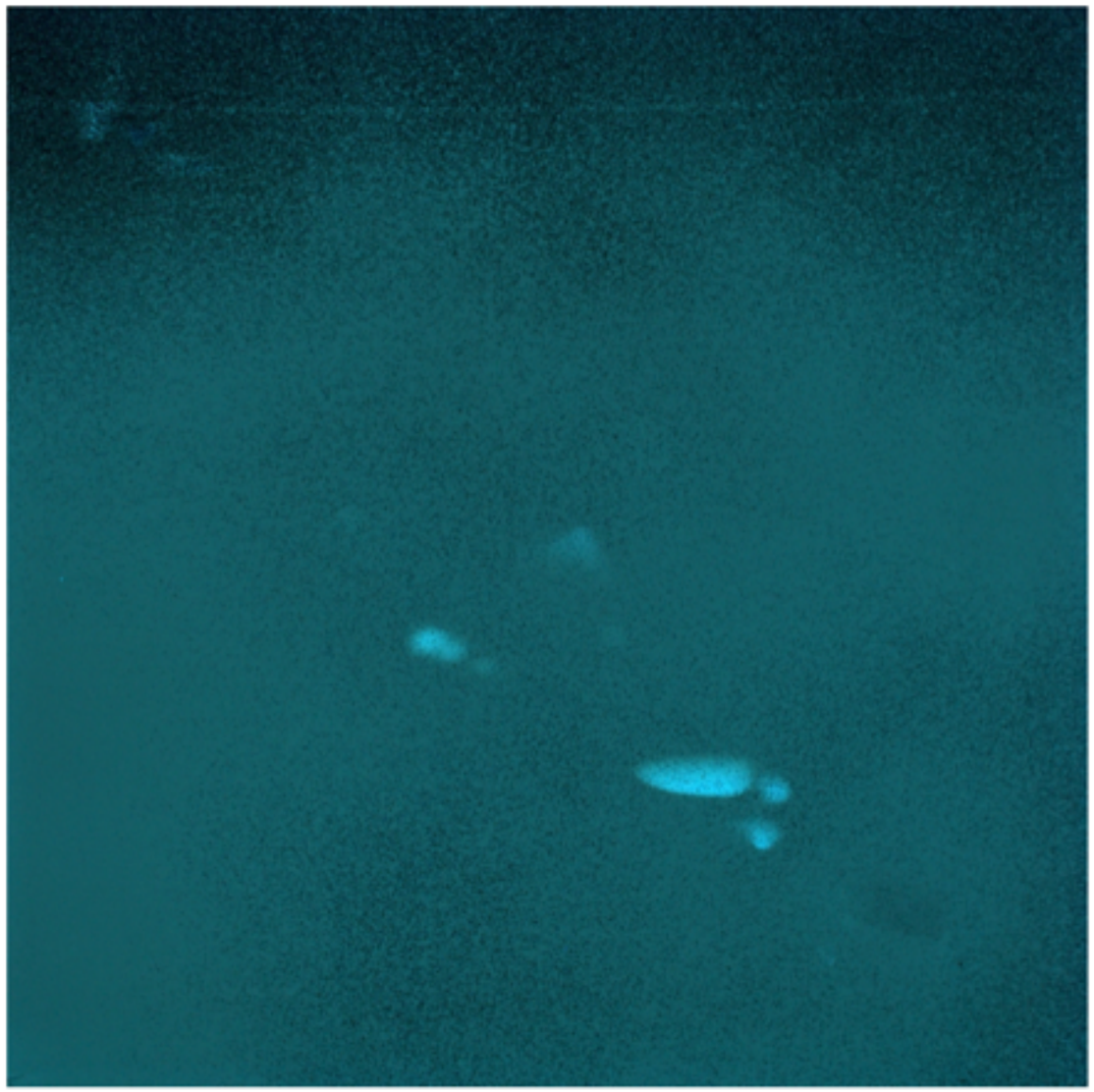

Phospholipid composition **non** affected by deuterated growth culture

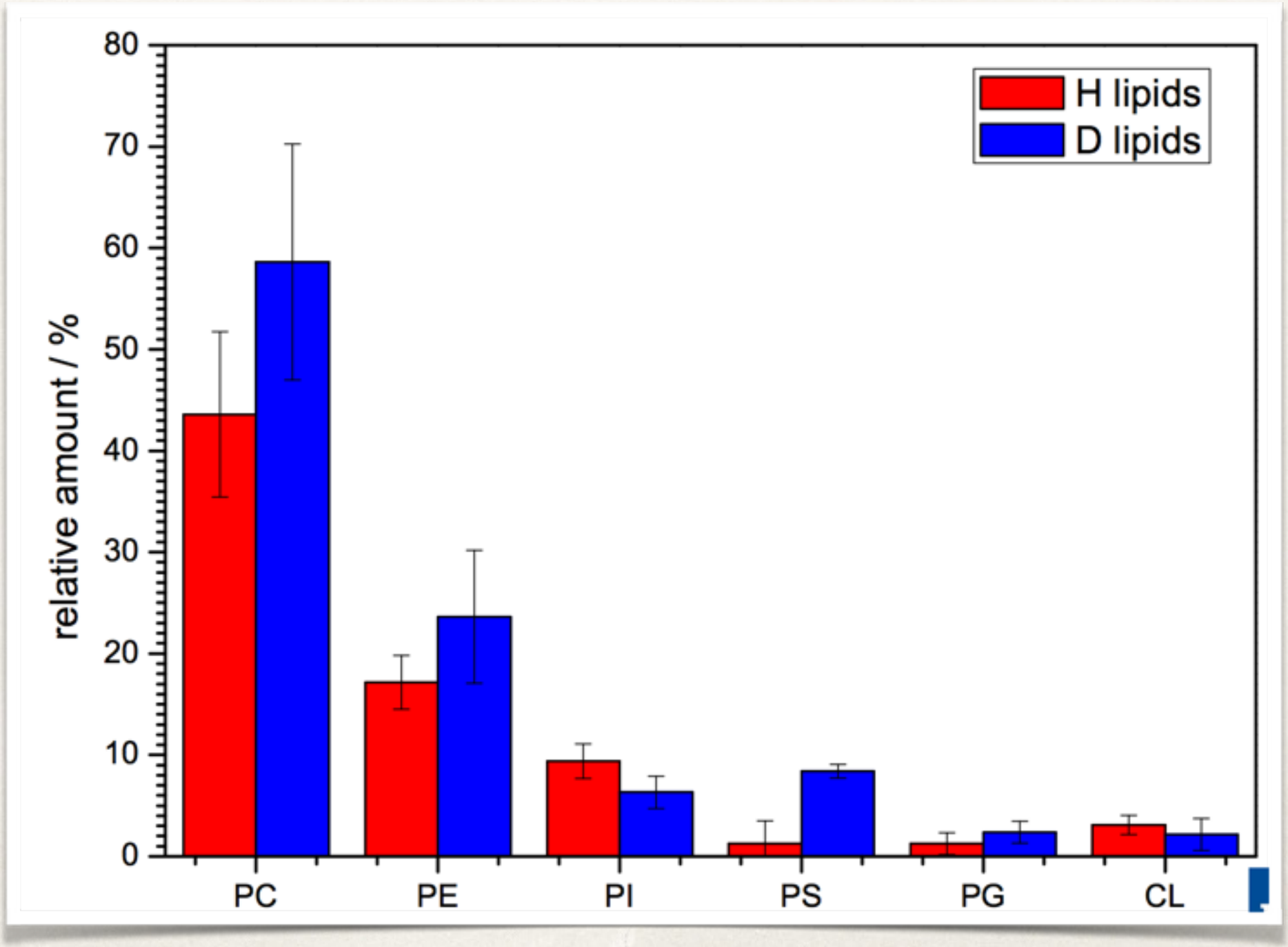

Fatty acid composition affected by deuterated growth culture

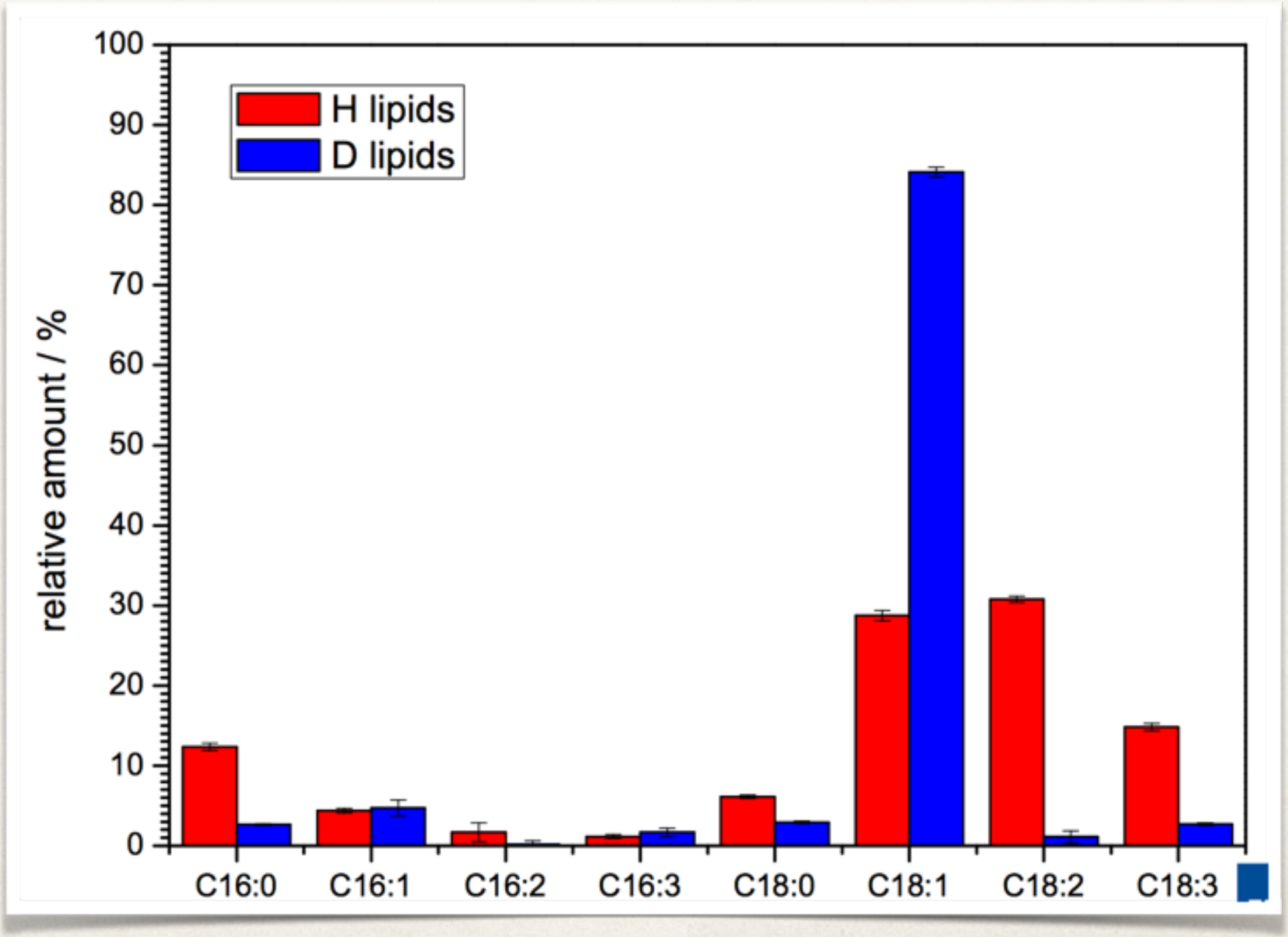

Deposition by vesicle fusion: Optimisation by QCM-D (PSCM labs)

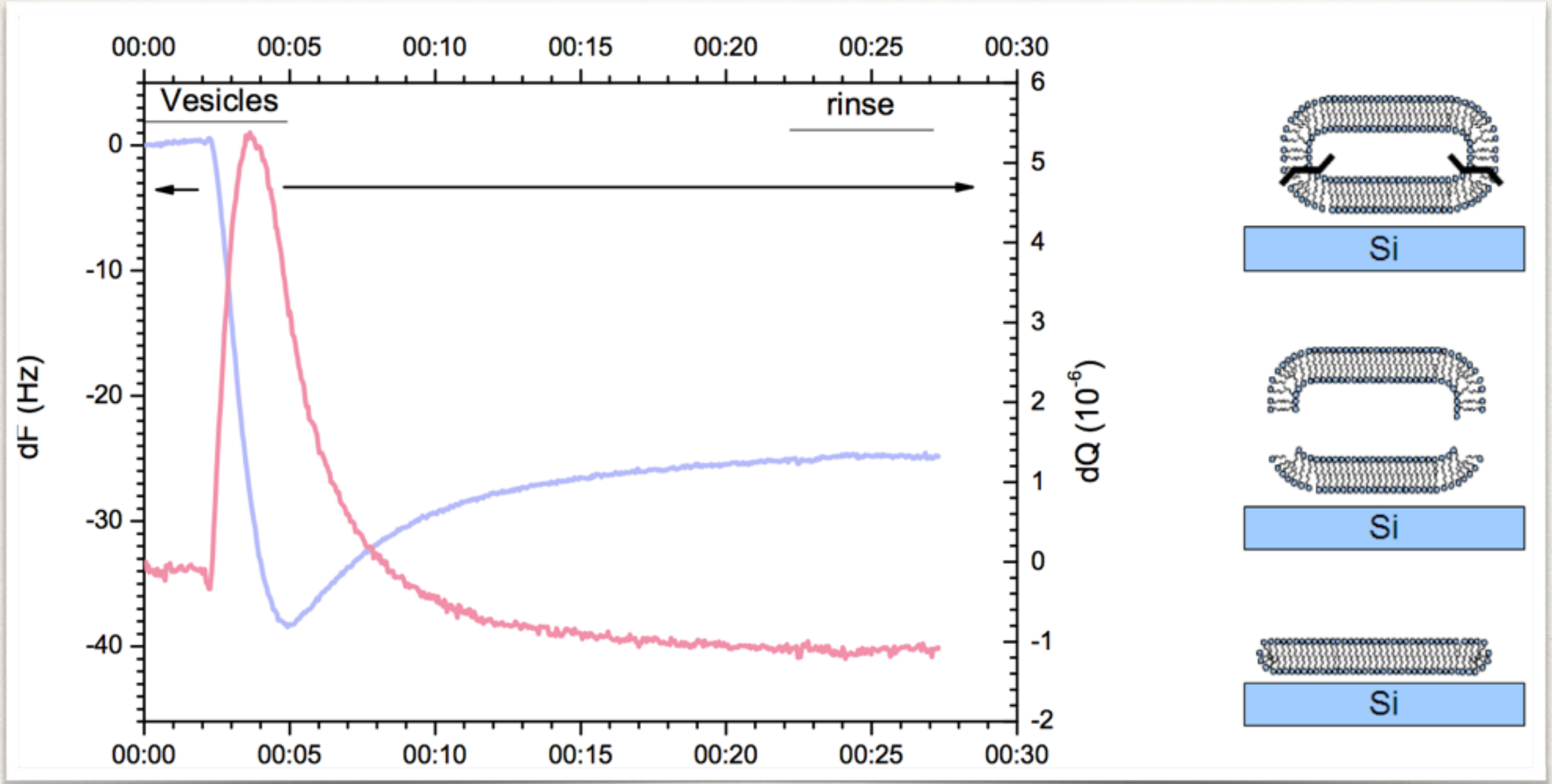

Structure of D-polar lipids

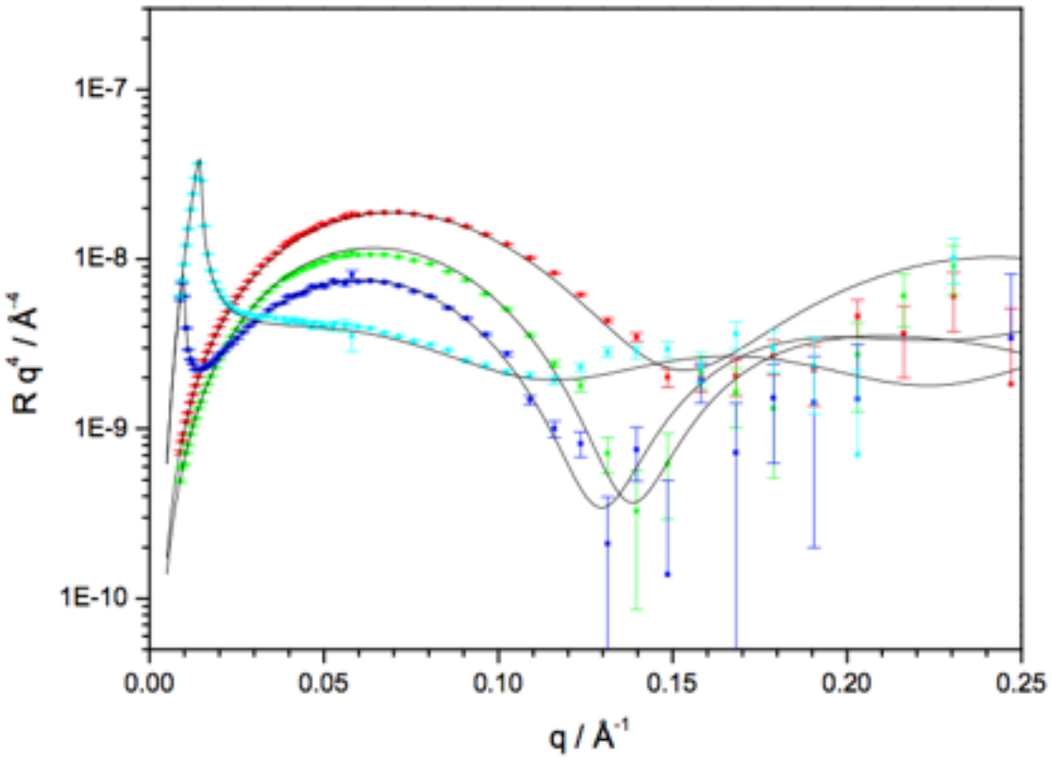

Neutron reflectivity from Figaro at the ILL

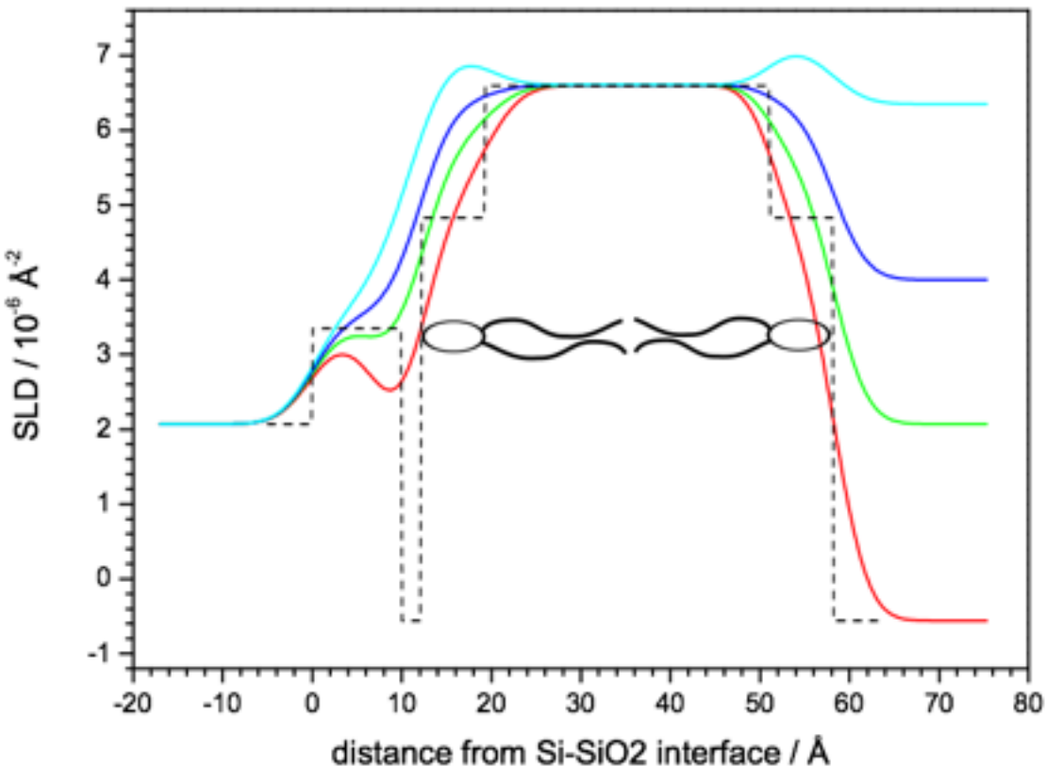

Full coverage
Full deuteriation
Structure similar to synthetic DOPC

Structure of H-polar lipids

- Full coverage
- Thinner than DOPC bilayer
- Rougher outer headgroup - tail interface

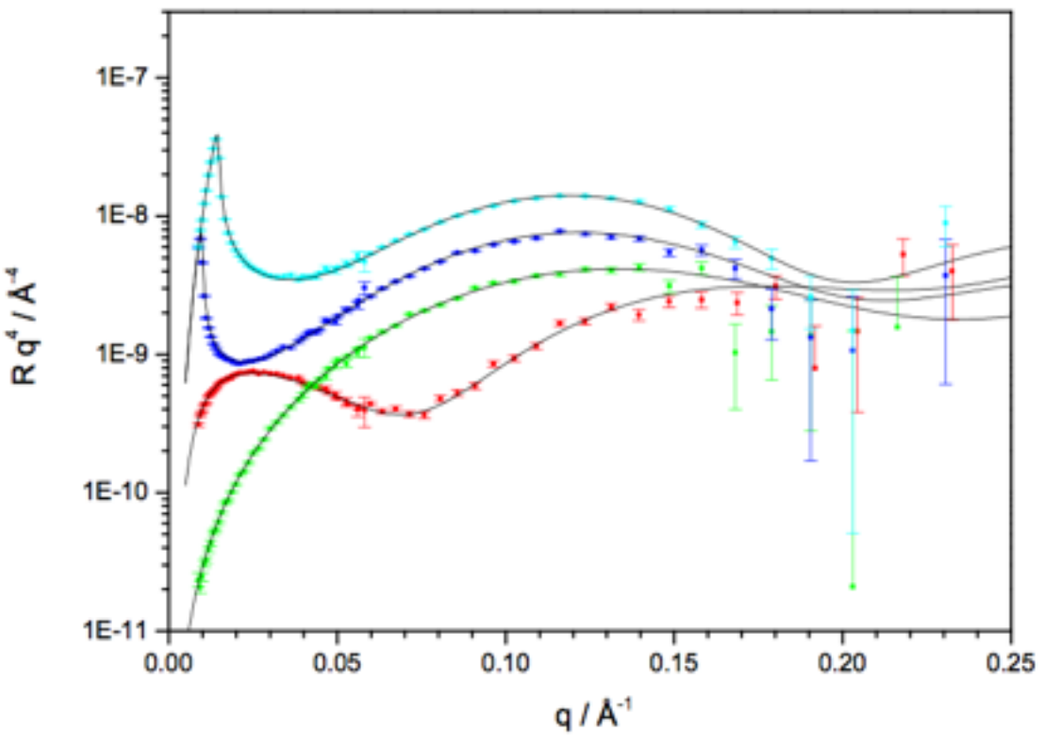

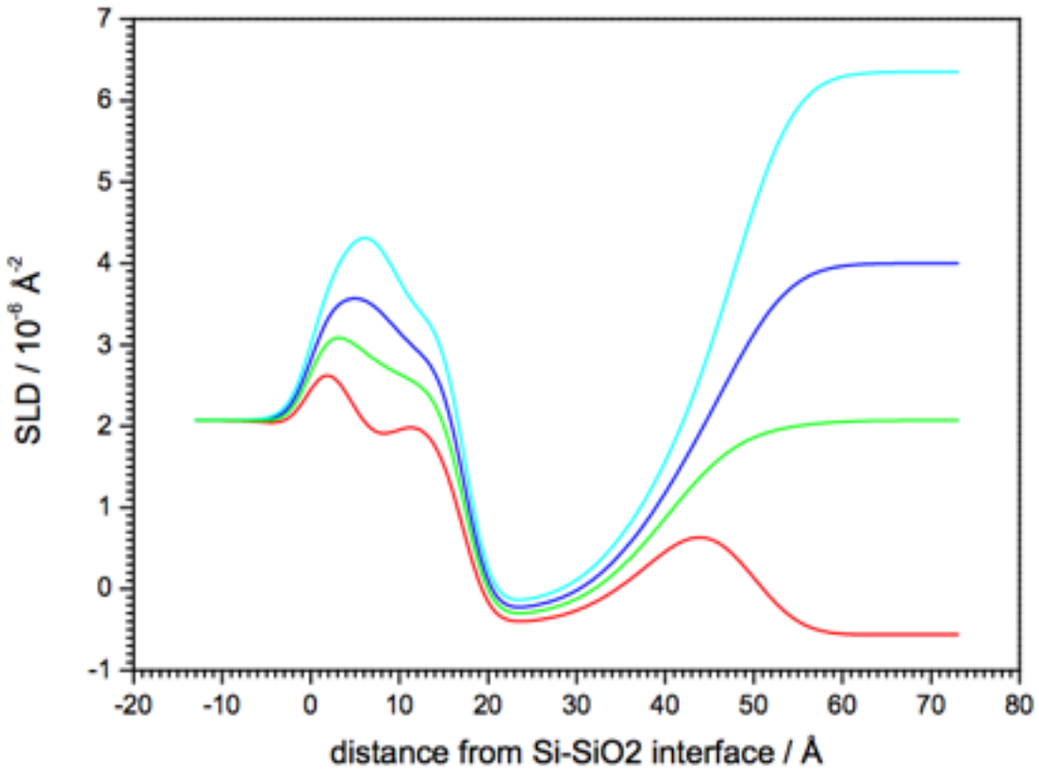

Neutron reflectivity from Figaro at the ILL

Structure of D-polar lipids + sterol

- Same thickness as D-polar lipids
- Increased roughness at the tail - headroup interfaces

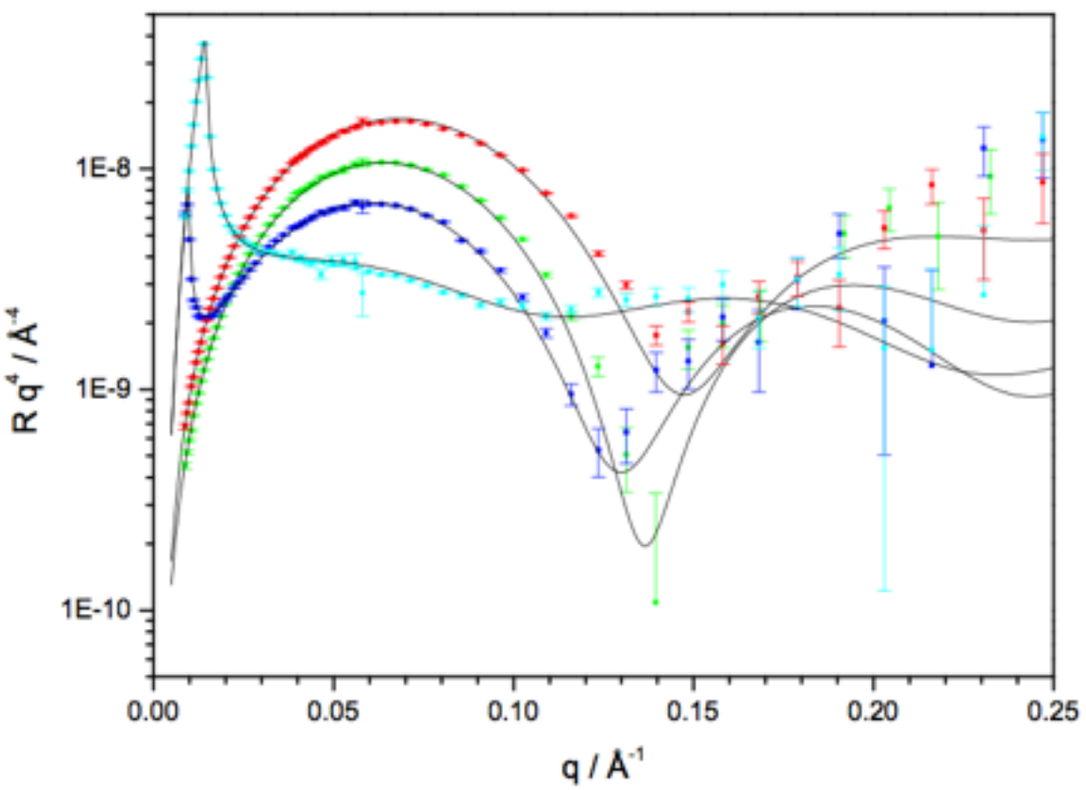

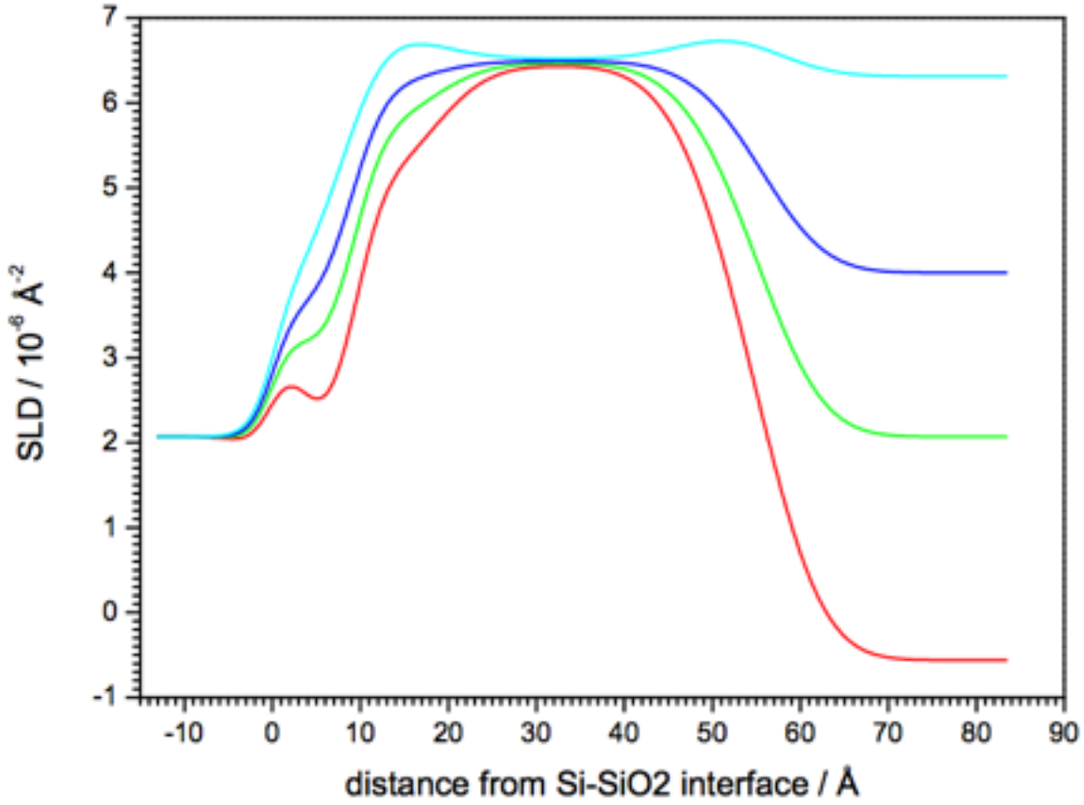

Structure of H-polar lipids + sterol

- Thicker than H-polar lipids

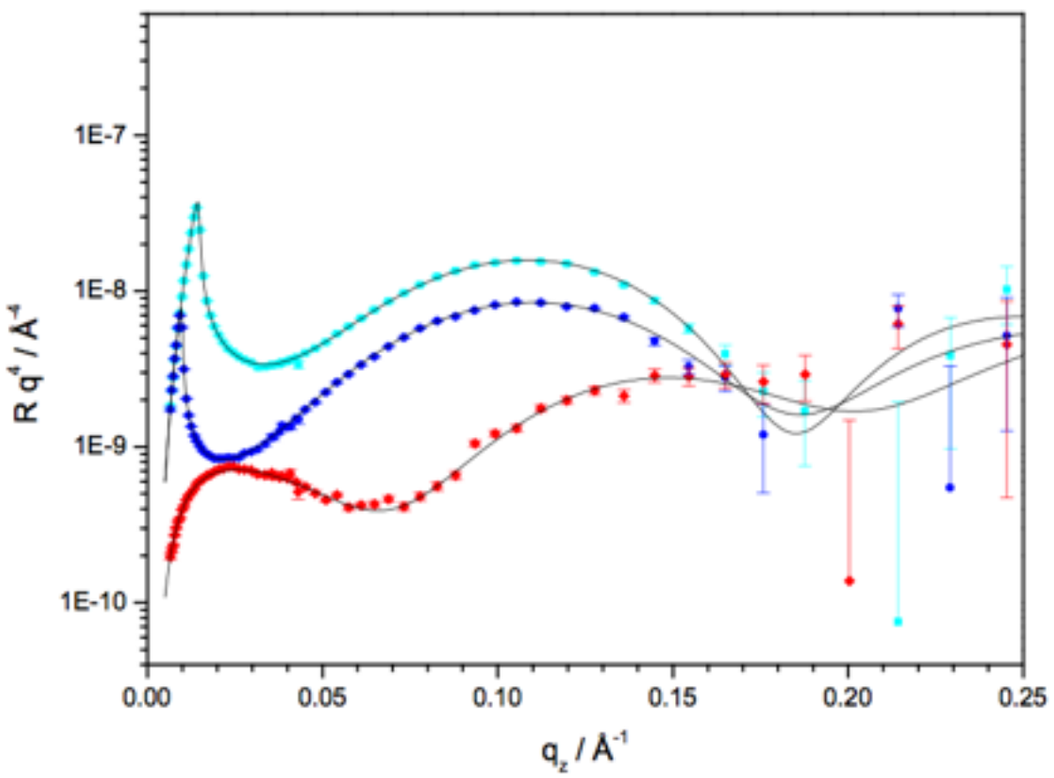

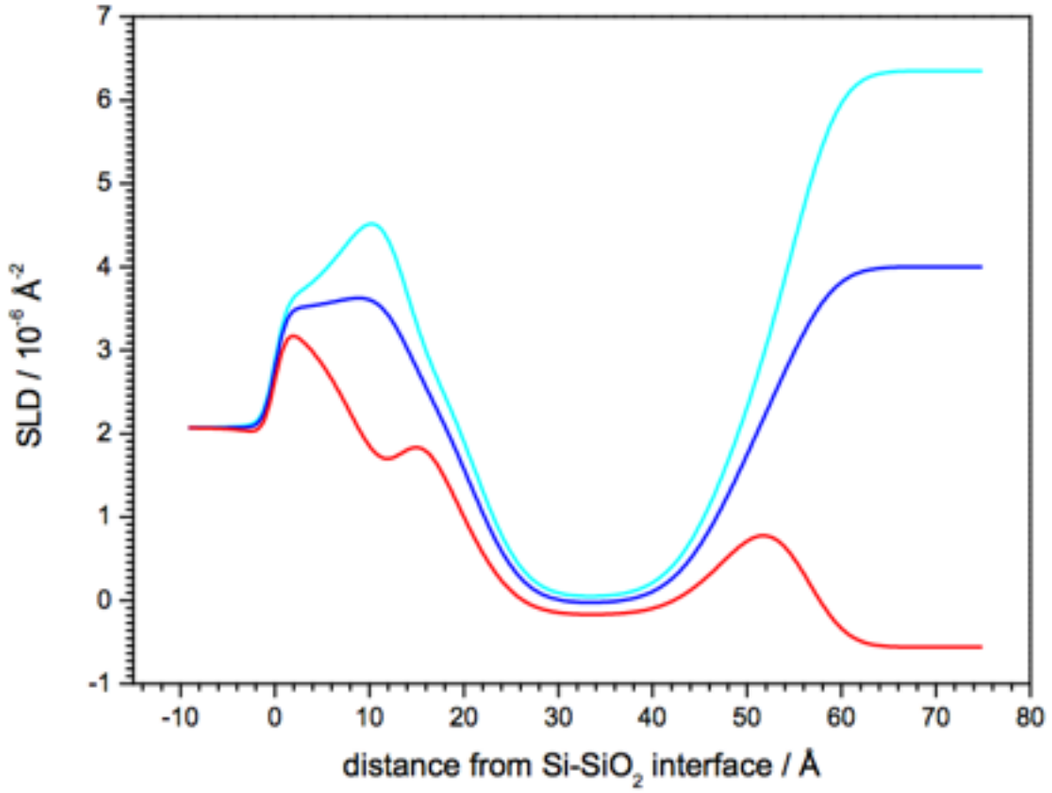

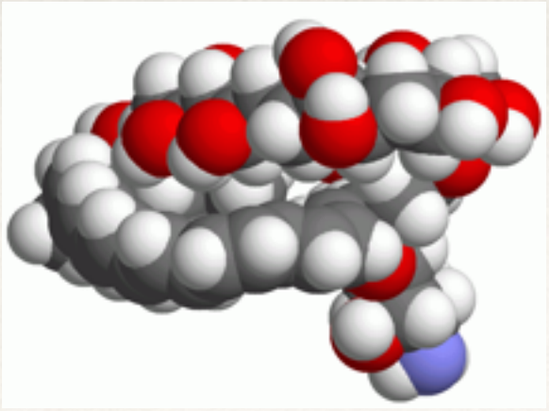

Interaction with antibiotic molecule: Amphotericin-B

✤Polyene antifungal drug used intravenously for systemic fungal/parasitic infections (AIDS & cancer patients)

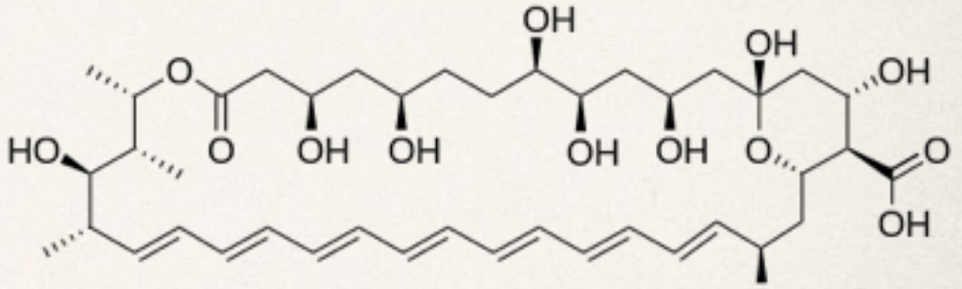

✤**AmB is well known for its severe and potentially lethal side effects**

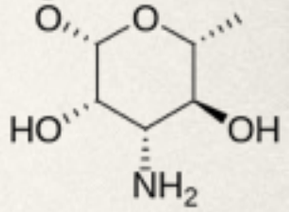

✤AmB binds with **ergosterol**, a component of fungal cell membranes, forming a transmembrane channel that leads to **monovalent ion leakage**, which is the primary effect leading to fungal cell death.

✤ Oligomeric pore formation

✤ Activity depends on aggregation state

✤**Recently evidence was found that pore formation is not necessarily linked to cell death.**

✤The actual mechanism of action may be more complex and multifaceted.

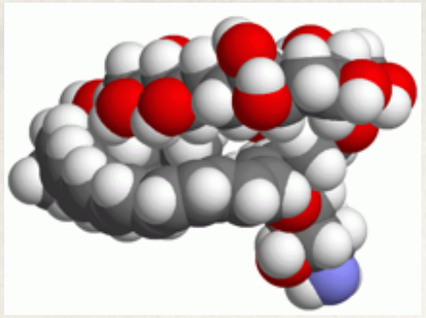

AmB effect on P. Pastoris yeast membranes: neutron reflectometry measurements

- AmB inserts in yeast membranes in the presence of ergosterol
- Amb also forms a dilute 30-40 Å layer on the top of the membrane
- Membrane thinning is more pronounced in H-lipids which are more polyunsaturated
- **No water filled pores are observed**

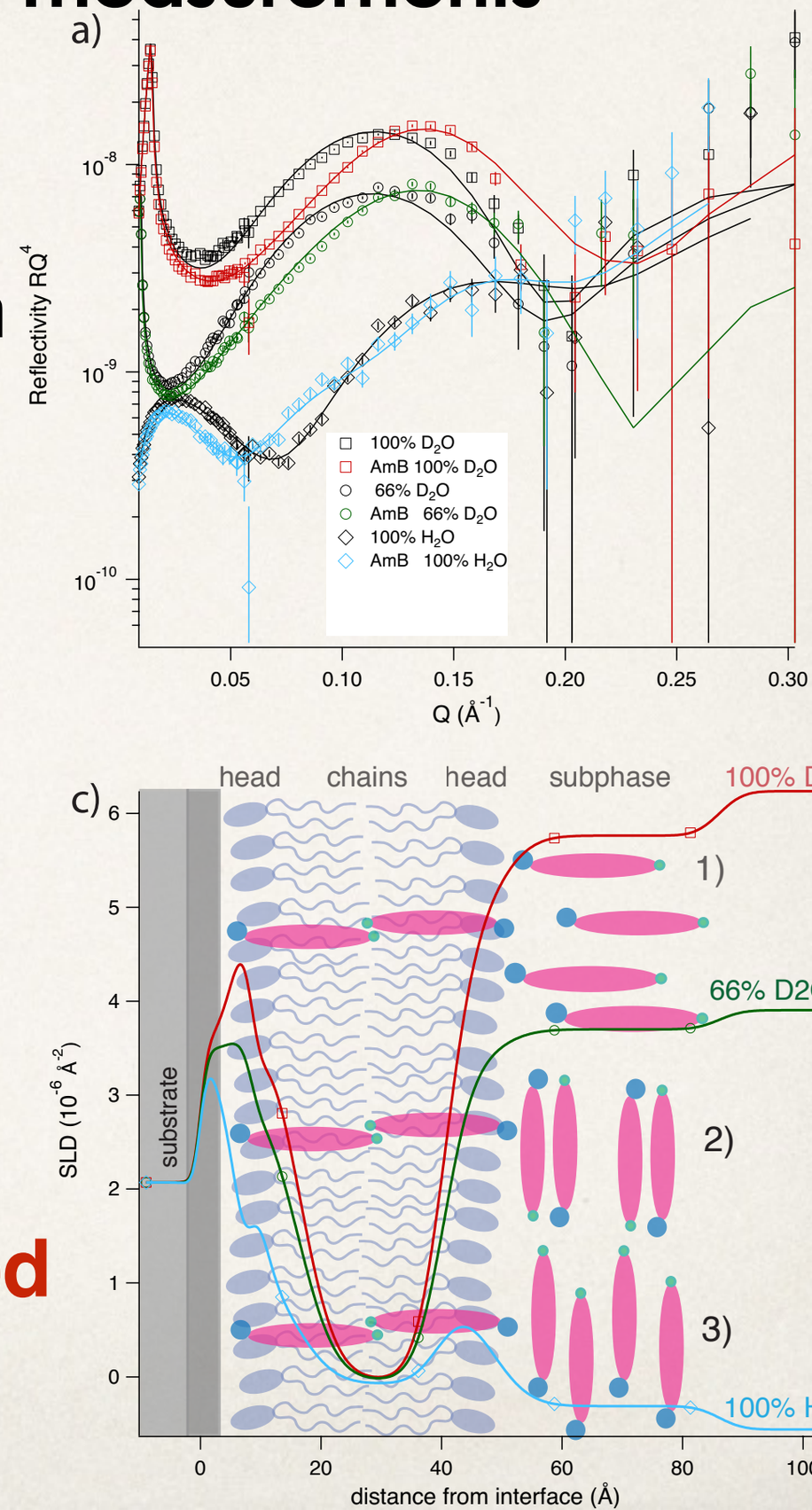

AmB extracts ergosterol !

ARTICLE
PUBLISHED ONLINE: 30 MARCH 2014 | DOI: 10.1038/NCHEMBIO.1496

nature chemical biology

Amphotericin forms an extramembranous and fungicidal sterol sponge

Thomas M Anderson[1,6], Mary C Clay[1,6], Alexander G Cioffi[2], Katrina A Diaz[2], Grant S Hisao[1], Marcus D Tuttle[1], Andrew J Nieuwkoop[1], Gemma Comellas[3], Nashrah Maryum[1], Shu Wang[1,4], Brice E Uno[1], Erin L Wildeman[2], Tamir Gonen[5], Chad M Rienstra[1-3]* & Martin D Burke[1,2,4]*

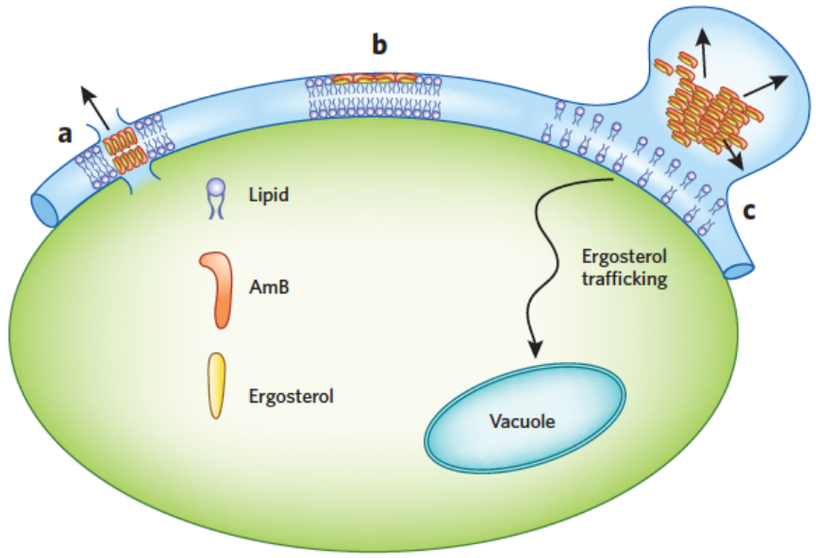

- Paramagnetic Resonance enhancement of ^{13}C-AmB by selectively spin-labelled lipids
- TEM + ultracentrifugation (cells)

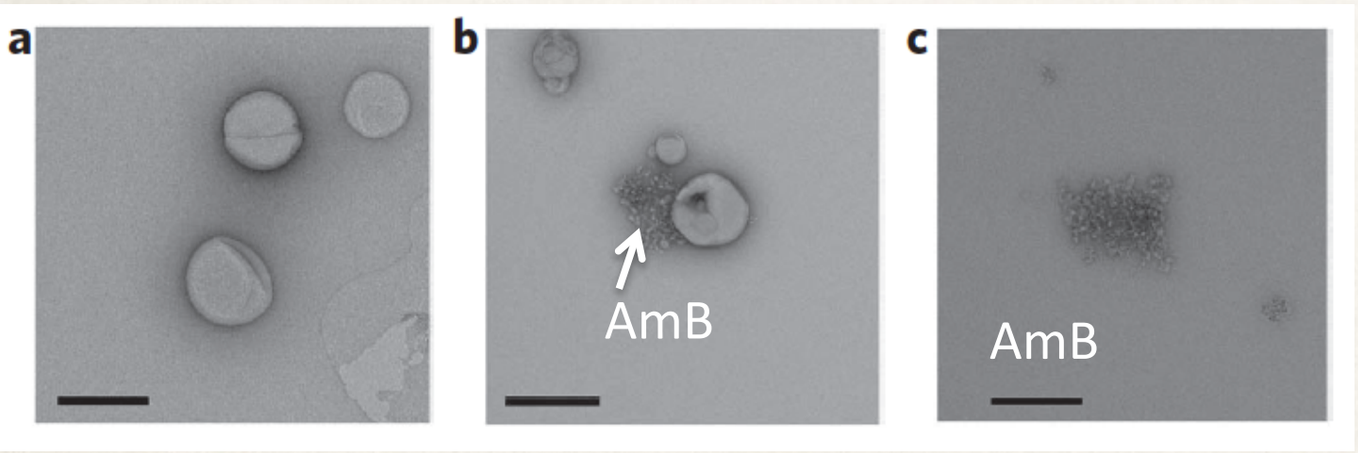

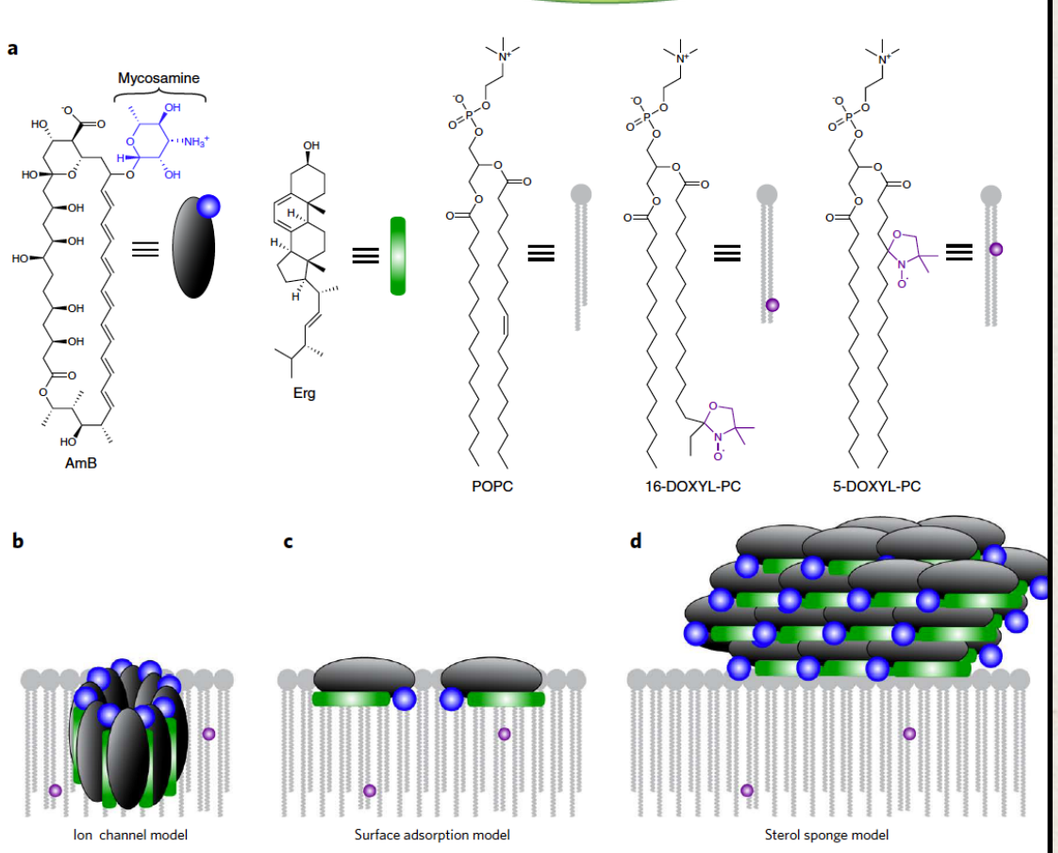

A closer inspection of NR data …

- sld of lipid chains (-0.14 10-6 Å-2) higher than for model bilayers due to PUFAs
- AmB exchanges protons with solvent
- Data allows for **AmB insertion into bilayer**, **ergosterol extraction** and **incorporation into AmB layer** and **decoupling of lipid head groups from each other** -> *better global fit*

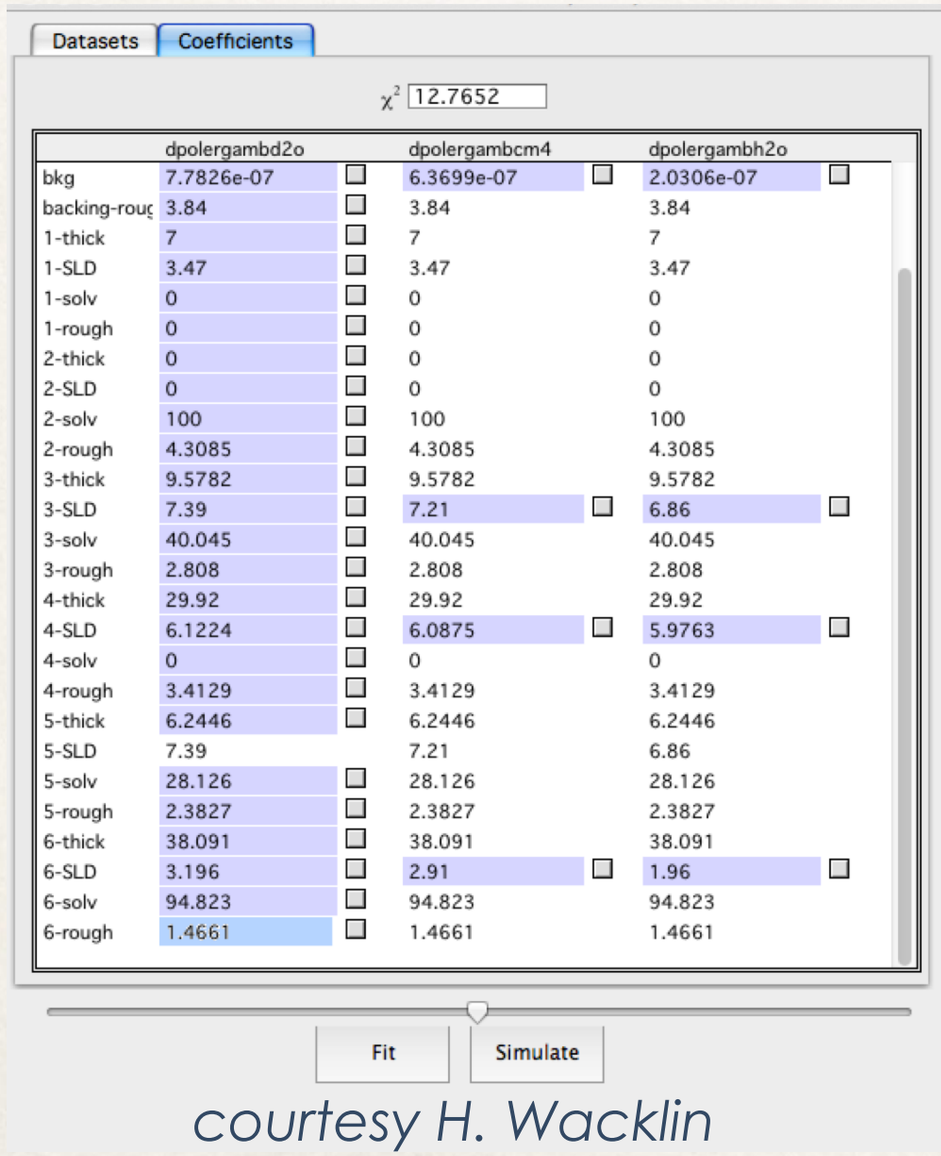

	dpolergambd2o		dpolergambcm4		dpolergambh2o	
bkg	7.7826e-07	☐	6.3699e-07	☐	2.0306e-07	☐
backing-roug	3.84	☐	3.84		3.84	
1-thick	7	☐	7		7	
1-SLD	3.47	☐	3.47		3.47	
1-solv	0	☐	0		0	
1-rough	0	☐	0		0	
2-thick	0	☐	0		0	
2-SLD	0	☐	0		0	
2-solv	100	☐	100		100	
2-rough	4.3085	☐	4.3085		4.3085	
3-thick	9.5782	☐	9.5782		9.5782	
3-SLD	7.39	☐	7.21	☐	6.86	☐
3-solv	40.045	☐	40.045		40.045	
3-rough	2.808	☐	2.808		2.808	
4-thick	29.92	☐	29.92		29.92	
4-SLD	6.1224	☐	6.0875	☐	5.9763	☐
4-solv	0	☐	0		0	
4-rough	3.4129	☐	3.4129		3.4129	
5-thick	6.2446	☐	6.2446		6.2446	
5-SLD	7.39		7.21		6.86	
5-solv	28.126	☐	28.126		28.126	
5-rough	2.3827	☐	2.3827		2.3827	
6-thick	38.091	☐	38.091		38.091	
6-SLD	3.196	☐	2.91	☐	1.96	☐
6-solv	94.823	☐	94.823		94.823	
6-rough	1.4661	☐	1.4661		1.4661	

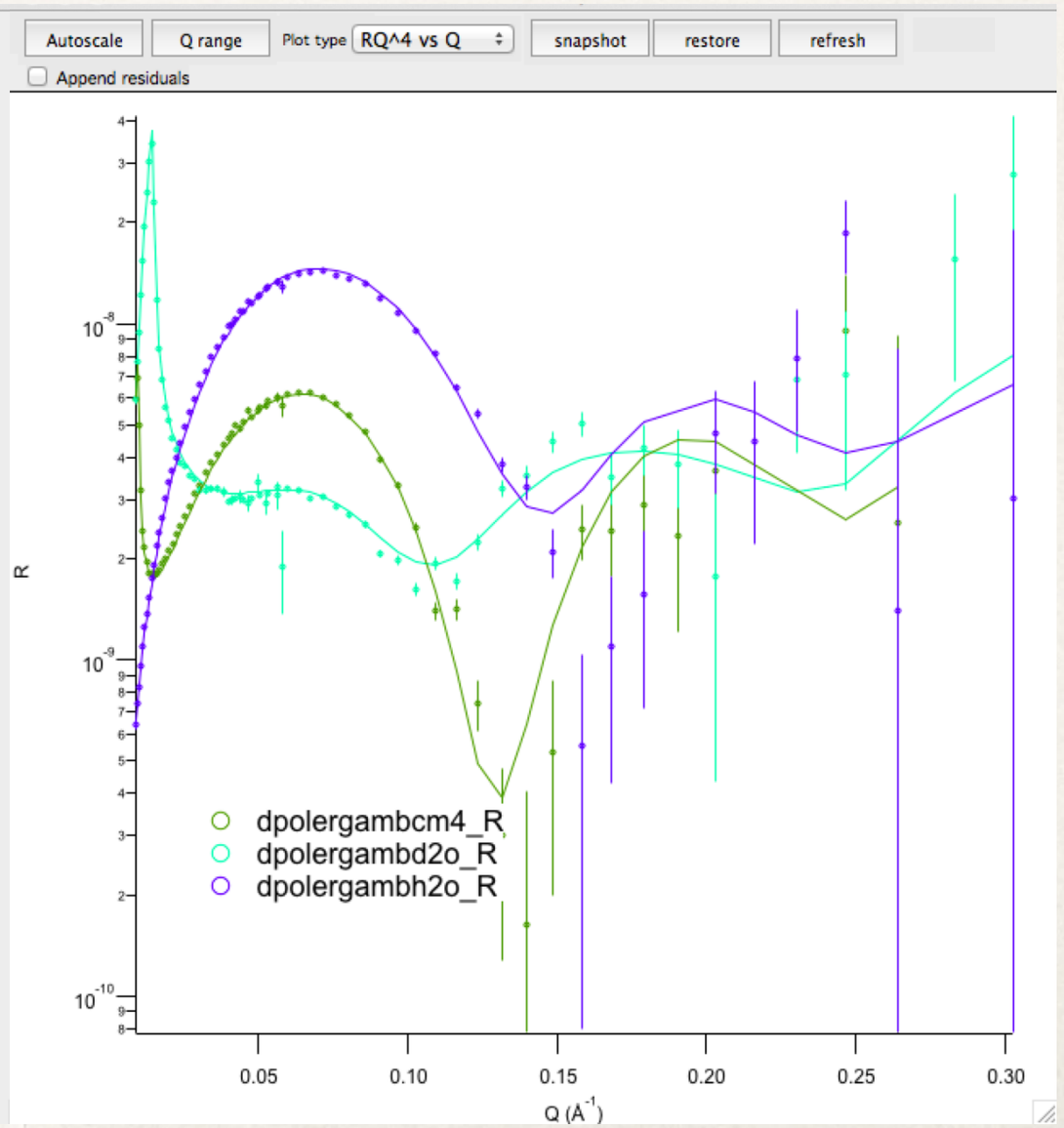

courtesy H. Wacklin

A closer inspection of NR data …

- sld of lipid chains (-0.14 10-6 Å-2) higher than for model bilayers due to PUFAs
- AmB exchanges protons with solvent

h-lipids

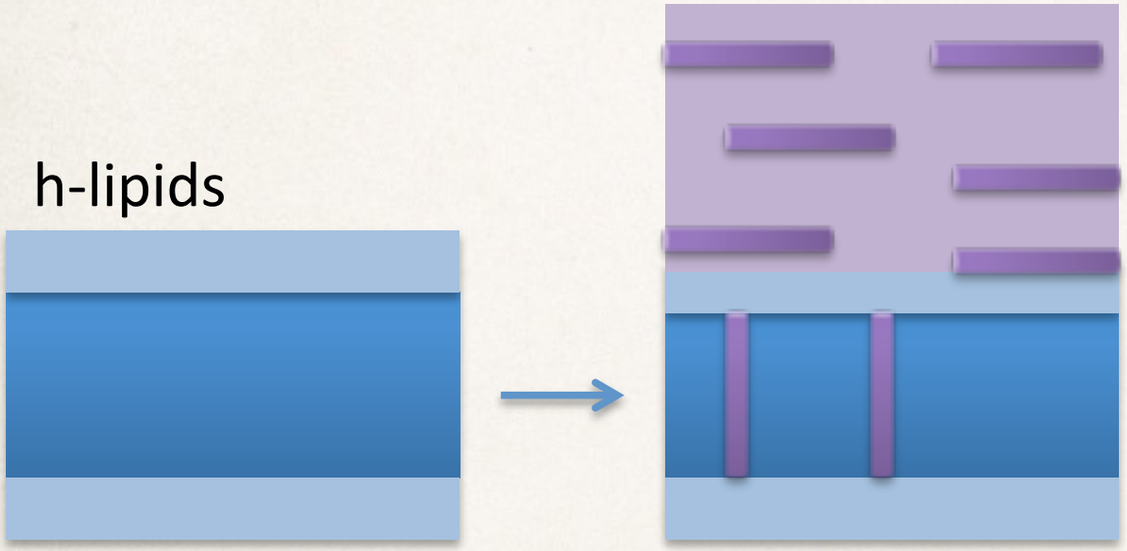

- only small amount of AmB inserts in the lipid bilayer (4v/v%)
- bilayer gets 4Å thinner
- 36Å thick Amb layer (83v/v% water) on top of bilayer much larger than AmB molecule

h-lipids+sterols

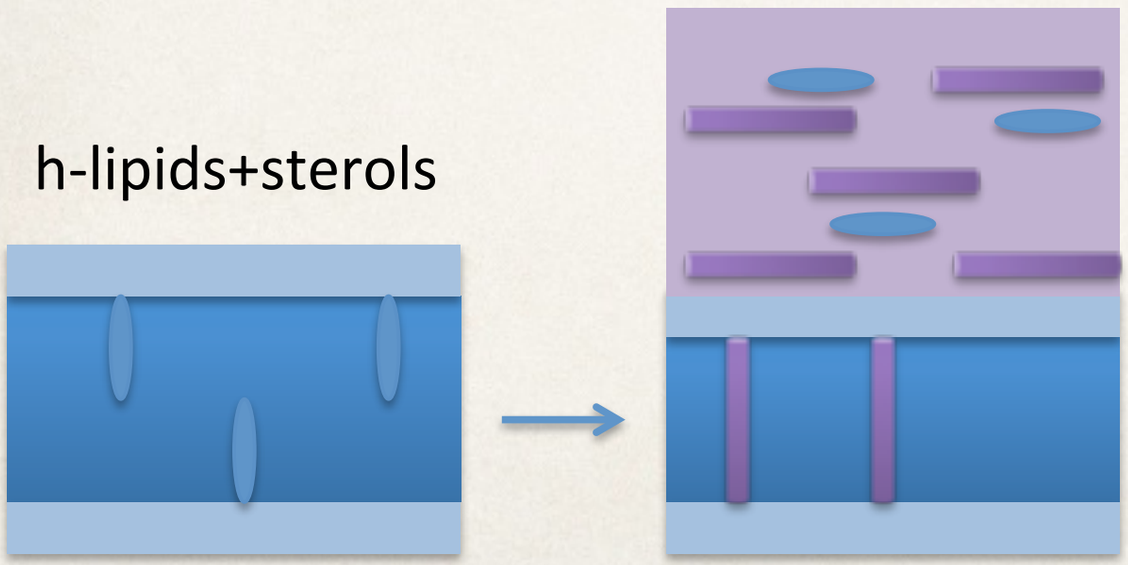

- h-yeast contains 14.5mol% ergosterol
- AmB insertion the same as above
- ergosterol all extracted into AmB layer above, which is 39Å thick (77v/v% water).
- Lipid bilayer gets 6Å thinner

A closer inspection of NR data …

- sld of lipid chains (6.61x 10^{-6} $Å^{-2}$) slightly smaller than estimated from lipid composition
- d-yeast contains mainly mono-unsaturated C18:1 lipids, and is thicker than h-yeast.

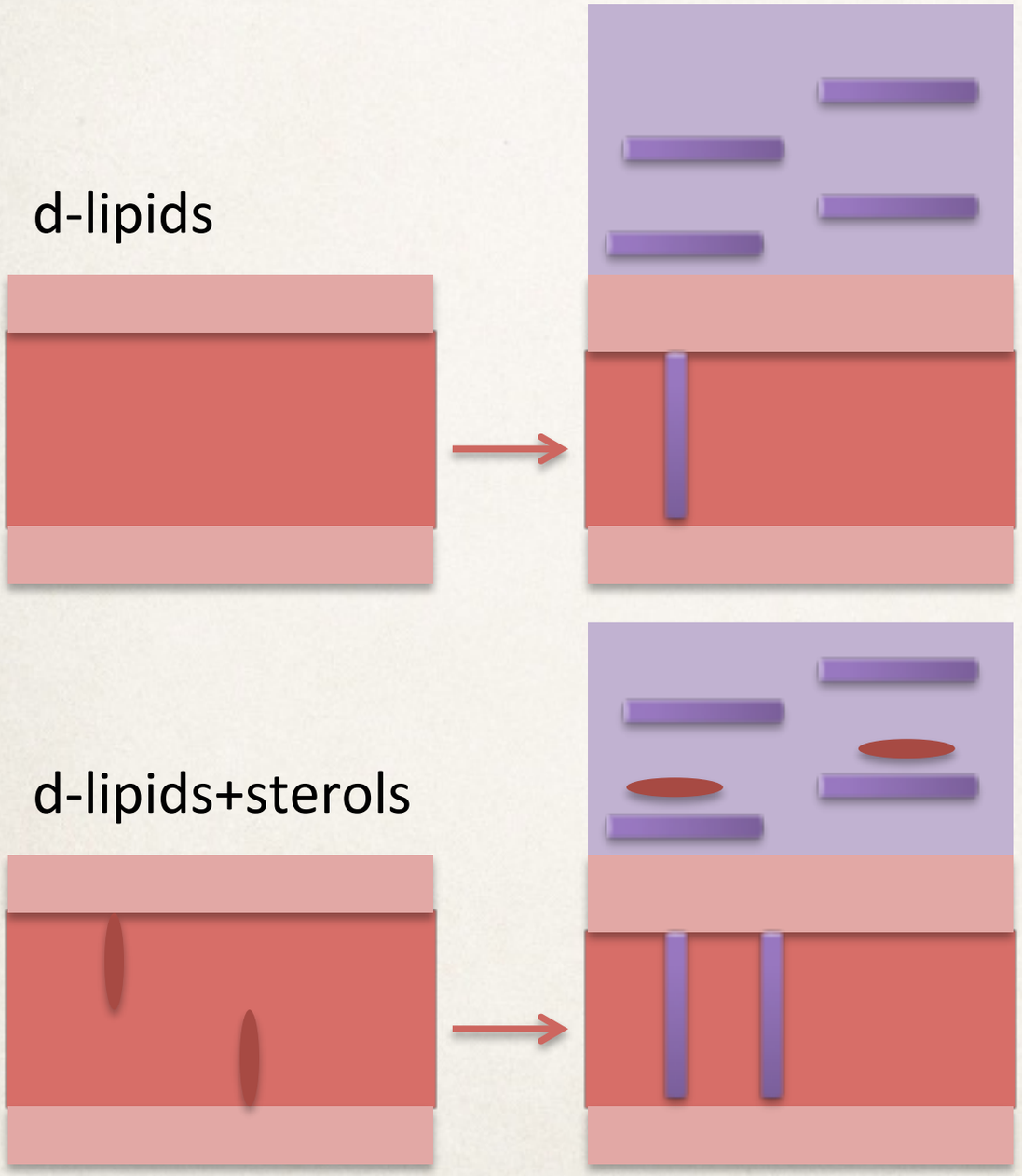

- less AmB inserts in the bilayer (1.5v/v%)
- bilayer does not get much thinner
- 47Å thick Amb layer (91v/v% water)

- d-yeast contains less ergosterol (6mol%)
- 12 v%v AmB insertion
- ergosterol all extracted into AmB layer above, which is 38Å thick (94% water).
- Lipid bilayer gets 3Å thinner

Conclusions

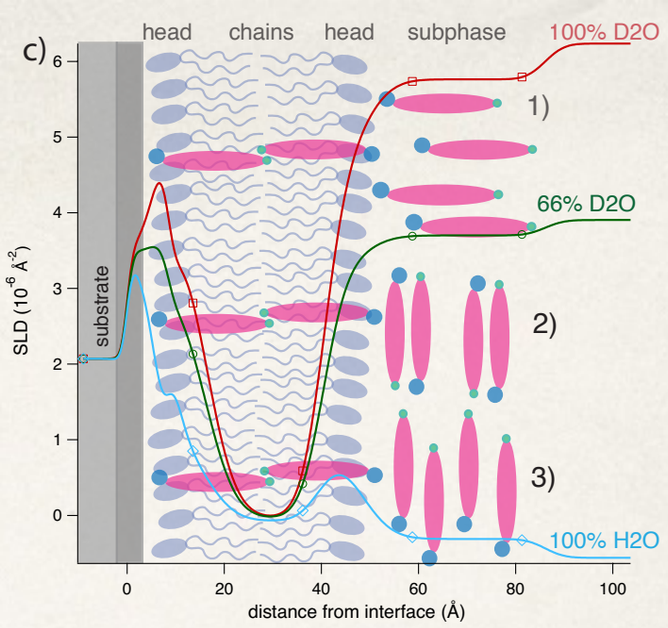

- Data more **consistent with new model for AmB** mechanism than pore model
- **Future scope** for investigating ergosterol extraction and dependence on membrane composition, the kinetics, effect of AmB formulation etc.
- Experiments possible due to **set up for extracting, separating and purifying lipid components** (PSCM) from deuterated cells grown at ILL D-Lab
- **Analysis of lipid composition** (in collaboration with CEA Grenoble, UMIL Dept. Translational Medicine) enabled effect of polyunsaturation to be observed

Examples:

- Ganglioside/cholesterol pair **(V. Rondelli, L. Cantù, et al.)**

- Interaction of antibiotic with natural membranes **(A. de Ghellinck, H. Wacklin, M. Sferrazza, J. Jouhet, M. Haertlein, …)**

- Neutron reflectometry and deuteriation to probe density profiles of proteins adsorbed onto polymer brushes **(E. Schneck, A. Schollier, A. Halperin, M. Sferrazza)**

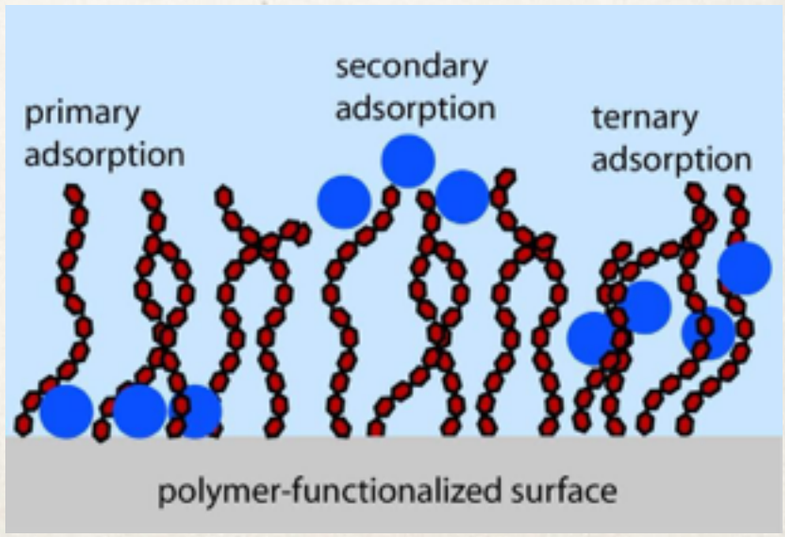

Density Profiles of Proteins in Polymer brushes

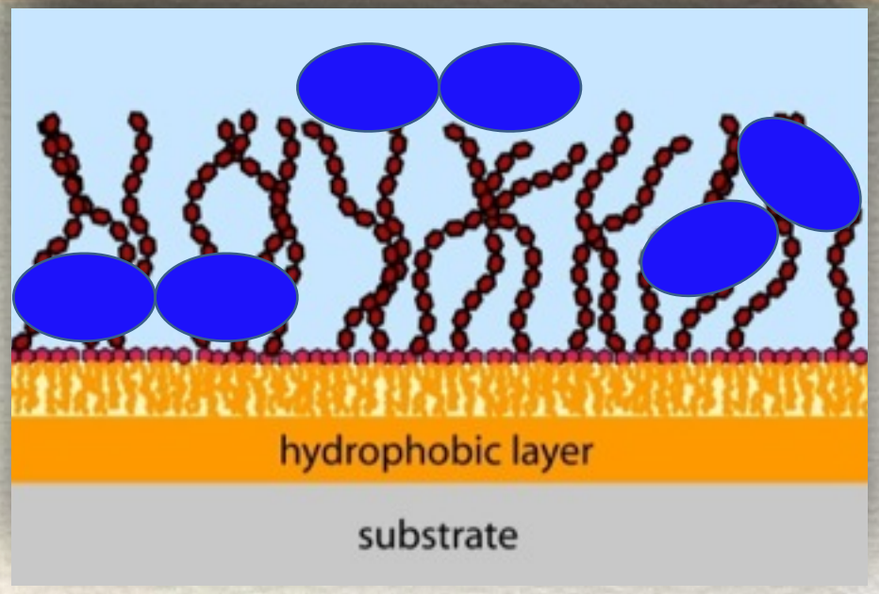

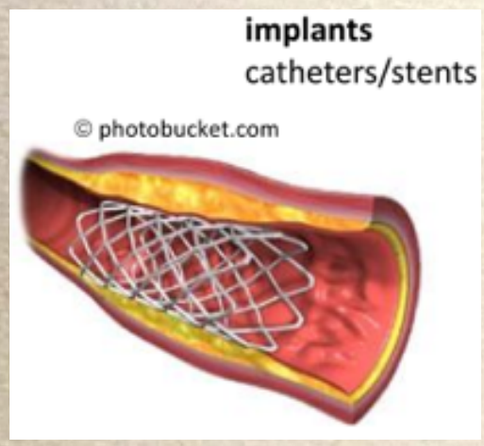

biocompatible surface functionalization

“brush failure” via protein adsorption

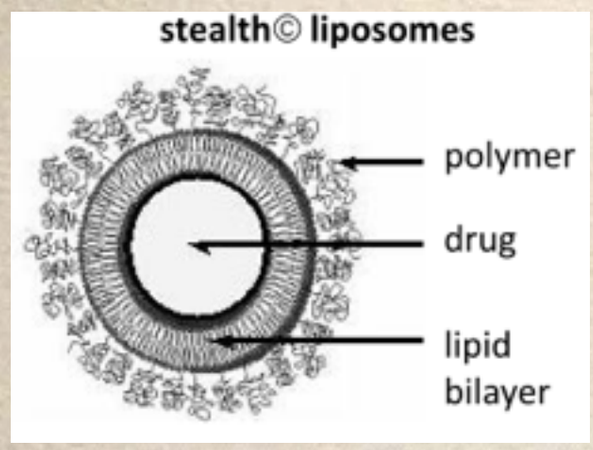

modes of protein adsorption:
primary, secondary, ternary

structural characterization
for “rational design” of protein resistant functionalization (role of grafting density and polymer length)

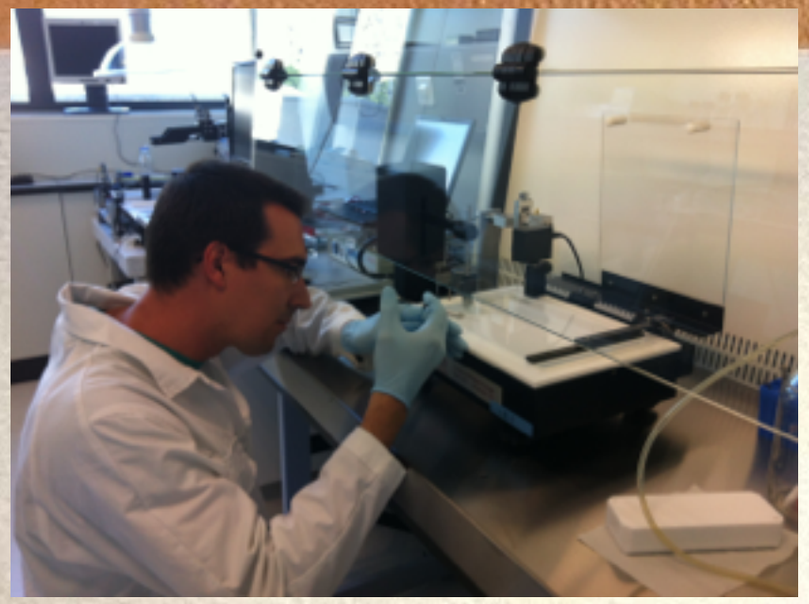

Sample Preparation

Preparation steps

- Planar silicon substrates
- Hydrophobic functionalization
- Brushes at air/water interface (Langmuir trough) of PS-PEG diblock copolymers or PE-PEG lipid anchored polymers

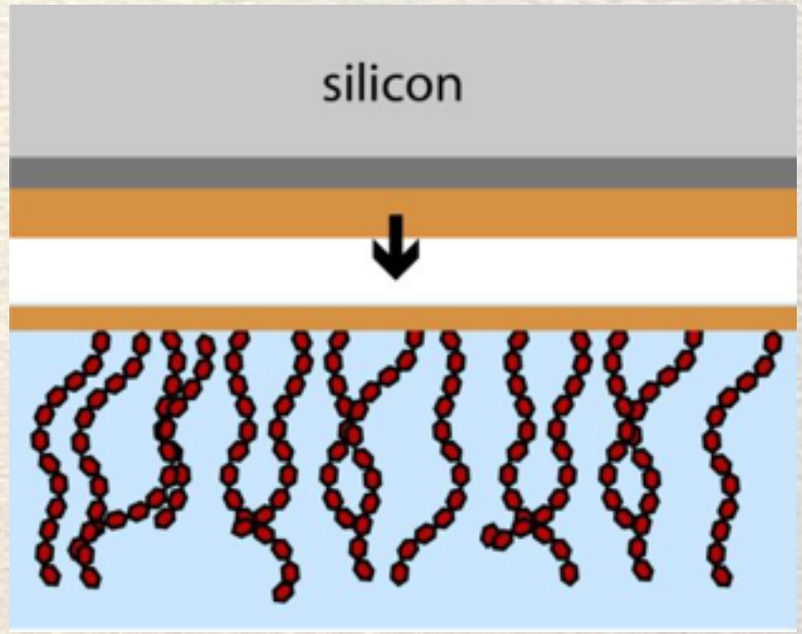

Resulting brush

- defined grafting density, **σ**
- defined polymer length, ***N***
- hydrophilic/hydrophobic grafting surface

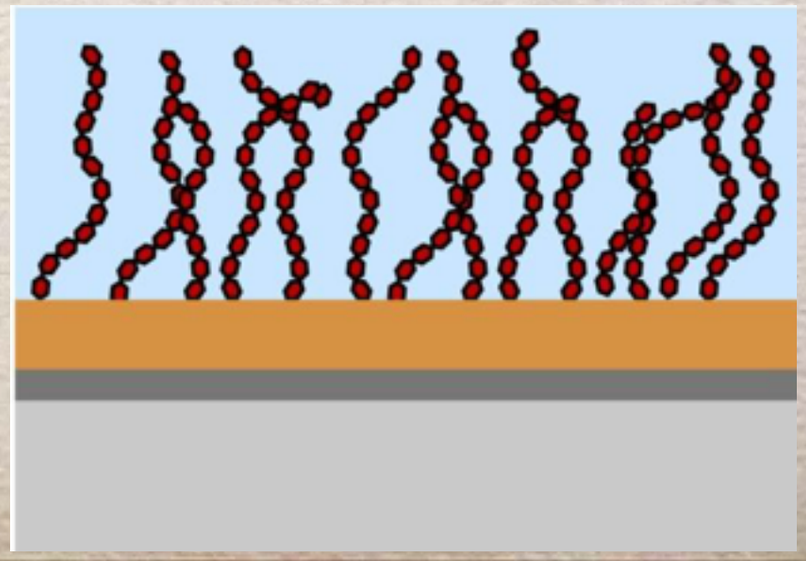

Data Analysis

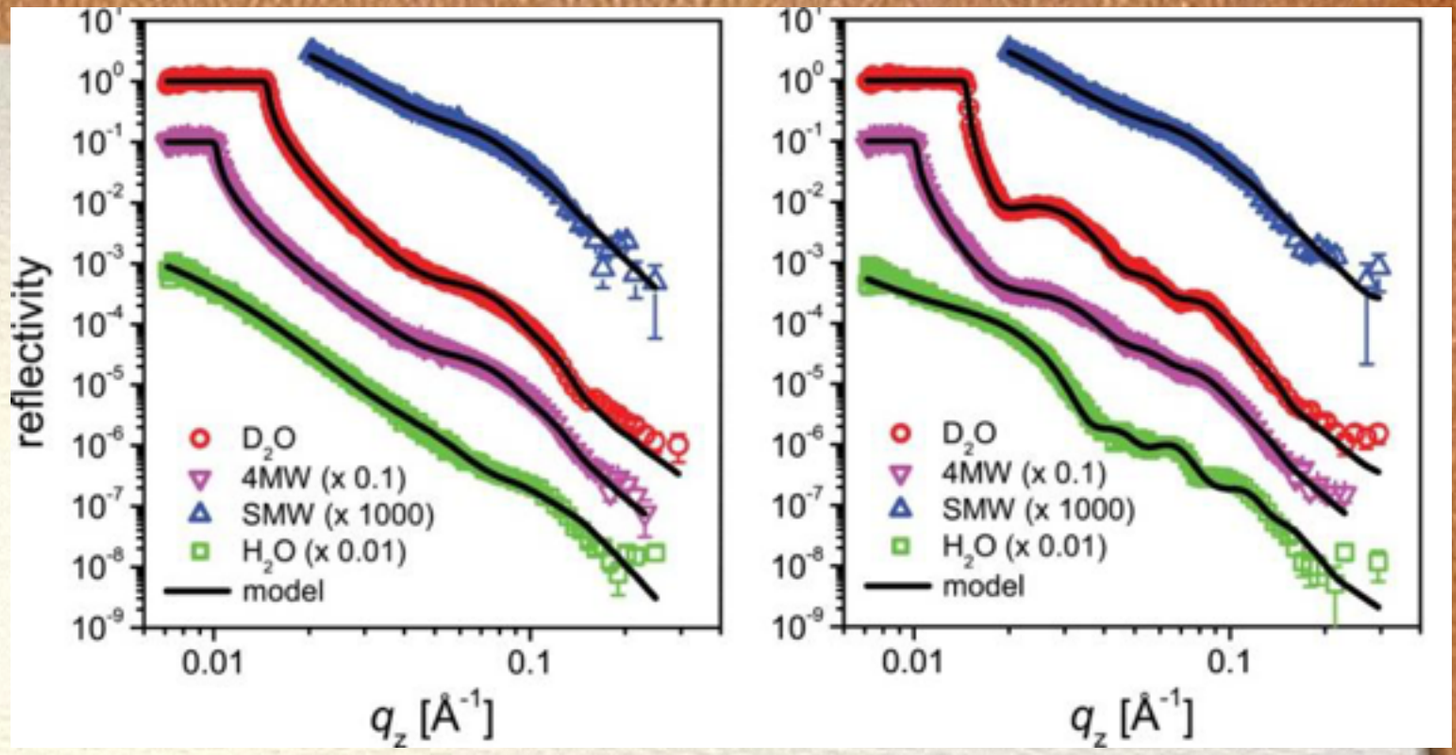

for each parameter set:

- compute SLD profiles corresponding to all measurement conditions;
- discretized into 1Å slices;
- compute corresponding reflectivity curves (dynamical treatment: Fresnel reflection coefficients, Parrat formalism)
- **parameters are varied** to achieve best agreement between measured and modelled reflectivity curves

Data Analysis

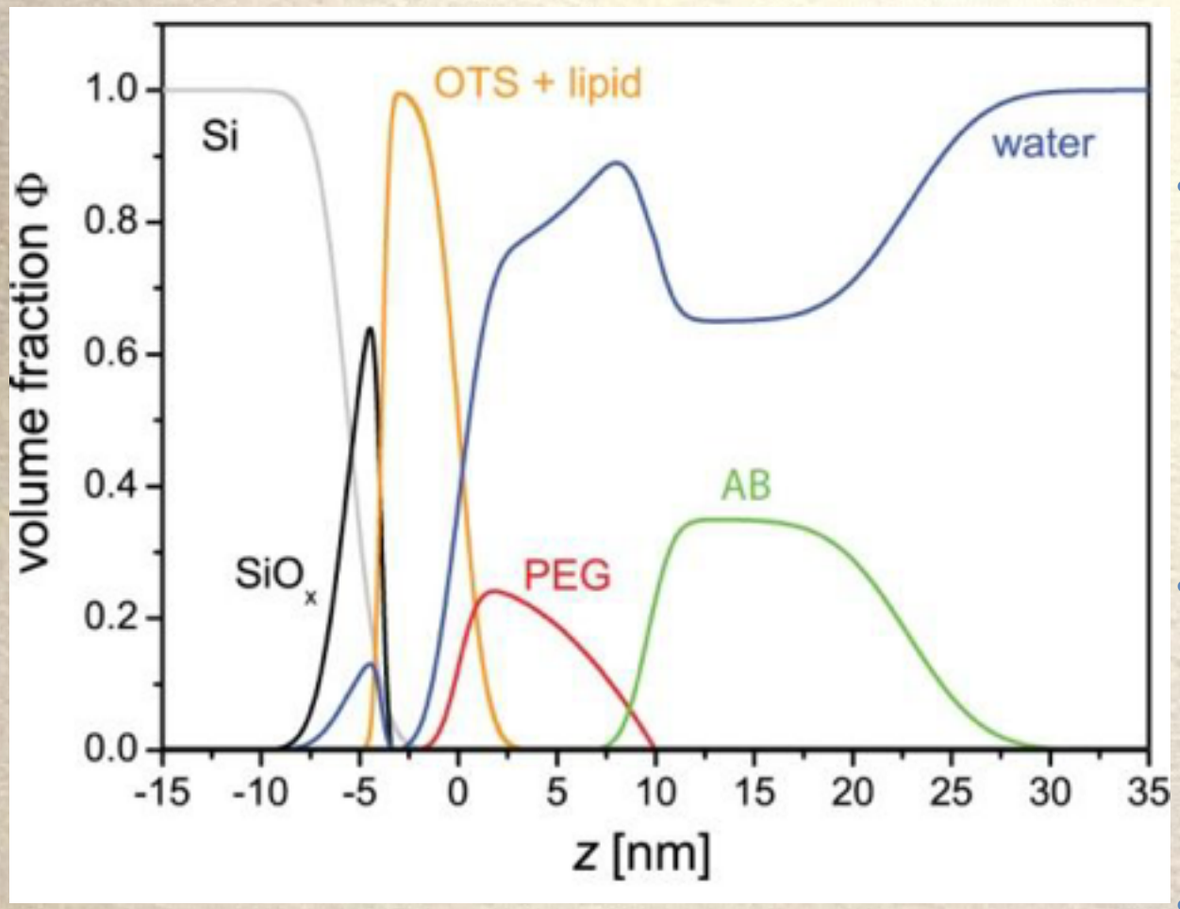

Schneck, Schollier et al., Langmuir 2013

Layers below grafting surface

- slabs with adjustable thickness, dry SLD, water content, interface roughness

PEG brush

- parabola (SCF theory) with adjustable brush length and density

After protein adsorption

- protein distribution that allows for primary, secondary, ternary adsorption (rough slabs+Gaussians)
- SLD of PEG and protein fixed
- dependence of protein SLD on water contrast (H/D exchange) taken into account

Bare Brushes
Results consistent with SCF theory

- PEG 114<N<770 up to σ ~ 2x10^{17}m^{-1} (*5nm^2 per chain*)
- **parabolic brush model** gives density, Φ_0 and length, H_0

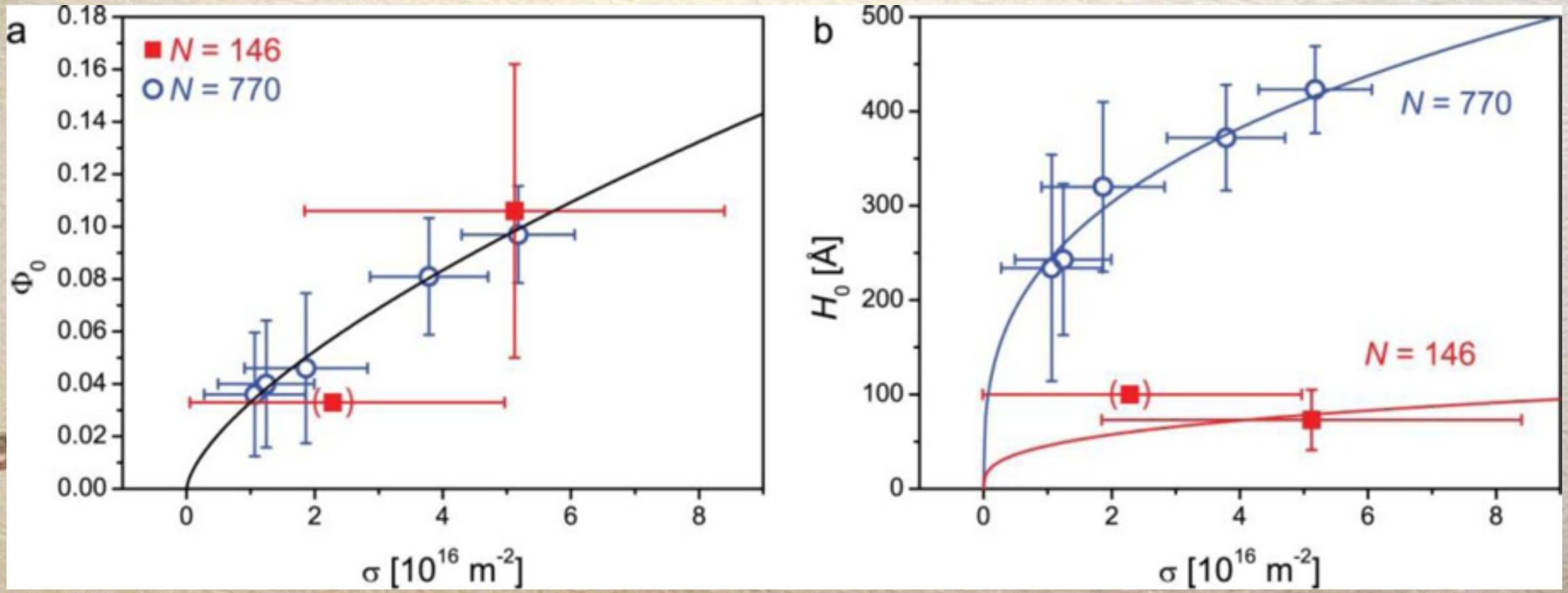

Adsorption of deuterated myoglobin to PEG brushes grafted on hydrophobic polystyrene surfaces

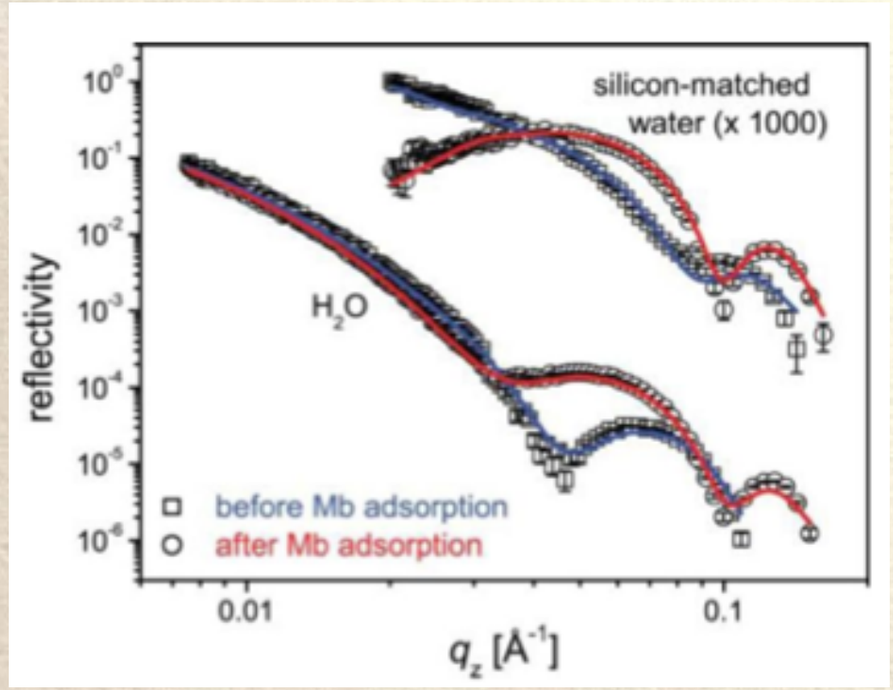

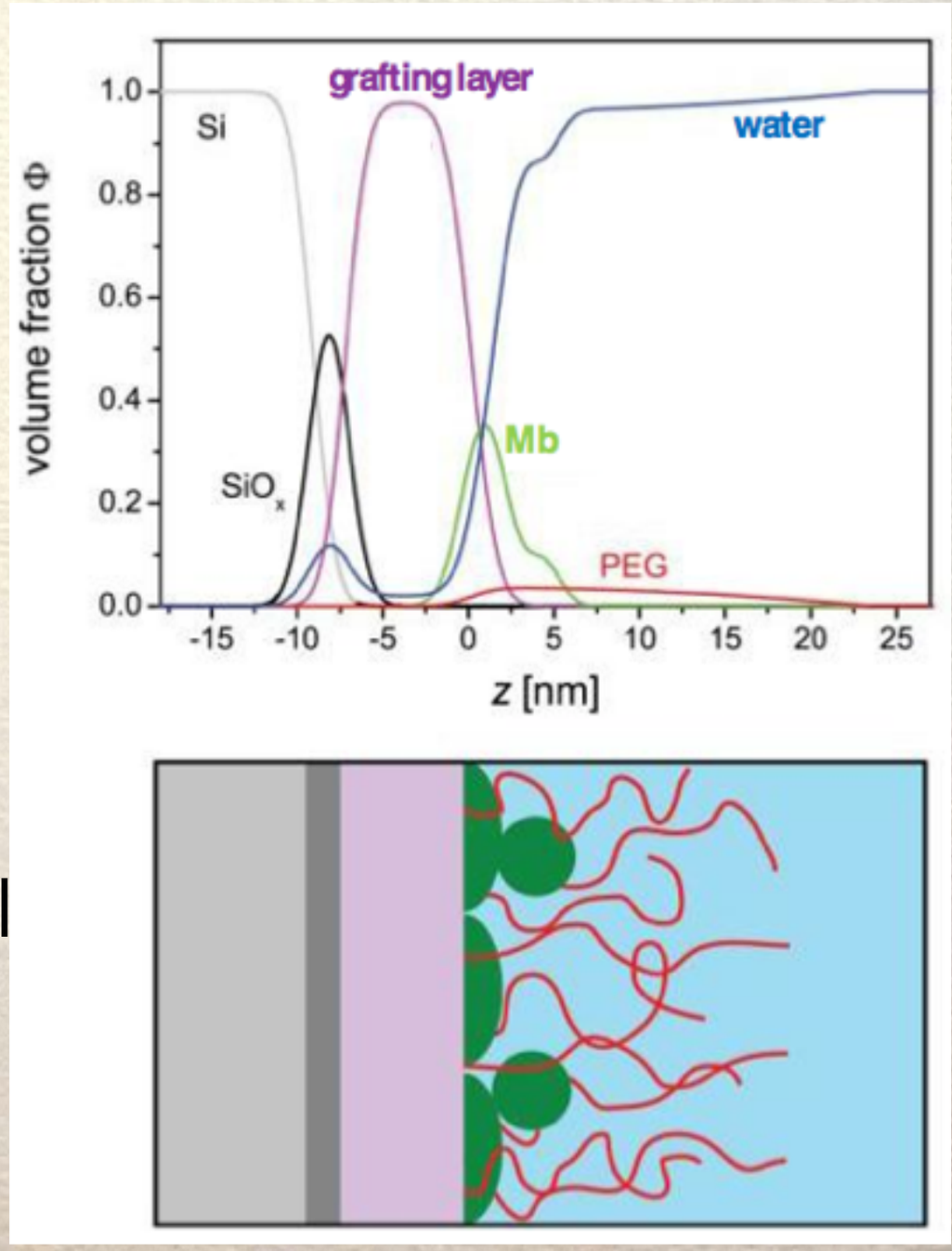

- Significant adsorption for all brush parameters
- only primary adsorption

Adsorption of deuterated myoglobin to PEG brushes grafted on hydrophobic polystyrene surfaces

- inner-layer: protein amount decreases with grafting density
- anchoring points obstacles adsorption
- outer protein layer depends on overall PEG amount and protein-protein interactions are altered by the presence of PEG
- **Information only accessible with neutron reflection combined with protein perdeuteration**

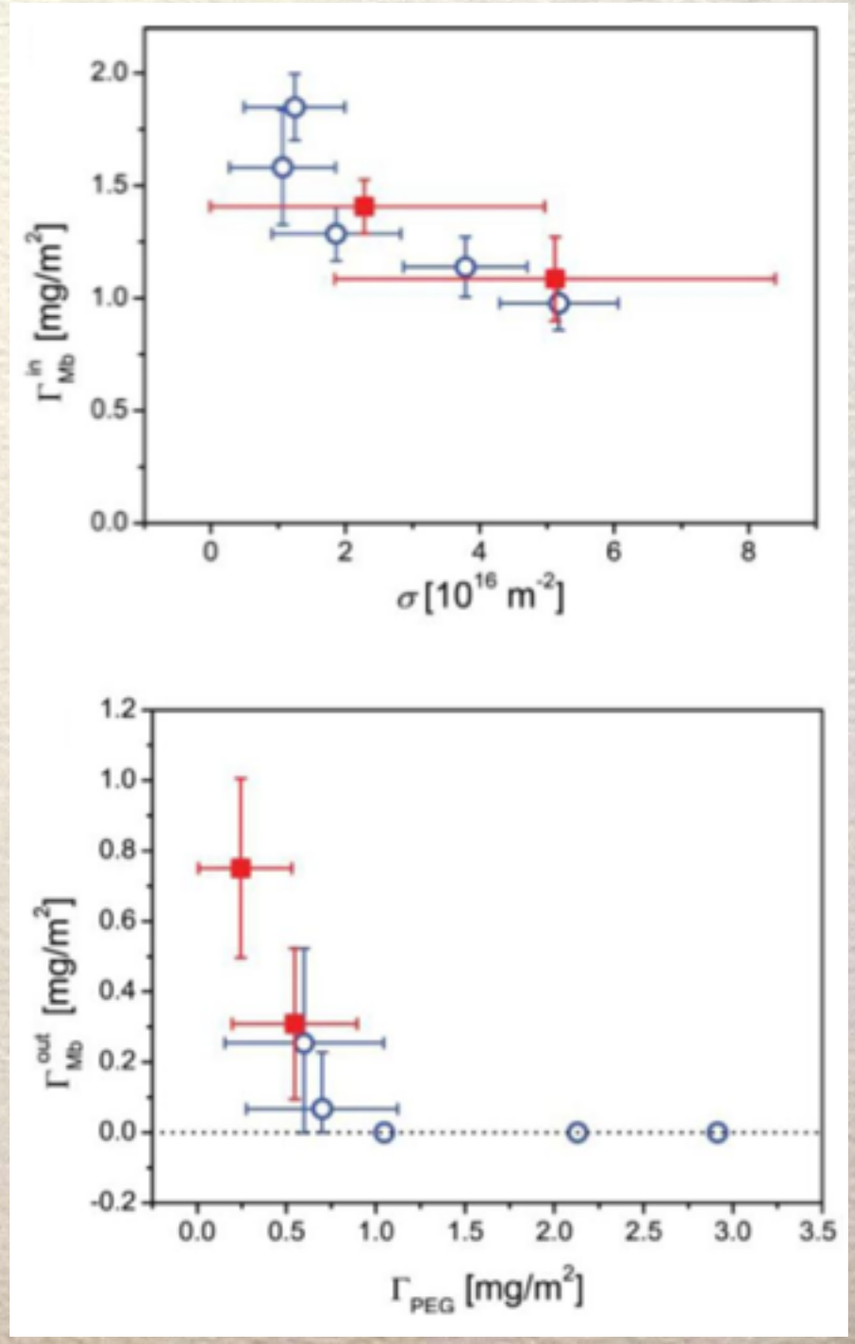

Specific adsorption: PEG antibodies

- **Classically PEG purely repellent, in fact it is antigenic**
- **PEG antibodies produces in animals (0.1% - 25% in humans)**
- **Implications on brush functioning - failure?**
- **IgG AB bind specifically to end segments of PEG**

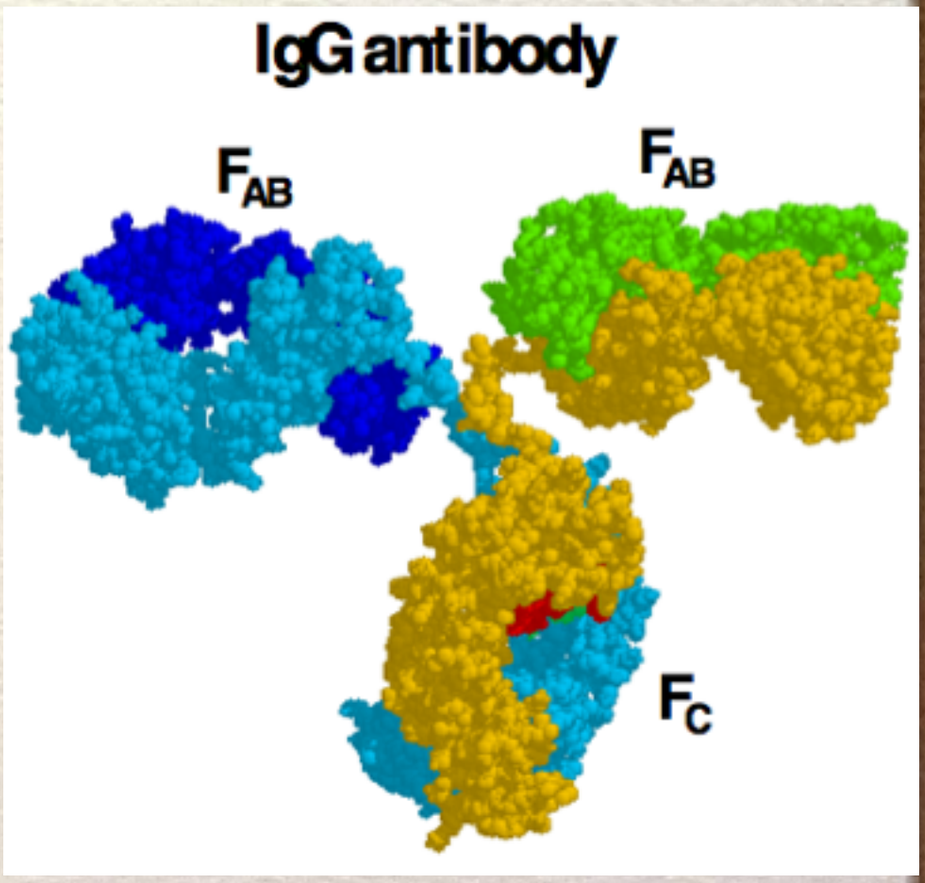

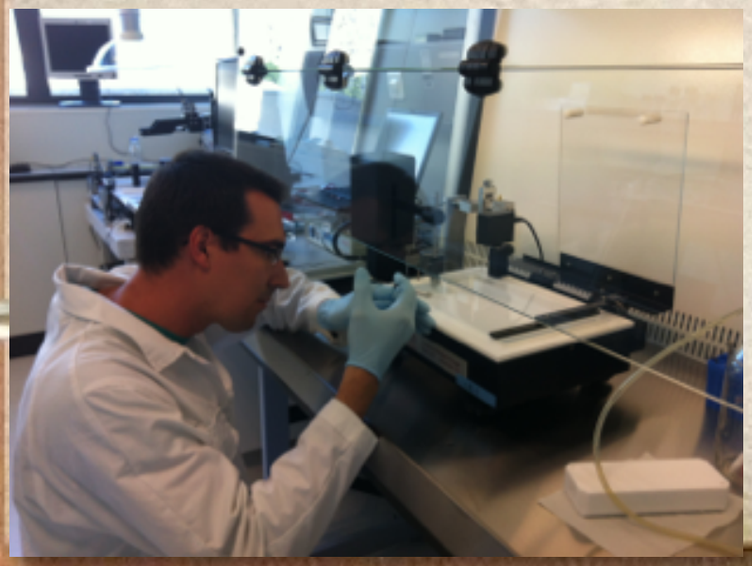

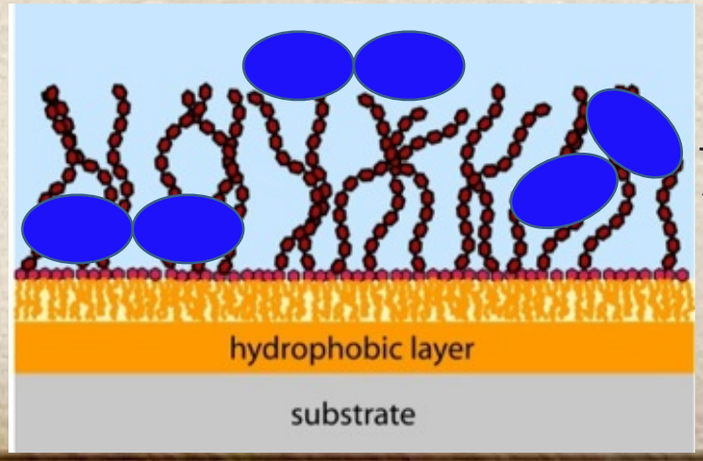

Brushes grafted to hydrophilic phospholipid surface to prevent primary adsorption

Specific adsorption: PEG antibodies

Neutron reflectometry measurements

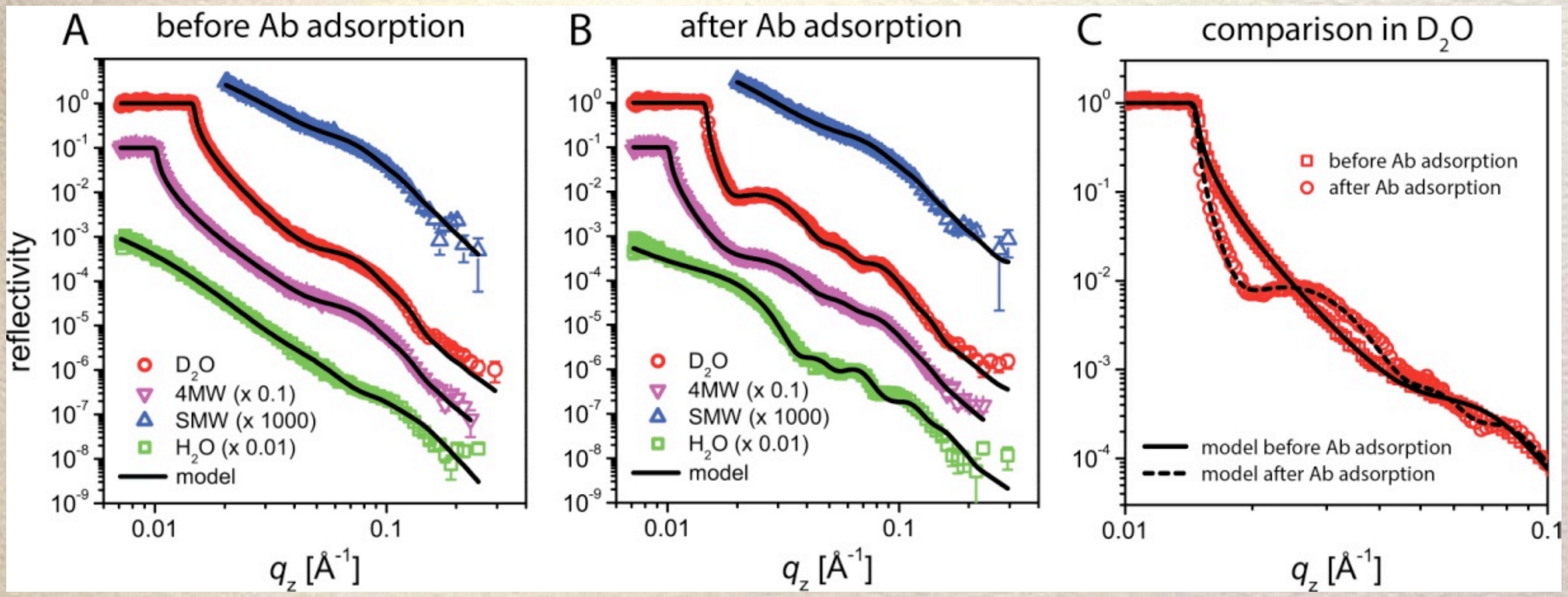

Brushes grafted to hydrophilic phospholipid surface to prevent primary adsorption

Specific adsorption: PEG antibodies

- **Antibodies adsorbs at brush periphery**
- **No primary adsorption**
- **Amount increases with grafting density**
- **Saturation - molecular crowding**

Antibodies become the dominant surface:
Brush no more functional
foreign-body reaction

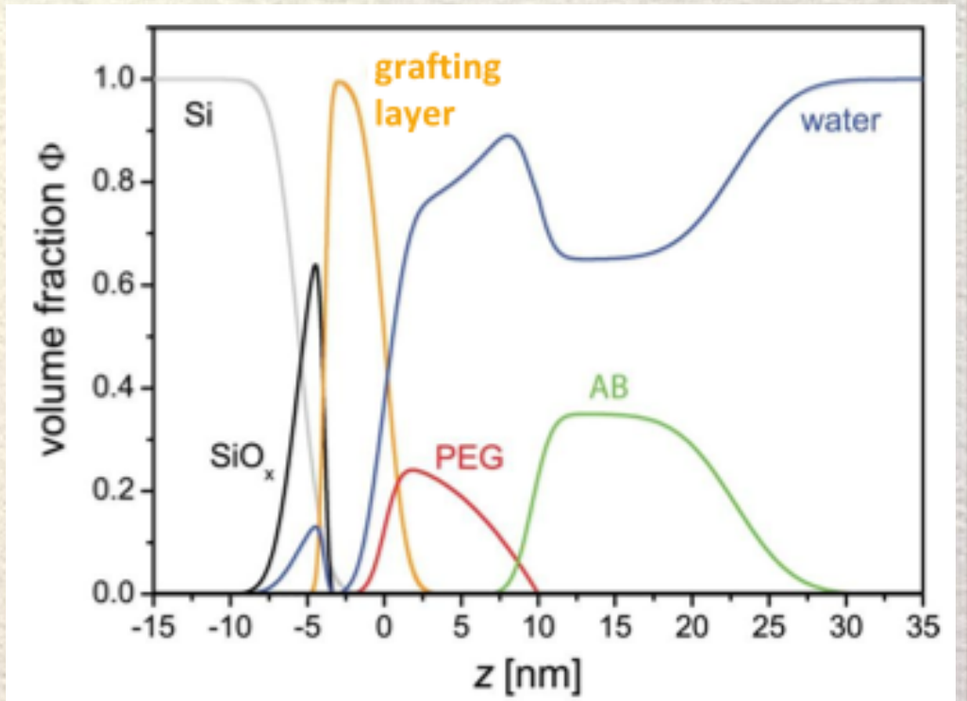

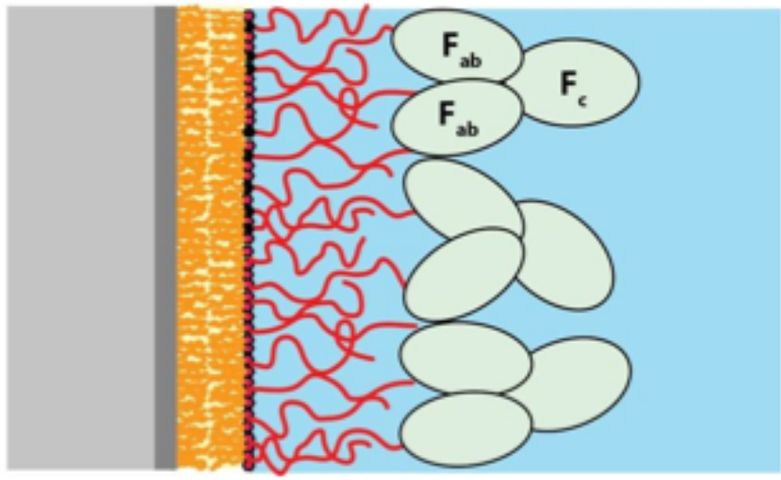

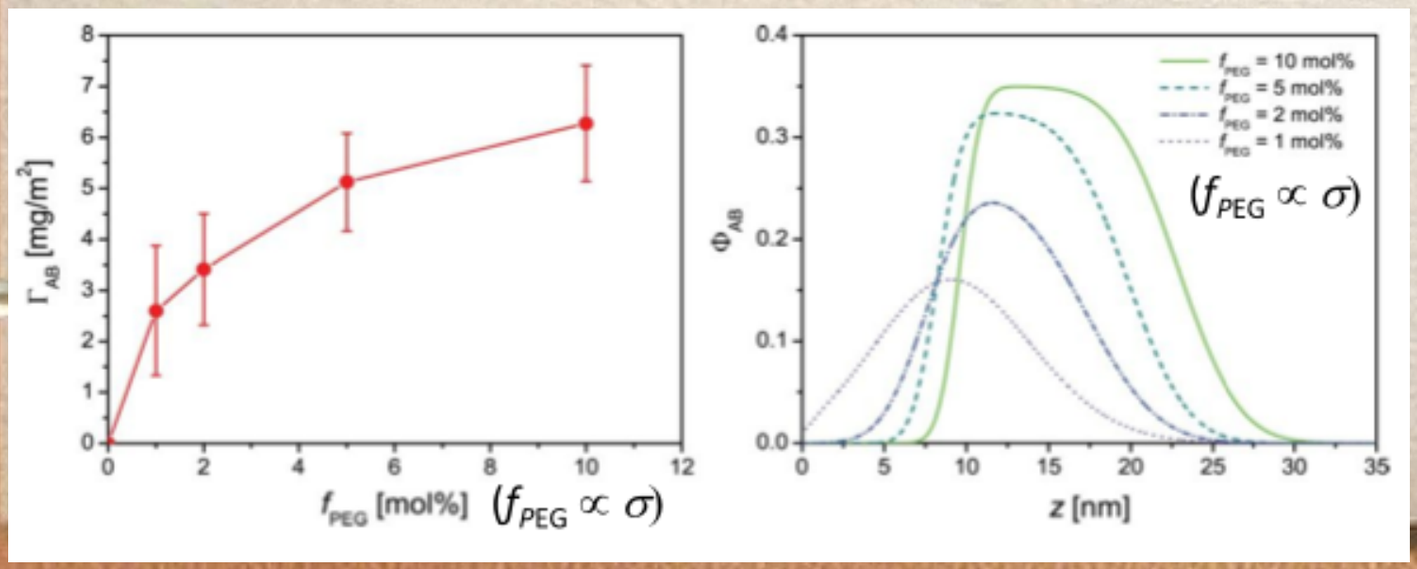

Schneck et al., in preparation

- Many open questions regarding protein adsorption to polymer brushes
- Neutron reflectometry (coupled to protein deuteriation) promising approach
- Detailed structural insight
- Unique tool to investigate the structure of biological interfaces and interfaces relevant for biotechnological applications

Conclusions

- Neutron reflectometry remains an essential tool for the study of structure at the nanometer level of soft self-assembled systems at interfaces.

- Complementary to x-ray and synchrotron radiation, advantages include high penetration, sensitivity to light elements (H, C, O, N, …) and isotopic labelling/contrast variation.

- Possibility to work in real (physiological) conditions

- Possibility for in-situ studies of systems under deformation.

- Need optimised sample preparation

- Perspectives in biology are very numerous.